TU Delft

Delft University of Technology

Magneto-/ electro-responsive polymers toward manufacturing, characterization, and biomedical/ soft robotic applications

Yarali, Ebrahim; Baniasadi, Mahdi; Zolfagharian, Ali; Chavoshi, Maede; Arefi, Fatemeh; Hossain, Mokarram; Bastola, Anil; Ansari, Mahdi; Foyouzat, Alireza; Dabbagh, Ali

DOI
10.1016/j.apmt.2021.101306

Publication date
2022

Document Version
Final published version

Published in
Applied Materials Today

Citation (APA)
Yarali, E., Baniasadi, M., Zolfagharian, A., Chavoshi, M., Arefi, F., Hossain, M., Bastola, A., Ansari, M., Foyouzat, A., Dabbagh, A., Ebrahimi, M., Mirzaali Mazandarani, M., & Bodaghi, M. (2022). Magneto-/ electro-responsive polymers toward manufacturing, characterization, and biomedical/ soft robotic applications. *Applied Materials Today*, *26*, Article 101306. https://doi.org/10.1016/j.apmt.2021.101306

Important note
To cite this publication, please use the final published version (if applicable).
Please check the document version above.

Copyright
Other than for strictly personal use, it is not permitted to download, forward or distribute the text or part of it, without the consent of the author(s) and/or copyright holder(s), unless the work is under an open content license such as Creative Commons.

Takedown policy
Please contact us and provide details if you believe this document breaches copyrights.
We will remove access to the work immediately and investigate your claim.

This work is downloaded from Delft University of Technology.
For technical reasons the number of authors shown on this cover page is limited to a maximum of 10.

Green Open Access added to TU Delft Institutional Repository

'You share, we take care!' - Taverne project

https://www.openaccess.nl/en/you-share-we-take-care

Otherwise as indicated in the copyright section: the publisher is the copyright holder of this work and the author uses the Dutch legislation to make this work public.

Applied Materials Today 26 (2022) 101306

Contents lists available at ScienceDirect

Applied Materials Today

journal homepage: www.elsevier.com/locate/apmt

Magneto-/ electro-responsive polymers toward manufacturing, characterization, and biomedical/ soft robotic applications

Ebrahim Yarali[a], Mahdi Baniasadi[a], Ali Zolfagharian[b], Maede Chavoshi[c], Fatemeh Arefi[c], Mokarram Hossain[d], Anil Bastola[e], Mahdi Ansari[f], Alireza Foyouzat[g], Ali Dabbagh[a], Mohamad Ebrahimi[h], Mohammad J. Mirzaali[i], Mahdi Bodaghi[j,*]

[a] School of Mechanical Engineering, College of Engineering, University of Tehran, Tehran 11155-4563, Iran
[b] School of Engineering, Deakin University, Geelong, Victoria 3216, Australia
[c] School of Electrical and Computer Engineering, College of Engineering, University of Tehran, Tehran, Iran
[d] Zienkiewicz Centre for Computational Engineering (ZCCE), Swansea University, Swansea, SA1 8EN, United Kingdom
[e] Centre for Additive Manufacturing (CfAM), School of Engineering, University of Nottingham, Nottingham NG8 1BB, United Kingdom
[f] Department of Mechanical Engineering, Arak University of Technology, Arak, Iran
[g] High Performance Computing Laboratory, School of Civil Engineering, University of Tehran, Tehran, Iran
[h] Department of Mechanical and Manufacturing Engineering, University of Calgary, Canada
[i] Department of Biomechanical Engineering, Faculty of Mechanical, Maritime, and Materials Engineering, Delft University of Technology (TU Delft), Mekelweg 2, 2628 CD Delft, The Netherlands
[j] Department of Engineering, School of Science and Technology, Nottingham Trent University, Nottingham NG11 8NS, United Kingdom

ARTICLE INFO

Article history:
Received 7 May 2021
Revised 24 November 2021
Accepted 1 December 2021

Keywords:
Magneto-/ electro-responsive polymers
3D/4D printing
Soft robotics
Tissue engineering
Drug delivery systems
Shape morphing

ABSTRACT

Magneto-/ electro-responsive polymers (MERPs) are a class of stimuli-responsive materials that are actuated when triggered by external magnetic/ electric fields. MERPs exhibit rapid, reversible, and safe multifunctional and dynamic (*i.e.,* changing with time) properties, which can effectively be manipulated at different length scales. These features make MERPs very attractive particularly in biomedical engineering (*e.g.,* drug delivery systems and tissue engineering), soft matter engineering (*e.g.,* soft robotics), and structural design of smart materials with unprecedented properties (*e.g.,* complex shape morphing). Due to the recent progress in the design and development of MERPs, here, we highlighted the current advances in fabricating MERPs using various manufacturing methods including 3D/ 4D printing and conventional techniques. We also summarized the methods used for the characterization of MERPs and discussed their important structure-property relationship. We also highlighted the potential applications of MERPs in biomedical engineering, soft robotic, and the design of smart materials and systems. MERPs show great potentials for creating smart materials with predictable dynamic properties. More studies are necessary to investigate the biological responses of MERP both *in-vivo* and *in-vitro*, which is essential for biomedical engineering applications.

© 2021 Elsevier Ltd. All rights reserved.

Abbreviations: AAm, acrylamide; 2PP, two-photon polymerization; 3D, three-dimensional; ABS, acrylonitrile butadiene styrene; Ag, silver; AM, additive manufacturing; AMF, alternating magnetic field; ATO, antimony-doped tin oxide; BMSCs, bone marrow mesenchymal stem cells; BTE, bone tissue engineering; CAD, computer-aided design; CIPs, carbonyl iron powders; CNFs, carbon nanofibers; CNTs, carbon nanotubes; CTE, cardiac tissue engineering; DDSs, drug delivery systems; DE, dielectric elastomer; DIW, direct ink writing; DLP, digital light processing; DLW, direct laser writing; DMA, dynamical mechanical analyzer; DOD, drop on demand; DSC, differential scanning calorimetr; ECM, extracellular matrix; EMREs, electro-magnetorheological elastomers; ERPs, electro-responsive polymers; ERSMP, electro-responsive SMPs; FDM, fused deposition modeling; FFF, fused filament fabrication; HAMP, heat-assisted magnetic programming; IOs, iron oxides; IPMC, ionic polymer metal composite; IPs, iron particles; LED, light-emitting diode; MERPs, magneto-/ electro-responsive polymers; MPs, microparticles; MR, magnetorheological; MREs, magneto-rheological elastomers; MRPs, magneto-responsive polymers; MRSMPs, magneto-responsive SMPs; MSCs, mesenchymal stem cells; NdFeB, neodymium–iron–boron; NIR, high near-infrared; NPs, nanoparticles; PA, polyamides; PAAm, polyacrylamide; PANi, polyaniline; PC, polycarbonate; PCL, polycaprolactone; PDMS, polydimethylsiloxane; PEG, polyethylene glycol; PEGDA, poly(ethylene glycol) diacrylate; PLA, polylactide acid; PLGA, poly (lactic-co-glycolic acid); PLLA, poly-l-lactic acid; PLMC, poly-lactide-co-trimethylene carbonate; PPy, polypyrrole; PVA, Poly(vinyl alcohol); PVDF, polyvinylidene fluoride; SEM, scanning electron microscope; SLA, stereolithography; SLS, selective laser sintering; SM, shape morphing; SME, shape memory effect; SMP, shape memory polymers; SPIO, superparamagnetic iron oxide; TE, tissue engineering; TGA, thermogravimetric analysis; TPU, thermoplastic polyurethane; UA, urethane acrylate.

* Corresponding author.
E-mail address: mahdi.bodaghi@ntu.ac.uk (M. Bodaghi).

https://doi.org/10.1016/j.apmt.2021.101306
2352-9407/© 2021 Elsevier Ltd. All rights reserved.

1. Introduction

The past two decades have witnessed a growing interest towards the use of stimuli-responsive polymers in high-tech industries and material science technology. Among different stimuli-responsive polymers, magneto- and (or) electro-responsive polymers (termed as MERPs here) are one of the most widely used polymers for achieving particular multi-functional properties. Examples of these multi-functional properties are tunable mechanical properties as well as complex (re-programmable) shape morphing (SM) capabilities at different length scales. One of the remarkable advantages of MERPs is their capability for the remote actuation when being triggered by the external magnetic and electric fields. This feature is a prominent and robust way of actuating objects particularly at small scale. This is because of their ease of use, fast actuation/ response time, compatibility in biological environment which is more feasible than other stimuli such as direct heating [1]. These unique features of MERPs make them a prominent candidate in biomedical engineering (*e.g.,* tissue engineering (TE), drug delivery systems (DDSs)), soft matter engineering (*e.g.,* soft robotics), design of smart structures and systems with dynamic properties [2–4]. Moreover, in the last decade, employing different motifs, *e.g.,* stimuli-responsive polymers such as shape memory polymers (SMPs) [5] as matrix, use of additive manufacturing (AM) techniques [6], and multiple stimuli [7,8], have created advanced MERPs-based applications with the ability to store/recover their temporary/ permanent shape(s) thanks to their shape memory effects (SMEs).

MERPs generally consist of two components including magneto-/ electro-responsive particles (= actuation particles), and non-magnetic/electric polymer matrix. However, in some cases, the polymer matrix has magnetic/ electrical properties itself and the need to add actuation particles becomes unnecessary. Elastomeric polymers (*e.g.,* silicones, acrylate-based polymers, and polyurethanes), SMPs (*e.g.,* polylactic acid (PLA)) and hydrogels are the most widely used polymers as matrix in MERPs. Particularly, if large deformations are needed, soft elastomeric polymers such as Ecoflex™, SYLGARD™, and polydimethylsiloxane (PDMS) are widely used thanks to their biocompatibility, mechanical/ thermal stabilities, and large deformation ability [9]. Common particles used in the fabrication of MERPs are metal particles (cobalt, iron and nickel (Ni)), iron oxides (IOs) (*e.g.,* Fe_2O_3 and Fe_3O_4, cobalt ferrite ($CoFe_2O_4$), nickel ferrite ($NiFe_2O_4$)), neodymium–iron–boron (NdFeB), graphene, carbon black, carbon nanofibers (CNFs), carbon nanotubes (CNTs), and multi-walled carbon nanotubes [10–13]. Such magneto-/ electro-responsive particles are generally responsible for the dynamic behavior of MERPs unless a polymer with SME is used as the matrix.

MERPs are classified into magneto-responsive polymers (MRPs) and electro-responsive polymers (ERPs) given the type of stimulation. As MRPs consist of magnetic particles, they will be activated upon the application of a magnetic field. In preparing MRPs, ferromagnetic particles are homogeneously (or sometimes non-homogeneously) distributed inside a non-magnetically active polymeric material before the solidification process. Furthermore, MRPs with particles aligned in a preferred direction can be produced when a magnetic field is applied during the curing (or solidification) process [14]. Given the hysteresis loop of magnetic particles and their coercivity, ferromagnetic particles are divided into two categories known as soft and hard magnetic particles. Soft magnetic particles such as IOs have low coercivity as compared to hard magnetic particles (*e.g.,* NdFeB) [15]. In soft MRPs, upon applying a magnetic field, magnetic particles are moved due to the dipole-dipole interactions between particles driven by magnetization. Such movement and rearrangement of particles induce internal stresses/friction with matrix which creates internal heat and consequently lead to deformations and property changes. However, in hard MRPs, there is also an internal interaction between particles even under a in the absence of magnetic field in such a way that they can deform under a uniform magnetic field (unlike soft MRPs that can be deformed under magnetic field differences). This is why soft MRPs such as magnetorheological elastomers (MREs) are mainly used in dynamic systems due to their capability in large deformation and mechanical property changes, and hard MRPs are mainly used in shape morphing applications [15–18].

ERPs have emerged as a class of soft multi-functional materials with outstanding electromechanical properties, which draw immense attention among researchers. Based on their transduction mechanisms, ERPs are usually divided into two main categories, namely electronically ERPs and ionically ERPs [19]. ERPs can be used as actuators when an electric field produces mechanical outputs, or as sensors via capacitance changes, or as energy harvesters when ambient mechanical motions produce electrical outputs. One of the most salient features of ERPs is that they can be deformed largely under electric stimuli while they are used as actuators [20].

In this review, we will first refer to the advances in the manufacturing procedures of MERPs, including 3D/ 4D printing, and conventional technologies. In the next step, experimental characterization of MRPs, as well as the electro-mechanical response of ERPs, will be scrutinized. Afterwards, the discussion will be oriented to widespread applications of MERPs in biomedical engineering including TE and DDSs, soft matters (*e.g.,* soft robotics), SM structures and dynamic systems. Finally, we will provide an outlook of future research directions and opportunities.

2. Manufacturing techniques

In general, two methods, namely AM and conventional (*e.g.,* template-based fabrication) techniques, have been employed to fabricate MERP-based polymeric structures. Several factors including the production type (*e.g.,* mass or customized fabrication), the complexity of the structures, dimensions of the specimens, polymer matrix diversity, application of the structure, and the characteristics (*i.e.,* morphological, mechanical, electrical, and magnetic) of the reinforced particles can determine the choice of suitable fabrication method. Although both AM and conventional techniques have several pros and cons, AM techniques have received more academic and industrial attention.

2.1. 3D/4D printing technologies

Additive manufacturing (also known as the 3D printing) is a manufacturing process for the rapid prototyping of 3D objects designed by 3D computer-aided design (CAD) models. The layer-by-layer nature of the 3D printing processes allows for creating porous structures with complex interconnected internal pores. Moreover, the advancement of multi-material 3D printing has provided unparalleled opportunities to arbitrarily deposit multiple materials in the 3D space. By rational design of the microarchitectures of porous structures and precise deposition of the multiple material phases in the space, one can create architected materials with tailor-made properties and functionalities [21–23]. The unique features of the 3D printing structures can be combined with the novel properties of the stimulus-responsive materials to create 4D-printed structures whose properties can dynamically change over time [24,25]. 4D-printed structures, due to their SME, time-dependent properties and the reduction of the need for external power or electro-mechanical systems to induce the property changes (*e.g.,* shape change), offer several advantages in the development of stimuli-responsive materials and structures with shape adaptivity/ multi-functionality [26,27]. Besides, 3D/4D printing techniques have several advantages including making complex

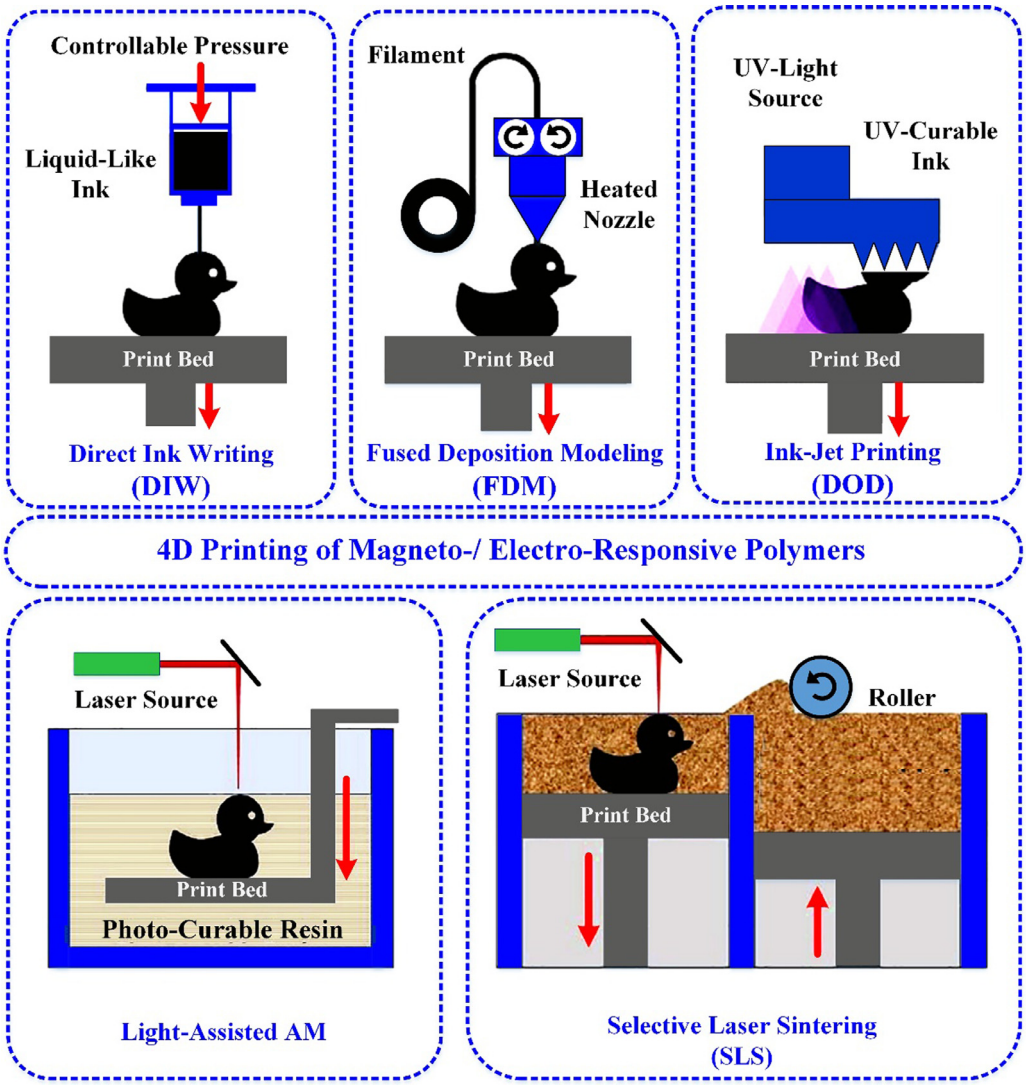

Fig. 1. A schematic summary of the 3D printing techniques used for the development of MERPs. The 3D printing illustrative sub-figures are adapted from [30].

geometries and easy-to-use products, single-step fabrication process, producing patient-specific biomedical devices, and ease of control [28,29]. Here, our focus is to provide the state-of-the-art 3D/ 4D printing technology used for developing the MERPs. As illustrated in Fig. 1, five different 3D printing techniques have been used for the development of the MERPs, namely direct ink writing (DIW), inkjet or drop on demand (DOD), fused deposition modeling (FDM), light-assisted AM and selective laser sintering (SLS).

2.1.1. DIW

DIW technique refers to a 3D printing method based on the extrusion of a viscous ink through a nozzle under pressure to construct the geometries in a layer-by-layer fashion utilizing a computer-controlled robotic dispenser. DIW is the most widely used 3D printing technique for the development of MERPs, thanks to its simplicity and extreme ability to dispense highly viscous inks. The physical properties such as viscosity and density of the ink can significantly be altered after adding the magneto/ electro-responsive particles such as CNTs and nanoparticles (NPs) of IOs into the non-active-matrix material [16,31,32]. Therefore, investigating the rheological properties of the ink is a key step for a successful DIW 3D printing. As summarized in Fig. 2.a, various rheological properties (*e.g.,* shear-thinning/thixotropy and the viscosity recovery [32]) have to be investigated and optimized for printability and shape fidelity by rotational and oscillatory tests. In addition to the physical properties of the inks, the printing parameters such as print speed, die swelling, extrusion rate and print height need to be optimized for the successful DIW 3D printing [33] (see Fig. 2.b). Examples of the DIW 3D printing technique of MERPs are given in Fig. 2c-e and include; First, DIW 3D printing can be used as a method to encapsulate multiple (active and non-active) materials. This means that the active particles such as CNTs/carbonyl iron powders (CIPs) can be mixed in a matrix such as silicone to develop an active ink, that can later be 3D printed and encapsulated within another non-active material [32]. Second example concerns the application of magnetic domains to adjust the orientation of hard magnetic particles such as NdFeB during the printing processes. This has been done via imposing magnetic field at the nozzle tip [16]. Third example includes a solvent evaporation method that can be used to 3D print MERPs. In this method, after dispensing the ink from the nozzle, UV light were used to evaporate the solvent and to cure the filament [34]. The solvent evaporation rate and diameter shrinkage ratio were the two major features, which needed to be investigated for the successful DIW 3D printing. The popular non-magnetic matrix for the DIW is heat-curable silicone-based elastomers, thanks to their nontoxic, non-flammable, and highly stable properties [16,32,35]. Moreover, hydrogels (*e.g.,* polyethylene glycol (PEG), poly(ethylene glycol) di-

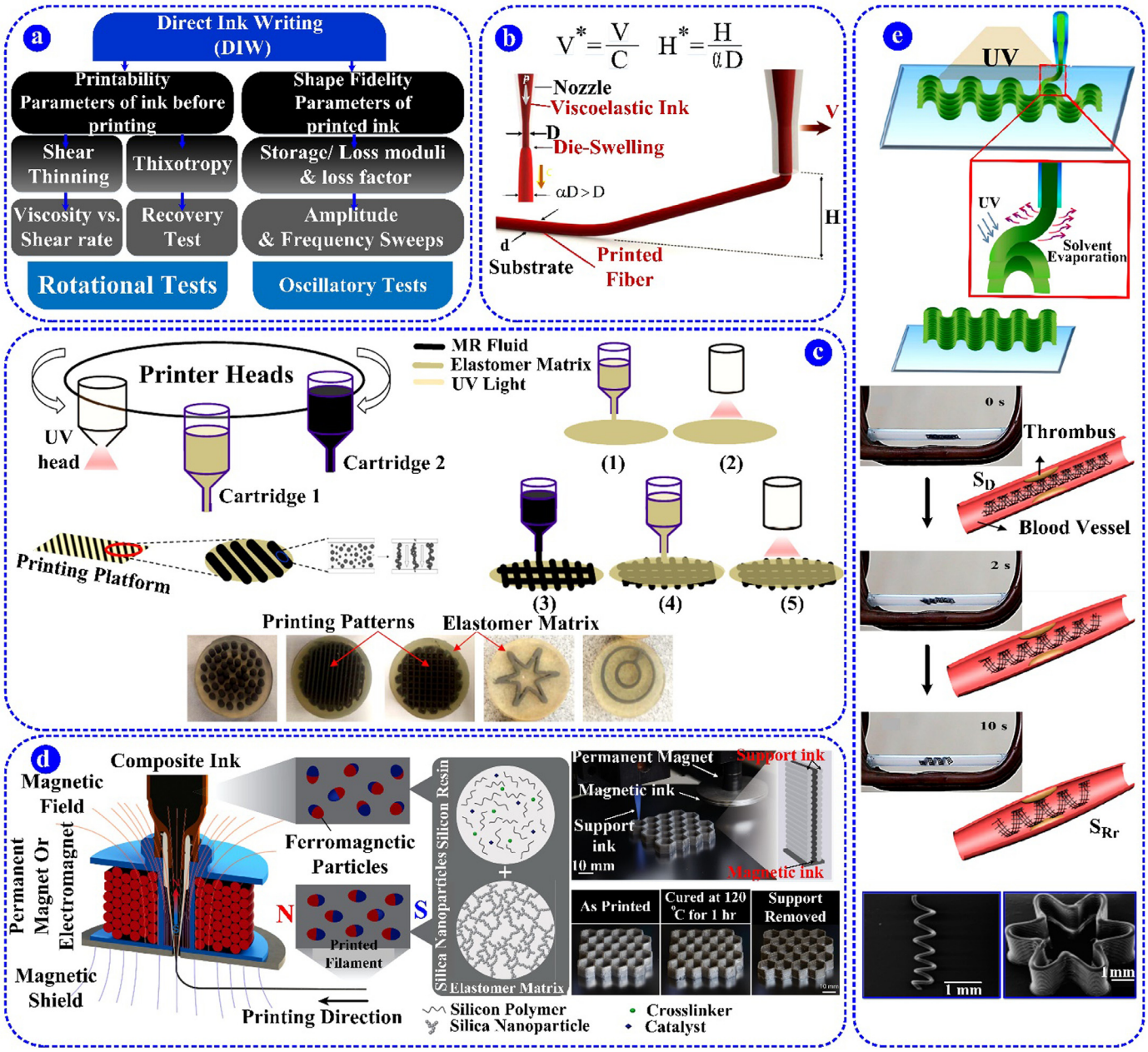

Fig. 2. (a) A summary of the rheological parameters for the development of inks in DIW. (b) Illustration of the optimization of the printing process [33], where V: speed of the nozzle/platform, C: speed of the extruded filament, H: printing height (distance between printing platform and nozzle tip), D: diameter of the extruded filament, α: die swelling ratio, V*: dimensionless print speed and H*: dimensionless print height. (c) Schematic illustration of the 3D printing of hybrid MREs using soft magnetic particles and examples of printed patterns [32]. (d) Schematics of the printing process of magnetic domains using hard magnetic particles, the magnetic domains were reoriented by applying a magnetic field generated by a permanent magnet or an electro-magnet placed around the dispensing nozzle and the example of the developed patterns [16]. (e) Schematic of the DIW 3D printing via solvent evaporation of UV cross-linked PLA-based ink and the 3D-printed structures [34].

acrylate (PEGDA), polyacrylamide (PAAm) and acrylamide (AAm)) involving IOs have also been 3D printed using DIW (*e.g.,* 3D-printed magneto-responsive hydrogels made from PAAm-Carbomer for soft robotics application [36]).

2.1.2. Inkjet

Inkjet technique refers to a 3D printing method based on depositing droplets of inks through a high number of micro-sized nozzles to construct the geometries in a layer-by-layer fashion utilizing, usually, a piezoelectrically controlled dispenser. Inkjet 3D printing is usually suitable for low-viscosity inks and small volumes of ink (~1–100 picoliters) [37]. The physical properties such as viscosity, surface tension, density, and droplet formulation of the inks play a critical role in this technique. Firstly, the ink is expected to be a Newtonian fluid (see Fig. 3.a). Secondly, for a stable droplet formation and a successful 3D printing process, the inks should have a Z-value between 1 and 10 [38,39] (see Fig. 3.b). To print MERPs by this method, the conductive inks, (either electrically or magnetically), are necessary. The ink can be dispensed continuously, *i.e.,* inkjet or DOD fashion (see Fig. 3.c) and can be polymerized either using heat or UV light (Fig. 3.d). Inkjet 3D printing is known for its high printing resolution; however, nozzle clogging is one of the biggest issues in this method. For example, the inkjet 3D printing with magnetic particles of micro-size loaded ink is not easily achievable as micro-sized magnetic particles can easily clog the nozzle. This is one of the reasons that inkjet 3D printing is less

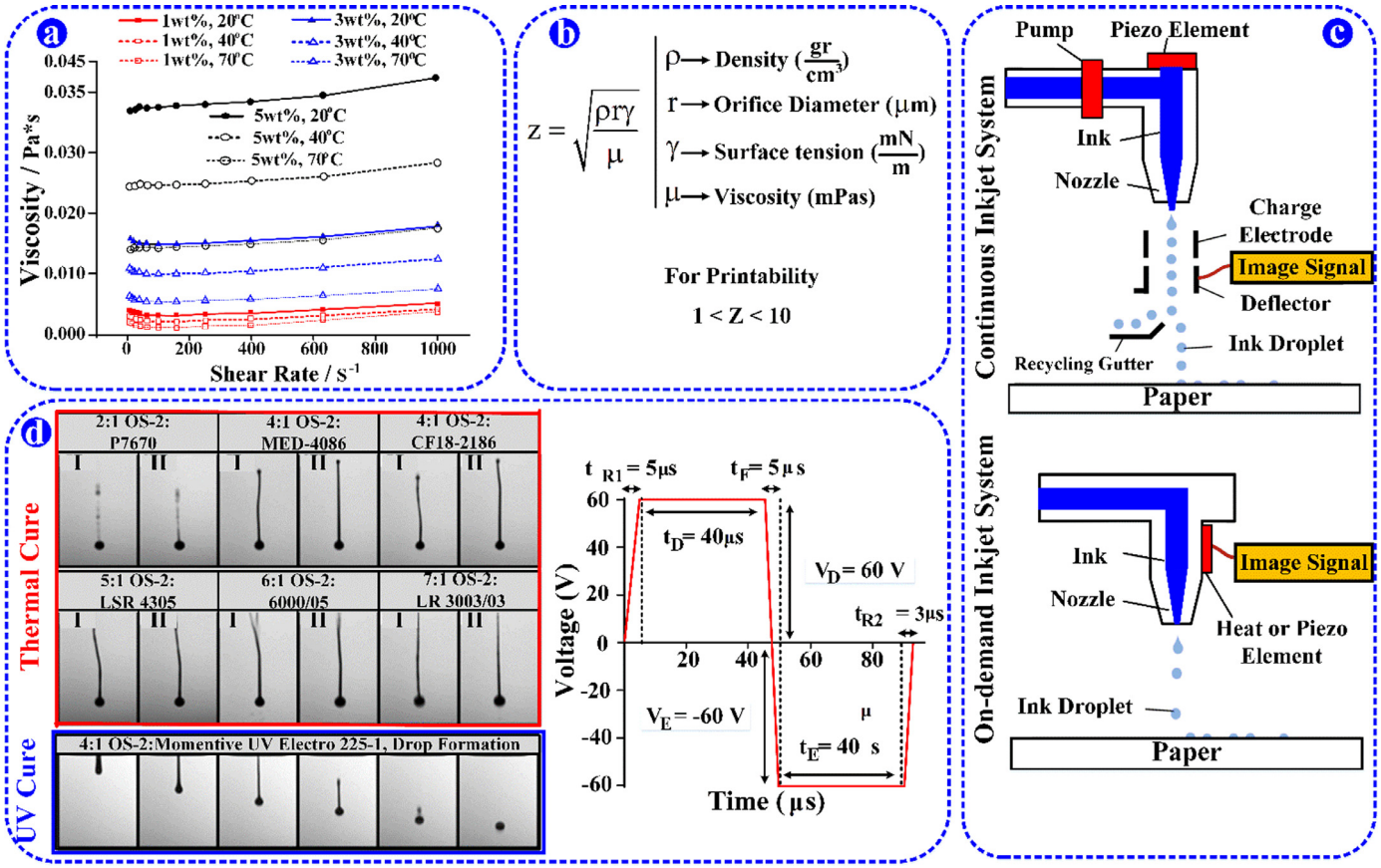

Fig. 3. (a) Example of the physical properties (*e.g.,* viscosity) of the ink in inkjet 3D printing [38]. (b) Important parameters that are necessary to be taken into account for the printability of the ink [38,39]. (c) Schematics showing a continuous inkjet printer and an on-demand inkjet printer [50]. (d) Examples of jetting droplets formed for thermal and UV curable silicone elastomer inks [41].

adopted for MRPs. There are very limited examples for the development of magneto-responsive actuators using inkjet 3D printing. One example is a magneto-responsive fluid encapsulated within a PDMS substrate via the DOD method [40]. On the other hand, there are several studies available for the inkjet 3D printing of ERPs [41–49]. For instance, dielectric elastomer (DE) devices with high performance and throughput (thermal and UV-curable silicone-based DE membranes with a thickness of 2 μm) were successfully 3D printed using a DOD inkjet 3D printing [41]. It should be noted that DEs as a subset of ERPs belong to the class of smart polymers that can produce large strains upon an electric field. Further details about DEs are presented in Section 4.5.2. The extremely high resolution and DOD technique make it always noteworthy to implement the inkjet 3D printing for the development of high-performance MERPs. However, the optimization of the inks to prevent the nozzle clogging is pivotal in this method.

2.1.3. FDM

FDM also known as the fused filament fabrication (FFF) 3D printing technique uses filaments made of thermoplastic polymers, which are melted and extruded through a nozzle to construct the geometries in a layer-by-layer fashion. The well-established materials for FDM 3D printing are PLA, acrylonitrile butadiene styrene (ABS), thermoplastic polyurethane (TPU), polycarbonate (PC), and polyamides/nylons [51–53]. Among them, PLA has extensively been attracted in the field of 3D/ 4D printing of MERPs. To print MERPs-based structures, again, it is necessary to modify the filaments of traditionally available materials by adding active particles such as CNT or silver (Ag) nanowires [54] and NPs of IOs [55]. Fig. 4 illustrates how the modified PLA filament can be achieved for MERPs development via FDM technique. For example, to develop a composite filament of PLA, first, pure PLA can be dissolved in $CHCL_2$ solvent at room temperature, and NPs of Fe_3O_4 can be added into the PLA solution to make the Fe_3O_4/ PLA composite [55]. Thereafter, the raw composite of Fe_3O_4/PLA can be added into the feeder of an extruder for the extrusion of the new composite filament for FDM 3D printing. Various parameters such as concentration of magnetic particles, extrusion temperature, filament diameter, and thermal behaviors of the composite filament (using differential scanning calorimetry (DSC) and thermogravimetric analysis (TGA) techniques) need to be optimized for this purpose [56–58].

2.1.4. Light-assisted AM

Stereolithography (SLA), digital light processing (DLP), and two-photon polymerization (2PP) are three common light-assisted AM techniques to create photo-curable polymers using light [59]. They all have the same mechanisms in a way that take the light-mediated conversion of a liquid resin comprising of monomer or oligomer photopolymers into a solid object (see Fig. 5.a and b). However, there are differences in terms of precision and resolution among these techniques. In the process of photopolymerization, as illustrated in Fig. 5.a, the absorption of photons by the photo initiator initiates the reaction by producing free radicals, which pass within the resin. Then the radical monomers are created, after that the interaction between radical monomers with other monomers produce heavier molecular weight radical polymers. Finally, non-radical polymers are produced given the interaction of radical monomers with each other and the reaction is terminated [60]. For DLP, the relation between UV light dose and curing depth of the resin has to be determined in detail. To print

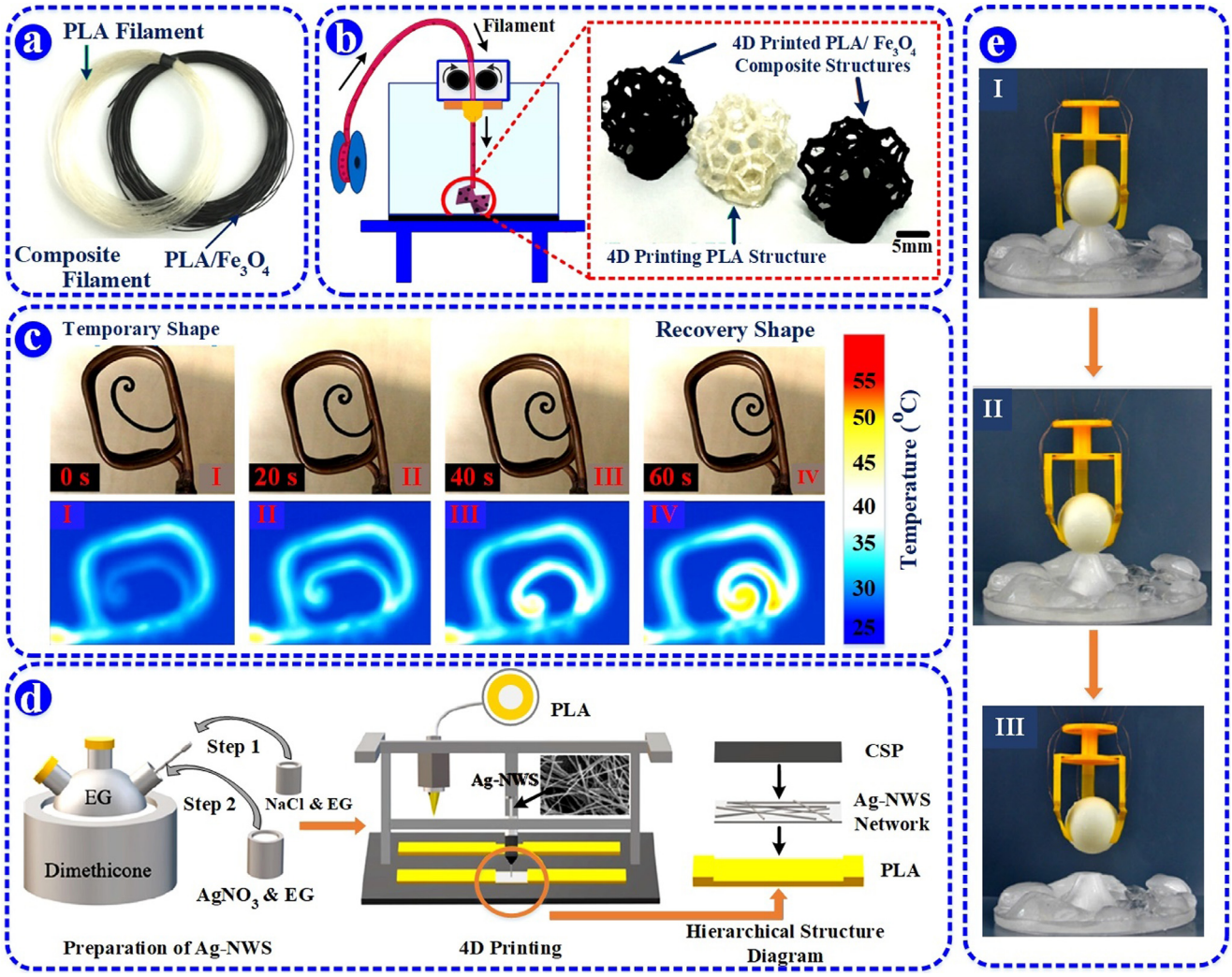

Fig. 4. Examples of the modifications and developments of filaments for 3D/ 4D printing of MERPs using the FDM technique. (a, b and c) FDM for magneto-responsive PLA composite [55]. (d and e) FDM for electro-responsive PLA composite [54].

MERPs by this method, like other methods, the liquid resin must be loaded with magneto-/ electro-responsive particles. Various parameters such as exposer time per projection, magnetic/ electric filler loading percentage, layer thickness, waiting time before exposure, and the effects of the additives should be optimized for the modified resin (*e.g.,* the optimization of the above-mentioned parameters for DLP 3D printing of MRPs [61] or the stability of a magnetic resin [54]). Fig. 5.c and d provide examples of the light-assisted AM techniques of MREs (*e.g.,* using urethane acrylate (UA) resins loaded with NPs of Fe_3O_4 to develop MRPs [62].

2.1.5. SLS

SLS 3D printing technique uses a thin layer of plastic powder, which is selectively melted by a laser to construct the geometries in a layer-by-layer fashion from the powder bed. The SLS technique is newer compared to other 3D printing techniques for the development of MERPs. In this regard, 3D printing of NP of IO functionalized polyamide powders using SLS techniques has been recently reported [63]. Similarly, CNTs loaded polyamide composites have been 3D printed using the SLS [64]. Again, similar to other 3D printing processes, proper adjustment of the material development and printing parameters (*e.g.,* printing height, hatch distance, laser power, and scan speed) are crucial factors for a successful SLS process. From material development viewpoint, the blending of the NPs of IOs or CNTs is shown in Fig. 5.e. The process involves colloid formulation followed by the laser fragmentation of liquids by irradiating of a laser light in a liquid jet setup. Thereafter, the resulted colloids can be mixed with polyamide 12 to develop composite polymer powders for SLS (also known as colloidal or nano-additivation).

In summary, 3D/ 4D printing provides a greater flexibility to develop innovative and intricate structures of MERPs for various applications. DIW is one of the widely adopted 3D printing techniques used so far owing to its facile printing method and compatibility to wide range of materials. However, different types of other 3D/ 4D printing techniques have also been adopted to develop MERPs. Table 1 summarizes studies on the 3D/ 4D printing of MERPs, where the type of materials, stimulus, and 3D printing technique are listed. One of the biggest challenges of the 3D/ 4D printing is the development and characterization of the printing materials as the well-established or commercially available materials cannot directly be used and need to be modified by adding the magneto-/ electro-responsive fillers. The modification of printing materials and optimization of each 3D printing technique is different from each other. The customization of materials and the printing process is inevitable to develop MERPs via 3D/ 4D printing. Therefore, the knowledge of materials science, polymer chemistry, and 3D printing techniques need to emerge for the success-

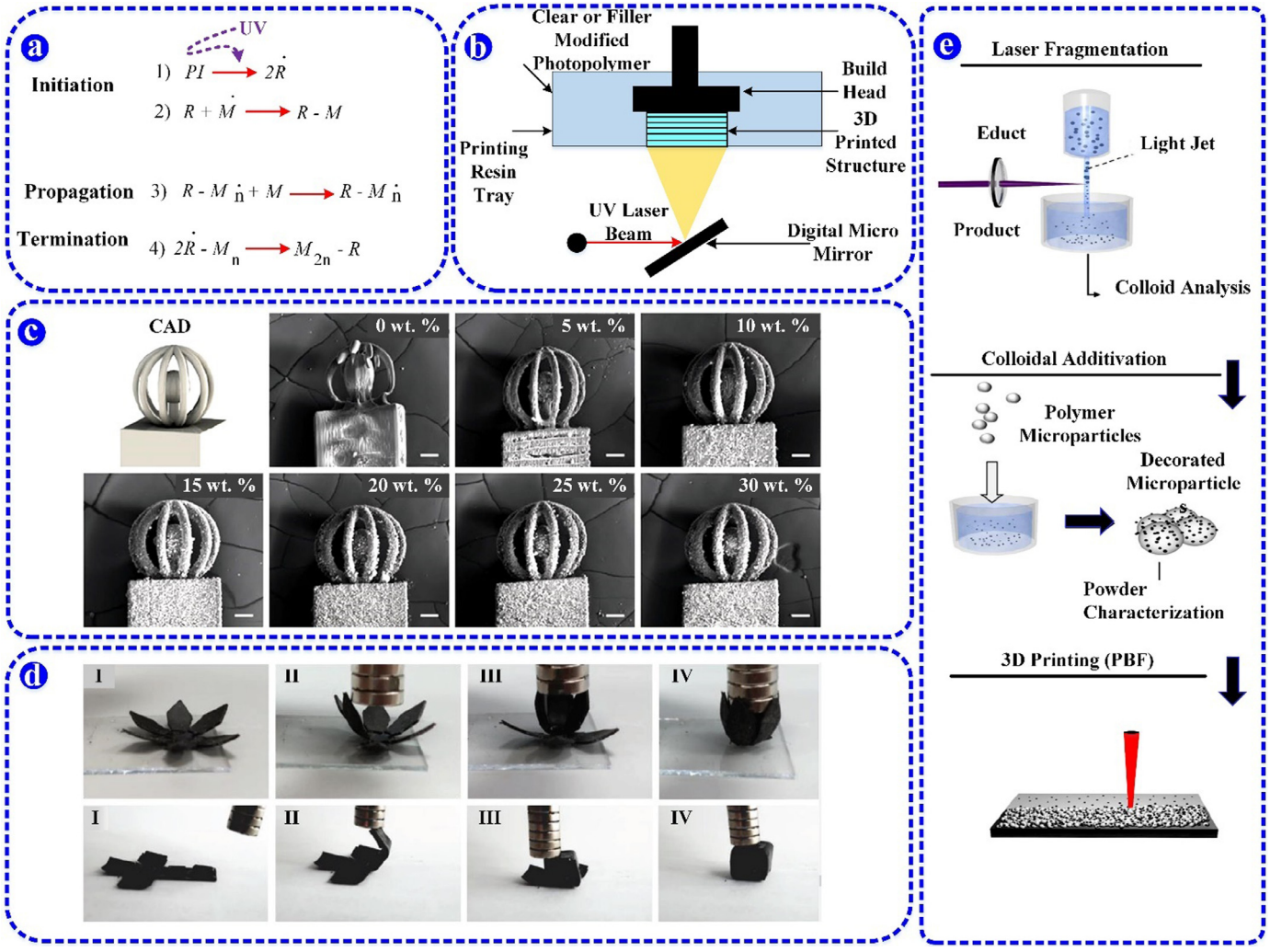

Fig. 5. (a) DLP photopolymerization reaction mechanism [60]. (b) Illustration of DLP 3D printing technique [61]. (c) CAD design of hollow spheres and corresponding 3D-printed samples using magnetic resin via DLP technique [54]. (d) DLP 3D-printed MREs, 3D-printed flower and 2D structure composed of flexible and rigid elements able to create a 3D cube when exposed to a magnetic field [62]. (e) Method to blend NPs of IOs into polyamide for nanocomposite powder development for SLS 3D printing [63].

ful 3D/4D printing of MERPs. In summary, Table 2 provides recommendations for the consideration of printing materials and methods for MERP development via 3D/ 4D printing techniques.

2.2. Conventional techniques

Despite the recent advantages of the 3D/ 4D printing process, conventional fabrication processes such as solution mixing, electrospinning, molding, and thermoforming are still used due to their unique benefits. For example, electro-spinning fabrication method is the key technology to create nano-fibers structures [84]. As mentioned before, various parameters such as complexity of the structures, production type (*e.g.,* mass or customized fabrication), size and the accuracy of the final product, applications, manufacturing lead-time and properties of the samples determine the choice of the fabrication technique. The main drawbacks of some of the 3D/ 4D printing techniques such as FDM are the degradation of drugs in DDSs owing to high temperatures created by the printing techniques, the discontinuity of the process, low material variability, low pressure, and long fabrication process time [84]. These factors cause non-uniform residual stresses, weak interlayer bonding, and micro-voids, which finally may lead to the strength reduction of samples [85]. Fig. 6 shows examples of conventional methods used for the fabrication of MERPs. More information on the fabrication methods, equipment used, and the characteristics of the MERPs can be found in Table 3. In this section, the fabrication of MERPs in four areas including material selection, material preparation, fabrication process, fabrication performance are summarized.

To make MRPs with a thermoplastic matrix, magnetic particles can be added to the matrix at a temperature either higher or lower than its melting temperature. To add the magnetic particles above the melting temperature, it is necessary to melt the polymer and uniformly mix the particles into the polymer matrix by mechanical processes [99]. The micro-compounder [100] and internal mixer [101,102] are standard mechanical devices used for this purpose. Melting temperature, mixing time, and mixing speed are essential factors influencing the uniformity of the mixture. The solution mixing (or solution casting) is another conventional method used to fabricate MRPs with thermoplastic matrices. Although this technique is not cost-effective and environmentally friendly, it has been frequently used in the past [103]. In this method, the polymer is dissolved in a solution and the polymer chains are separated. It should be noted that the solution temperature can be lower than the melting temperature of the polymer to facilitate the separation of the polymer chains. Also, to disperse microparticles (MPs) or NPs into the polymer matrix, a mixing machine (*e.g.,* ultrasonic or stirrer) can be used [93,104]. Dissolution time, as a crucial parameter, depends on the solvent type, polymer type,

Table 1
A summary of studies focusing on the 3D/ 4D printing of MERPs. The table summarizes the printing process, the polymeric base materials, type of the responsive particles and stimuli.

Printing Technique(s)	Base material(s)	Stimuli	Particle type(s)	Category	Refs.
DIW	AAm/PEG	Electric	Lithium Chloride	DE	[65]
	PDMS/AAm	field	Lithium Chloride		[66]
	PLA		Ag	SMP	[67]
	PLMC		CNT		[68]
	UA	Heat/ magnetic field	NdFeB	MRSMP and magnetic soft material	[69]
	PLA/ Benzophenone	Magnetic	Fe_3O_4	SMP	[34]
	PDMS	field	Fe NPs		[70]
	PUA		Modified Alumina Platelets		[71]
	PDMS/SiO_2		NdFeB	MRE	[16]
	Silicone		CIPs		[32,72-74]
	PEGDA		Carbomer	Hydrogel	[36]
FDM	PLA	Magnetic field	CIP	MRP	[75]
	Nafion	Electric field	Functionalized Potassium Hydroxide & Dimethyl Sulfoxide	IPMC	[76]
	Aquivion/Nafion		–		[77]
	PLA		Carbon fiber	SMP	[78]
		Heat/ magnetic field	Fe_2O_3		[55]
		–	Ag nanowires		[54]
DOD	Silicone	Electric field	–	DE	[41]
Light- Assisted AM	UA	Magnetic field	CIPs	MRP	[79]
			Strontium Ferrite/NdFeB		[61]
			Fe_3O_4		[62]
			Modified Alumina Platelets	MRE	[80]
	PEGDA		NPs of IO		[81]
			Fe_2O_3	Permanent magnet	[82]
	Hexanediol Diacrylate		–	Metamaterial	[83]
SLS	Polyamide	–	Fe_2O_3	SMP	[63]

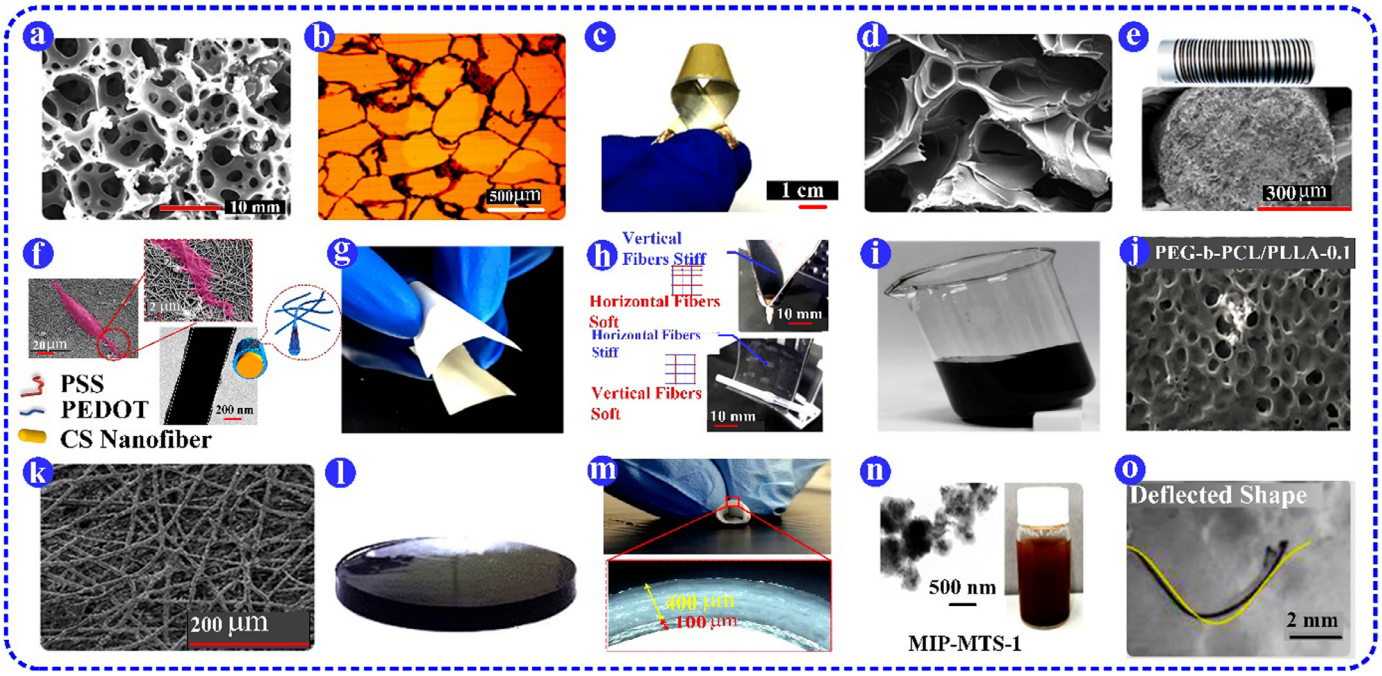

Fig. 6. Examples of various fabrication methods and their ability to create a wide range of dimensional, geometric, mechanical, physical, and biological properties. More details related to the images are provided in Table 3.

weight ratio of the solvent to polymer, temperature, mixer rotational speed, and container dimensions. As an example, increasing the temperature effectively reduces the dissolution time of the polymer [105,106]. Various solvents such as poly(ethylene glycol) (PEG), ethylene glycol(EG), DMF, tetrabutylammonium perchlorate (TBAP), THF, dimethyl sulfoxide (DMSO), and sorbitol have been used in the solution mixing fabrication process [107]. In the selection of the solvent, parameters such as polymer solubility, solvent boiling temperature, polymer morphology, and safety need to be taken into account [108]. After dissolving the polymer, the solution can be poured into a mold, and the solvent can be removed from the polymer matrix using a vacuum oven. Noted that it is also possible to fabricate thin sheets and coat samples by the solution mixing method [109].

Table 2
Categories of the 3D/ 4D printing methods for MERP development and recommendation to select a suitable printing process in terms of printing materials, crucial printing parameters, and pros and cons of the printing process.

Method	Printing material (s)	Crucial print materials parameters	Crucialprinting parameters	Pros and cons of 3D printing method	
				Pros	**Cons**
DIW	Low to high viscous link	Shear-thinning Thixotropy Viscosity recovery Rheology	Dimensional less print speed (V*)	Facile customization Wide range of materials	Low printing resolution
	Heat/ photo-curable	Stability of fillers (dispersion/sedimentation/agglomeration)	Dimensionless print height (H*)	High viscosity ink	Poor layer bonding
	Non-Newtonian fluid	Uniformity of filler distribution-morphology		Micro to nano size active particles	Anisotropy
FDM	Thermoplastic polymer filament (*e.g.,* PLA)	Modification of filaments Concentration of fillers Thermal behavior of modified filament (DSC and TGA) Uniformity of filler distribution-morphology (SEM)*	Extrusion temperature Extrusion diameter	Simple printing process Low cost	*Re*-extrusion of modified filament is needed Better with nanofiller
DOD	Low viscosity link	Density Surface tension Viscosity Rheology	Droplet formulation (Z value) Curing	High print resolution Very low viscosity	Only nanosize filler Nozzle clogging is biggest issue
	Heat/ photo-curable	Stability of fillers (dispersion/sedimentation/agglomeration)			
	Newtonian fluid	Uniformity of filler distribution-morphology			
Light- Assisted AM	Low viscosity ink	Filler loading percentage Effect of additives Rheology	Exposer time	High rresolution	Only photo-curable resin
		Stability of fillers (dispersion/sedimentation/agglomeration)	Layer thickness	Fast print process	Micron-sized particles are difficult to use
	Photo-curable ink only	Uniformity of filler distribution-morphology	Wait before next exposer	High surface finish	
SLS	Thermoplastic polymer powder (*e.g.,* polyamide)	Colloid formulation	Printing height Hatch distance	No support material required	Materials medication and print parameter optimization is the difficult task
		Laser fragmentation of liquid Colloidal additivation	Laser power Scan speed		Expensive machines
		Uniformity of filler distribution-morphology (SEM)	Energy density	Tough and stable materials such as polyamide	Nanofillers only

* Scanning electron microscope (SEM).

The process of solvent evaporation from the polymer matrix is accompanied by residual stress and shrinkage, which cause small dimensional changes in the samples after the solvent evaporation [110]. To overcome such shrinkages, the structure can be placed in a hot press (compression-molded) machine after the evaporation of solvents. By controlling various parameters such as time, temperature, and the press pressure parameters, the dimensions of the films can be adjusted [111,112]. Despite the simplicity of the hot press machine, there is also a possibility to induce micro-cracks and unwanted orientation in the polymer matrix [106]. In addition, methods such as spin coating/ drop-casting and photopatterning can be used to create extremely high-resolution patterns on the surface of the MERPs at small scale [113]. The advantage of these methods is the ability to fabricate a uniform and smooth layer with a predictable and repeatable thickness. To successfully create those small-scale features, several fabrication parameters need to be tuned. For example, in the spin coating method, the adhesion of the solution, the angular velocity of the substrate and the rotation time are among those parameters that have to be adjusted. In the photopatterning method, though, line widths, alignment and defects are some of the important fabrication parameters, which have to be initially determined.

Electro-responsive SMP (ERSMP) and magneto-responsive SMP (MRSMP) as two sub-sets of MERPs can also be fabricated using such conventional techniques [114] or hybrid techniques (*i.e.,* a combination of 3D/ 4D printing and conventional techniques). For example, as mentioned in the FDM 3D printing section, conventional filaments such as PLA can first be melted, then by adding suitable MPs/NPs (*e.g.,* Fe_3O_4), new magneto/ electro-responsive filaments can be fabricated using an extruder machine [78,115–117]. The new magneto/ electro-responsive filaments are used to make MERPs. The stimulation mechanism in MSMPs and ESMPs is based on inductive heating and Joule heating, respectively [13]. Therefore, while fabricating MSMPs or ESMPs composites, parameters such as type, percentage, size, and homogeneous distribution of MPs/NPs in the polymer matrix must be considered. NPs are more recommended as compared to MPs due to their higher surface-to-volume ratio, less adverse effects on mechanical properties, and better interface properties.

To fabricate the ERPs, the synthesis of NPs should be greatly taken into account. For example, synthesis of the 3D-graphene network increases electrical conductivity, decreases threshold percolation, and improves mechanical strength, thermal conductivity, and glass transition temperature [118]. Also, another way to improve the electrical and thermal properties of the polymers is to use hybrid NPs rather than single NPs [119,120]. Although polymers such as Polyaniline (PANi) as a conductive polymer [121] and Poly (3,4-ethylenedioxythiophene) (PEDOT) with piezoelectric properties [84] already have intrinsic electrical properties (without adding MPs/NPs), adding such particles remarkably can improve their electrical properties. The fabrication process of MERPs with a thermoset matrix is somewhat similar to the solution mixing process. Stabilization of the particles in the polymer solution and thermoset polymers (with a long solidification/ curing time) is of great importance due to the possibility of particle sedimentation.

Table 3
An explanatory information to Fig. 6 describing the primary and sub-fabrication processes, equipment, and characteristics of MERP structures.

Labels in Fig. 6	Type	Primary fabrication process	Sub-fabrication process/equipment	Characteristics	Refs
(a)	Magnetic Polymer Foam	Synthesis	• Ultrasonic mixer • Foaming	• Highly Porous • Good Candidates in Microwave Absorption Applications • Good Magnetic Properties • Good Strong Microwave Absorption	[86]
(b)	Electro/ Light-Responsive SMP composite	Hot-press	• Ball milling • Internal mixer	• Segregated Structure	[87]
(c)	Electro-/ Moisture-Responsive SMP	Sandwich layering	• Melting • Mixing • Chemical cross-link • UV-curing	• Quick Reversible Response • Lightweight • Low Cost • Easy Fabrication • Flexible • Highly Sensitive	[88]
(d)	Electro-Responsive Hydrogel Bulk	UV-polymerization	• Freeze dryer • Mixing	• Higher Thermal Stability Than Non-Conductive Hydrogel • The High Impedance at Low Frequencies and Low Impedance at High Frequencies	[89]
(e)	Electro-Responsive Hydrogel Fiber	Microfluidic spinning	• Ultrasonic • Stirrer • UV and free radical polymerization	• Faster Swelling • Faster Electro-Response Rate by The Increase of Graphene Oxide Content • Improve Mechanical Property	[90]
(f)	Conductive and Piezoelectric Nanofibers	Electro-spinning	• Recrystallization	• Nanostructure • Ultrasensitive Piezoelectric Property • High Electrical Conductivity • High Electro-chemical Stability • Low Interfacial Charge Transfer Impedance • Partly Biodegradable	[84]
(g)	Piezoelectric	Electro-spinning	• Stirrer	• Improve the Proliferation, Adhesion, Osteogenesis Differentiation of Bmscs	[91]
(h)	Dielectric and Thermo-Responsive SMP	Stacked layers	• Solution mixing • laser cutter	• Multi-Stable and Reconfigurable Shape-Morphing	[92]
(i)	MR Gels	Synthesis	• Stirrer • Ultrasonic vibrator • Vacuum dryer	• Characterize the Stress-Strain Hysteresis • Phenomenological Modeling	[35]
(j)	Piezoelectric Thin Film Nanocomposite	Solution mixing	• Ultrasonic	• Good Cell Viability • Formation of Calcium Deposits	[93]
(k)	Piezoelectric 3D Fibrous	Electro-spinning	• Solution mixing • Ultrasonic • Coating	• Higher Osteoblast Cell Adhesion and Proliferation • Stimulating the Growth of The Bone Tissue • Biodegradable	[94]
(l)	MREs	Curing	• Mixture • Vacuum chamber • Molding	Very High Increase in Storage Shear Modulus Potential Application in Adaptive Noise and Vibration Control	[95]
(m)	Piezoelectric Nanocomposite Elastomer	Spray deposition machine	• Solution mixing	• Excellent Biocompatibility • Higher Burst Strength • Application in the Field of the Vascular Prosthesis • High Stability • Candidate a Small Vascular Prosthesis.	[96]
(n)	Magneto-Responsive Composite	Coating	• Thermomixer • Homogenizer • Sonicator • Coprecipitation	• Releasing the MTX Drug By The Magnetic Field in Nanoscale	[97]
(o)	MREs	Curing	• Laser spot • Molding • Magnetizing • Sandwiching (forming)	• New Time-Varying Shapes • Significant Potential to Achieve Mechanical Functionalities • Universal Programming Methodology	[98]

Curing the thermoset polymers, similar to the polymerization process, is a chemically one-way process due to the formation of cross-links [122]. Before the curing process, synthesis processes are used to make monomers [123]. Fig. 7 shows examples of chemical reactions to fabricate the MERPs based on the synthesis, curing (by Light [88], heat [124], and additives [125]), and polymerization steps. In fabricating the MERPs with a thermoset matrix, the desired mechanical properties can be controlled by regulating the curing/ synthesizing process (*e.g.,* time-temperature cycle in the curing and post-curing process, the amount of curing agent, and the percentage of additives) [90]. The incomplete curing process during the fabrication, may lead to the release of toxic substances in biological applications [126]. Moreover, a shrinkage and residual stress will still occur during the curing process of samples [127]. In these techniques, the inhomogeneous mixture of particles, their aggregation, and the improper adhesion of particles are issues influencing the interaction of particles and matrix polymer, which can be somehow controlled by optimizing the fabrication parameters or particle surface modification (*e.g.,* improving the chemical and colloidal stability, homogeneous mixture of NPs,

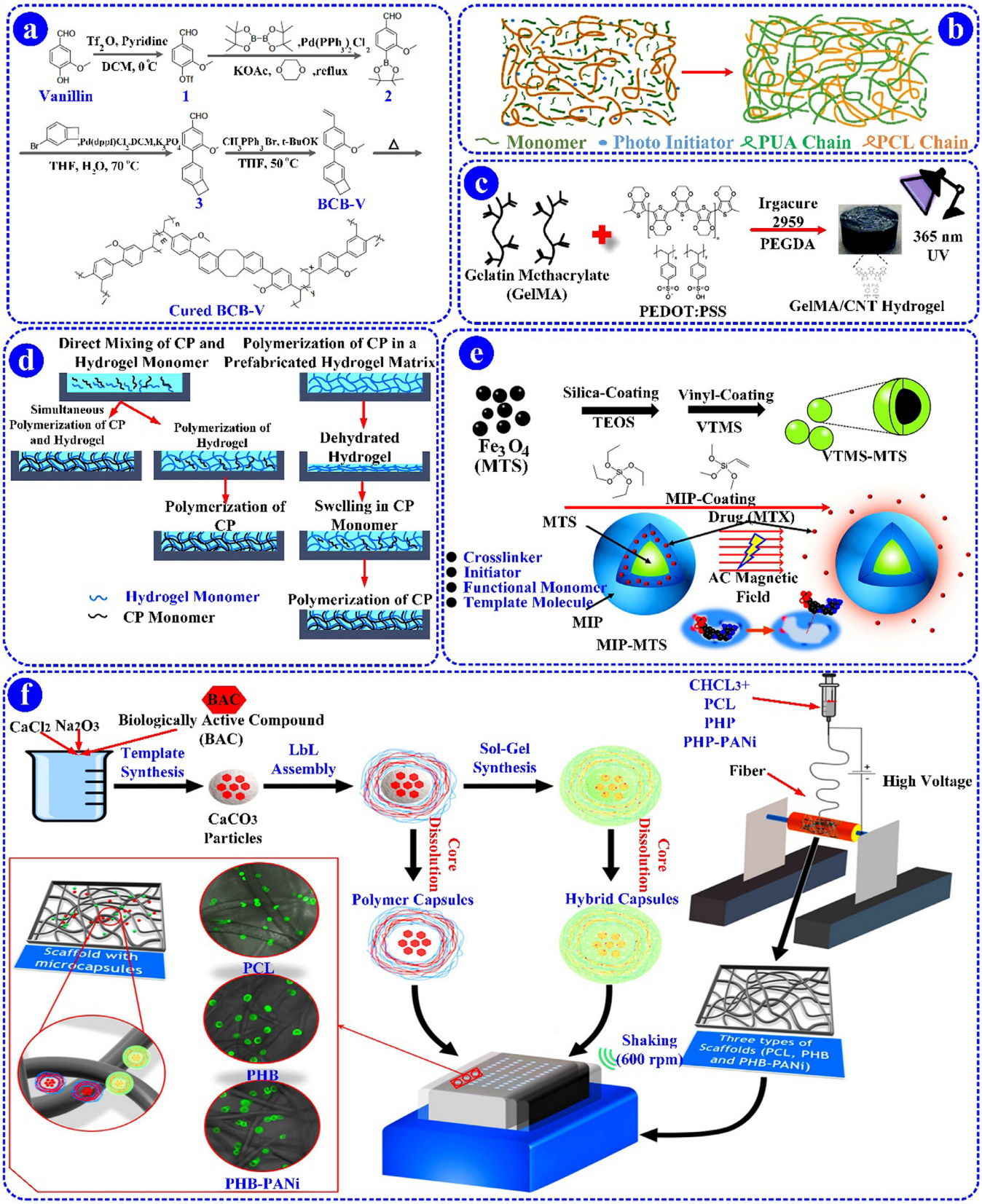

Fig. 7. Some examples of chemical reactions in fabricating MERPs. (a) BCB-V synthesis process in four steps to fabricate a DE. After increasing the temperature, BCB-V becomes a cross-linked network [123]. (b) Schematic of the cross-linking process of poly(urethane acrylate)/ polycaprolactone (PCL) SMP by UV light to fabricate ERPs [88]. (c) Schematic of the polymerization process of a conducting hydrogel [89]. (d) Drawing of a synthesis process of gelatin methacrylate/ CNT conductive hydrogels [130]. (e) Illustration of the preparation of a magneto-responsive drug-release composite system [97]. (f) Schematic of scaffold fabrication processes by the conventional electrospinning setup, synthesis of polymer using layer-by-layer technique and immobilized hybrid capsules [131].

tensile strength, initial permeability, rated current, and magnetic loss) [128,129].

The electro-spinning process can also be used to fabricate MERPs in fibers/ mats shapes at nano- and micro-scales with a diameter/thickness of around 350 nm up to 1 μm [132]. To this end, similar to the solution mixing method, the polymer must be dissolved. The solution is converted into fibers by establishing a high voltage difference between the needle and the collector. Solution flow control, needle diameter, voltage, the distance between needle and collector, type of collector movement, collector speed, and solution additives are important parameters controlling the fabrication process (*e.g.,* fibers diameter, the cross-sectional shape of the fibers, mat morphology, and the mat thickness) [132]. MERP-based samples made by electro-spinning have been widely used in biological applications due to the simplicity of their process, porous structure, and the possibility of adding a wide range of additives [91]. For the bio-related applications, natural polymers such as silk fibroin are suitable candidates for the fabrication of MRPs due to their excellent cell viability and remote stimulation particularly for the bone regeneration [133]. In the electro-spinning method, since the thickness of the fiber is in the micron range, and the bond between the fibers is weak, samples made by this technique do not have remarkable mechanical properties [133]. Nevertheless, the out-off-plane strength of structures fabricated by electrospinning can be increased by applying pressure and heat [134].

Spray-machine deposition can also be used to fabricate samples with axial symmetry and small cross-sections such as piezoelectric vascular grafts [96]. In this method, the diameter of the mandrel is small, and no voltage is used to shape the polymer. Also, several spray-machines in this method can be used simultaneously to spray different types of polymer composites. For this purpose, foaming methods have been used to fabricate MERPs with 3D porous structures. To fabricate the MERP foams, physical or chemical blowing agents can be used. By mixing gasses, such as N_2, CO_2, CH_4, and H_2, in the polymer melt, a porous structure is created. Also, porous structures are created in the polymer matrix by penetrating the gas at a temperature lower than the melting temperature and by controlling the thermodynamic conditions.

3. Experimental characterizations of MERPs

3.1. MRPs

To measure various MR properties of an MRP, either a universal testing setup equipped with a device that can apply a magnetic field or a dynamical mechanical analyzer (DMA) attached to a device capable of applying a magnetic field is used. These rheological properties include measuring pure mechanical moduli (*e.g.,* shear modulus, storage, and loss moduli) and the corresponding magnetic field-dependent moduli. The differences between pure mechanical properties and field-dependent properties will quantify the influences of the magnetic field. For instance, if E_0 is termed as the elastic modulus at the null magnetic field while E_1 is the same at a specified magnetic field, then, the difference between the two moduli, *i.e.,* $(E_1 - E_0)$ will simply give the absolute value of the so-called MR effect. Sometimes, it is convenient to calculate the MR effect in terms of the relative value [73]. It should be mentioned that in this section, we will elaborate on the characterizations of soft MRPs only. However, these experimental techniques can also be applied to hard-magnetic soft MRPs.

The characterization of MRSMPs/ERSMPs and magnetic (or electric) hydrogels, as the two main subsets of MERPs in biomedical applications, have widely been investigated [116,135–139]. Nevertheless, further efforts are needed to elucidate the characterization of such materials, particularly, MRSMPs/ERSMPs. More specifically, in the modeling of MRSMPs/ERSMPs and magnetic (or electric) hydrogels, there are not enough constitutive modeling capturing their SME coupled with stimuli responsiveness. Despite the mentioned advantages of MERPs such as fast response, remote actuation, two-way behavior and SME, the main advantage of employing magnetic and electric responses in hydrogels and SMPs is their ability to make them more biocompatible in biomedical applications. For example, the glass transition temperature of PLA, as a common SMP, is around 60 °C-80 °C, which is larger than body temperature. One promising way to decrease the activation temperature in such SMPs is to use magnetic particles not only to make them remote actuation, and fast, but also to decrease the activation temperature around body temperature [116]. To model this phenomenon, there is only one model developed by the authors [8], which can effectively predict such temperature decreases upon magnetic and electric fields in MRSMPs/ERSMPs. Another interesting characteristic of employing magnetic particles into SMPs and hydrogel matrices is to increase their stiffness. For example, in thermo-responsive SMPs, during the recovery of SMP (*i.e.,* heating step), SMP behaves very softly which limits its ability, particularly, in soft robotic applications. To settle this issue, magnetic particles (or droplets of magnetorheological fluids) can be encapsulated into a matrix to give a purely MRSMPs, which is not sensitive to heat [136]. Similarly, in electro-responsive hydrogels, by spatially controlling the distribution of electric field, more freedoms can be added to the hydrogel in achieving complex SM structures [140]. To do so, the characteristics of the hydrogel including the effect of salt or different electric fields or different polarities should be investigated [140]. The current challenges in the characterization and manufacturing of MRSMPs/ERSMPs and magnetic (or electric) hydrogels are biocompatibility, biodegradability, energy efficiency, ability at small scale and response time [141].

In addition to characterizing the MR properties of MRPs, it is essential to investigate the mechanical responses of MRPs (*e.g.,* stress-strain behavior) under a magneto-mechanically coupled load. For this purpose, several modes of deformations including uniaxial (both compression and tensile) tests, pure shear tests, and equi-biaxial tests are usually tested. Among others, due to their vast applications, the shear and uniaxial compression tests are widely used. All major testing modes used in magneto-mechanical characterizations are schematically illustrated in Fig. 8.a.

3.1.1. Uniaxial compression and tension tests

One of the earliest applications of MRPs was in the area of shock and vibration absorption [18]; hence compression and shear modes of deformations under magneto-mechanically coupled loads have extensively been investigated so far [73]. For compression tests, a traditional testing machine that is usually employed to perform mechanical compression tests can be used. However, it needs to be equipped with a magnetic device using either electromagnets or permanent magnets. For instance, Kallio [142] performed static compression tests on MRPs up to 6.5% strain in which a magnetic flux of 1.0 T was used (see Fig. 8.c(I)). Similarly, Gordaninejad et al. [143] conducted compression tests up to 20% strain on RTV615A (vulcanized at room temperature) and RTV615B silicone elastomers as the matrix materials in which compressive moduli *versus* strains at various magnetic field strengths are reported, which clearly depicts the increase of moduli under an applied magnetic field (see Fig. 8.c(II)). It has been shown that the IP concentrations used in various experiments for MRPs vary ranging from 4.45% to 33% by volume [73].

Similar to compression tests, a significant amount of tensile test data for MRPs are available in the literature. A representative stress-strain data under magneto-mechanically coupled tensile load is given in Fig. 8.d [144,145]. As expected, under a magnetic field, the total stress is increased compared to the stress measured under a pure mechanical load. However, the influence

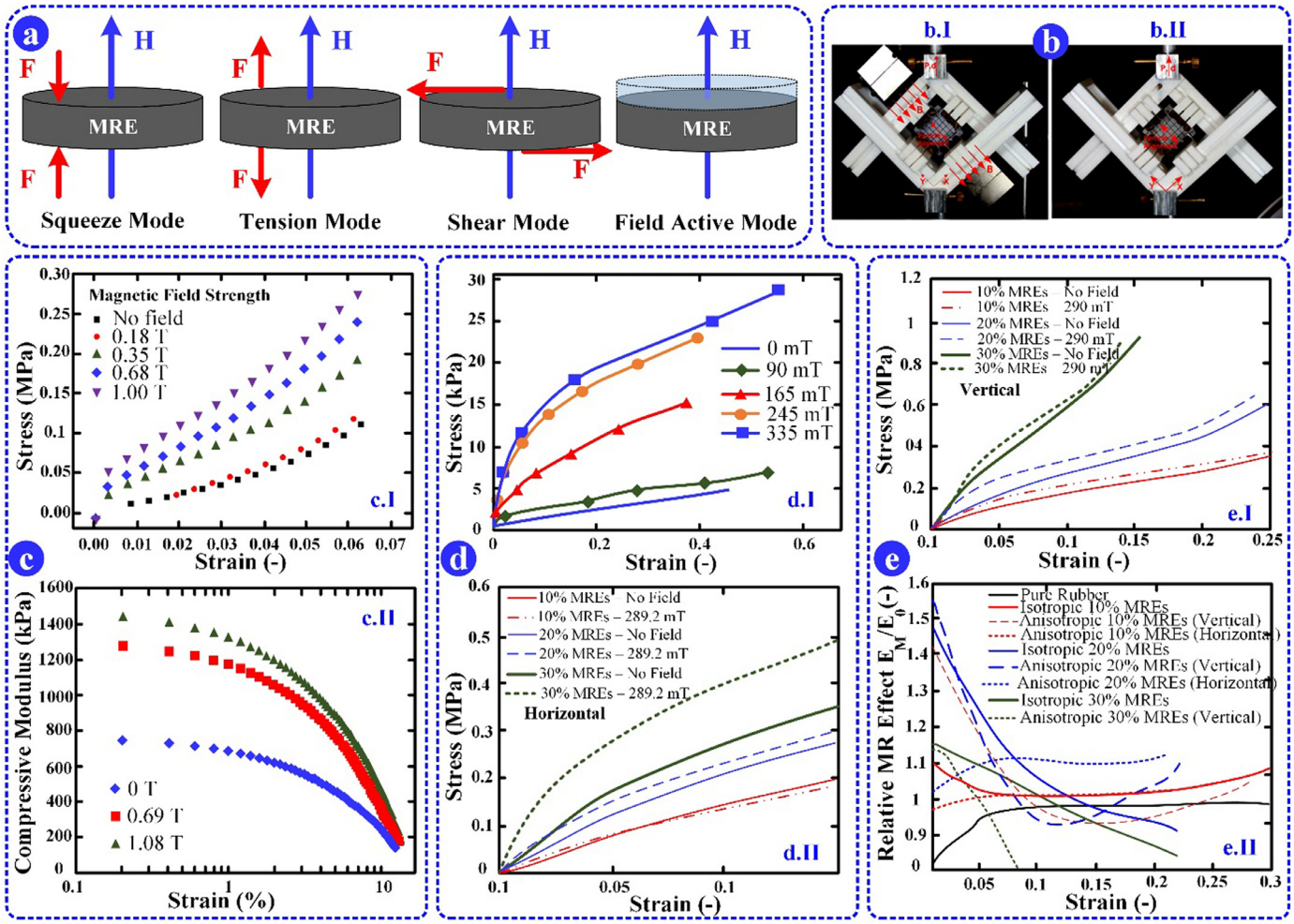

Fig. 8. (a) Experimental samples prepared for magneto-mechanically coupled study in various modes of deformations taken from Bastola and Hossain [73]. (b) a bespoke biaxial test setup made by Harrison and Schubert and Harrison [147]; (I) an anisotropic MRP sample for the pure mechanical test (II) Experimental set up while a magnetic field is applied in a MRP sample in which the field is applied in y-direction parallel to the particle chains of aligned MRPs. (c) Uniaxial compression test results with varying magnetic field as obtained (I) by Kallio [142] and (II) by Gordaninejad et al. [143]. (d) Uniaxial tensile test results under different amounts of magneto-mechanically coupled loads. (I) Stepanov et al. [144] performed tests on isotropic MRPs while (II) Schubert and Harrison [145] used anisotropic MRPs. (e) Pure shear experiments of isotropic and anisotropic magneto-responsive composites conducted by Schubert and Harrison [145]; (I) The influence of magnetic field at the various percentage of fillers, (II) MR effect in both isotropic and anisotropic MRPs.

of the applied magnetic field is much more pronounced at small strains. That is because MRPs are being separated resulting in weak particle-particle interactions at large strains, which will further reduce the magnetic part of the total stress. Similarly, the MR effect decreases rapidly with increasing strain levels in the tensile tests. As Bastola and Hossain [73] systemically analyzed, magneto-mechanical experimental data under tensile loads are available up to 100% strains with varying concentrations of (iron particles) IPs both for isotropic and anisotropic composites. Furthermore, Hernández et al. [146] performed tensile tests on isotropic MRPs with particle contents ranging from 20% to 70% (by wt.%) in which Ecoflex, a widely applied silicone elastomer, was used as the matrix material. To the end, they concluded that with a magnetic flux density of 52 mT, a MRP composite with 63 wt.% of IPs could demonstrate the maximum MR effect of 140%. However, this relative MR effect is still lower compared to the MR effect reported by Stepanov et al. [144].

3.1.2. Simple shear tests

As mentioned in the previous section, MRPs were mainly used in the areas of vibration isolators and shock absorber devices [73]. Therefore, it is imperative to perform experimental studies under magneto-mechanically coupled shear loads. Therefore, both single lap shear and double lap shear tests have been conducted before. Strain levels and strain rates are much lower in the shear mode of deformation, comparing to uniaxial tension/ compression setups. Shear experimental results conducted by Schubert and Harrison [145] provide a comprehensive picture. Therein, it was found that there is a contrary dependency between strain and the MR effect (see Fig. 8.b).

3.1.3. Biaxial tests

As explained in the previous section, sometimes, particles are aligned in a preferred direction during the curing process of MRPs fabrication [14]. It is not always the case that particles are aligned perfectly in a particular direction. Therefore, experimental characterizations should be performed taking into account the directional-dependent mechanical responses. However, experimental study using biaxial setups is not trivial. Hence, very few data are appeared out of biaxial or equi-biaxial tests. For the first time, Schubert and Harrison [147] have successfully performed equi-biaxial tests both on isotropic and anisotropic MRPs under magneto-mechanically coupled loads. For the study, they used commercially available silicone rubber MM 240TV and samples

were extended up to 10% in both directions. For that, they developed a bespoke test rig as shown in Fig. 8.b. Such a rig is more suitable for experimenting anisotropic MRPs in which magnetic fields can be applied in two different directions either along the particle alignments or perpendicular to them. The relative MR effect up to 74% at a magnetic flux density of 67.5 mT was reported for the anisotropic MRE when the applied magnetic field is parallel to the chains of particle alignment. Moreover, Zhou et al. [148] and Gorman et al. [149] used bubble inflation test setups that represent equi-biaxial mode of deformation, to measure the fatigue behavior of MRPs.

Fatigue life is a critical parameter for determining the performance of MRPs as they often experience cyclic loadings in their lifetime. For this reason, several studies have been conducted on MRPs to quantify their fatigue lives not only under purely mechanical loads but also under magneto-mechanical types of loading. For an extensive overview on the topic of MRPs' fatigue behavior, more information can be found elsewhere [73]. As polymers are usually susceptible to temperature fluctuation, the fatigue tests of MRPs have to be conducted in temperature-controlled conditions.

3.2. ERPs

In contrast to the vast efforts of synthesizing novel ERP materials, extensive experimental investigations consisting of all major characterization techniques are scarcely available in the literature. ERPs are typically viscoelastic materials. Hence, they need to be characterized considering all key techniques suitable for investigating a large deformable viscoelastic material. These procedures include loading-unloading cycling tests at various strain rates, simple and multi-step relaxation tests, creep tests under stress/ force-controlled mechanisms, time-dependent fatigue-fracture tests, quasi-static tests at very slow strain rates. Moreover, the same tests must be reproduced under electro-mechanically coupled loads to understand the influences of electric voltage on the material responses. Pure viscoelastic characterizations of typically used DEs (*e.g.,* VHB, silicones, PU) were extensively conducted before [35,150–153]. In the following sections, some major experimental characterizations will be described, which have been used over the years to understand electro-viscoelastic behavior of ERPs, particularly for use in actuators.

3.2.1. Electro-viscoelastic characterizations

In practical applications, ERP samples are mainly deformed under three basic modes of deformation, *e.g.,* uniaxial tension, equi-biaxial tension, and pure shear. Moreover, in most of cases, polymers are pre-stretched up to 200%−500% to make them thinner enough before applying electric voltages in all of the three deformation modes. For the uniaxial mode, a sample is stretched in one direction (typically this direction is much longer compared to two other directions) and the other two directions are kept free to contract. Some common applications of the uniaxial deformation mode include wearable multi-function textiles such as smart shirts and sensorized sleeves [154]. In contrast, most energy harvesting devices, soft micro-robots, artificially moving fish, micro-pumps, disk drives, and pneumatic valves loudspeakers [155] mimic the so-called equi-biaxial deformation mode in which an ERP expands in two directions and contracts in the third direction in order to maintain the incompressibility characteristics of a polymeric material. Moreover, in some technological applications such as haptic feedback, prosthetics hands, artificial muscles, artificial skins, and soft grippers, ERP materials are pre-stretched using a pure shear mode [154]. In this section, we will briefly outline some of the key electro-viscoelastic experimental characterizations under the three deformation modes.

3.2.1.1. Uniaxial tensile tests. Experimental characterizations of ERPs under electro-mechanically coupled loads are very rare in the literature. Several bottlenecks are responsible for such scarcity of experimental data. In order to obtain reasonable amount of actuation, a high voltage (in the range of 5–10 kV) is required, which needs to be generated using high amplifier machines (*e.g.,* TREK 610E high voltage amplifier from Trek Inc, USA). These are costly and complicated setups associated with high human risk factors. Moreover, most of the commercially available polymers used as ERPs appearing in several millimeters thickness, which need to be reduced to micrometer scales to induce sufficient amount of actuation strains. It should, however, be noted that pre-stretching also requires a delicate experimental setup, which also reduces the service life of ERPs [156]. In the case of uniaxial tests under electro-mechanical coupled loads, the situation becomes even worse. Typically, for a homogeneous uniaxial geometry, a 10:1(length: width) ratio is maintained. Moreover, a small portion of the width needs to be excluded for the compliant coating, which eventually violates the uniaxial geometrical conditions (all parts should be under electro-mechanical loads). Therefore, so far, there is no ideal test setup for conducting uniaxial tests under electro-mechanically coupled loads.

An efficient test procedure, which is very close to a uniaxial geometry that creates an almost homogeneous strain without pre-stretching the samples has recently been demonstrated [157]. A simple but efficient custom-made holding frame to prepare the samples were developed as shown in Fig. 9.a and b. The framework helps preparing the samples efficiently with minimum disturbances prior to any actual tests. The free length between two clamping plates is 70 mm while a 30 mm coated width is used for applying the voltage. In order to prevent any short-circuiting, a few millimeters (5–10 mm) area is kept uncoated on both sides throughout the entire length of the sample. Such experimental data help validating novel electro-mechanically coupled constitutive models at large strains [158].

3.2.1.2. Pure shear tests. For homogeneous pure shear tests, a sample is prepared in a way that the mechanical loading direction is much smaller than the width direction (Fig. 9.d.I). Hence, this mode of deformation has the advantage of creating a larger ratio of active area (*i.e.,* area with an electrode) to the passive area (*i.e.,* area without an electrode). Despite several efforts in conducting experiments for the pure shear case under mechanical loads, experimental characterizations using electro-mechanically coupled loads are very few in the literature. Moreover, few available tests were performed only on pre-stretched samples. For instance, Chen et al. [159] create pure shear geometry after pre-stretching the sample ($10 \times 160 \times 0.7$ mm^3 in dimensions after pre-stretching) with 100% strain in the lateral direction before clamping it with two pairs of plastic plates, see Fig. 9.c. In pure shear setup, a sample has sufficient space in the lateral direction. Hence, it can be coated with a conductive electrode (*e.g.,* a conductive grease in most cases) with small free areas in both sides to avoid any short-circuiting. It should be noted that the magnitude of pre-strain has a remarkable effect on the stress-strain response and electro-mechanical coupling of ERPs. Afterwards, they conducted standard electro-viscoelastic tests using loading-unloading cycles, single-step relaxation tests, and creep tests, which also are useful in validating electro-viscoelastic models. Note that what Chen et al. [159] did is a modified version of the pure shear test performed by Hossain et al. [160]. There are also some other studies that pure shear geometry with pre-stretched samples was used to predict various instabilities, significantly, observed during the operation of the devices made of ERPs [161–164]. Noteworthy to mention that all mentioned studies used VHB (3 M), one of the most widely used polymers for the electro-mechanical characterisations.

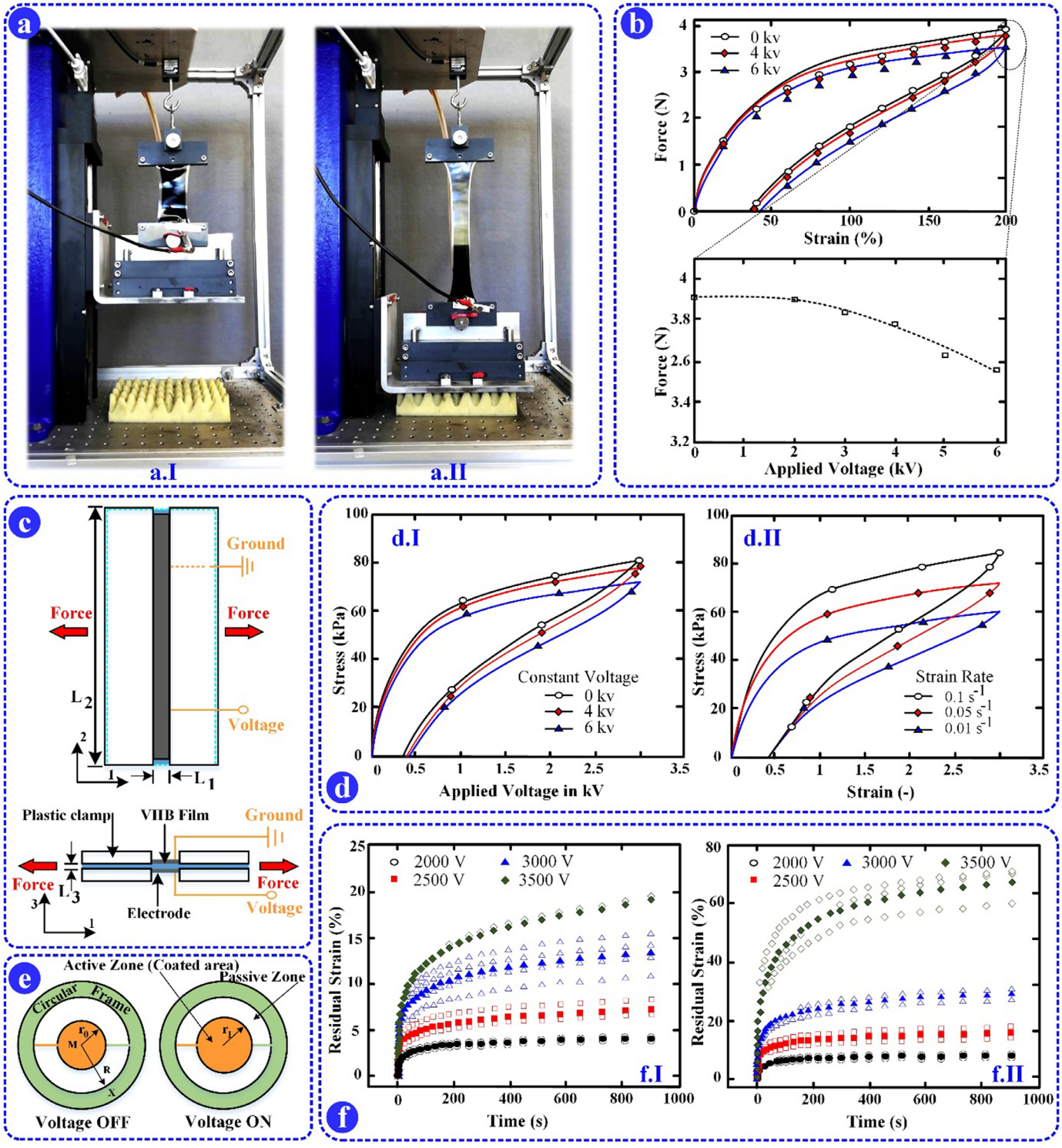

Fig. 9. (a) a bespoke experimental setup for uniaxial tests prepared by Mehnert et al. [157]; (I) an undeformed coated sample (II) Deformed sample under an electro-mechanically load. (b) Stress-strain cycles at different voltages, and the influence of electric voltage on the thickness direction, *i.e.,* release of stress in the vertical direction [157]. (c) a pure shear experimental setup advocated by Chen et al. [165], top view of a coated sample maintaining pure shear geometry and a cross-sectional view of the sample and clamps. (d) Electro-viscoelastic response of VHB 4910 polymer; (I) Stress-strain response at different voltages (fixed strain rate) (II) The same behaviour with different strain rates [165]. (e) a classical setup for conducting equi-biaxial electro-mechanical tests, a centrally coated sample before the application of electrical voltage, and actuated sample surrounded by a passive zone, taken from Wissler and Mazza [166]. (f) Time and voltage-dependent radial strain for (I) a 300% pre-strain (II) a 400% pre-strain [166].

3.2.1.3. Equi-biaxial tests. In contrast to the electro-mechanically coupled experimental characterizations of uniaxial and pure shear types, there have been significant efforts in producing biaxial and equi-biaxial experimentations. The reason is that the preparation of biaxial and equi-biaxial geometries for electro-mechanical tests are comparatively easier in which a larger geometry can be prepared, which helps in obtaining a significant amount of actuation. Moreover, in these settings, thinner samples can be obtained after a sizeable amount of pre-stretching. In addition, large uncoated free areas can be kept to avoid short-circuiting. For actuation purposes, most of the ERP geometries are of very thin sheets that are prone to various kinds of instabilities, *e.g.,* buckling, wrinkling, creasing, pull-in and pull-out instabilities [167,168].

A sizable number of experiential studies dealing with instability analyses of ERPs has been characterized using biaxial and equi-biaxial geometries. For instance, Wissler and Mazza [166] used an equi-biaxially stretched circular actuator to carry out tests characterizing ERPs under loading-unloading cyclic deformations in which electro- and mechanical loads were applied simultaneously. The study revealed that the circular actuator expanded gradually in the radial direction under an applied voltage (Fig. 9.e and f). Furthermore, using the experimental findings, they formulated a large strain model that explored the so-called quasi-linear viscoelastic approach. The model can predict the increasing radial strain as a result of the Maxwell stress, which was originating from an electric voltage. Similarly, Bai et al. [169] performed experiments on a circular DE actuator under a loading-unloading cycle. For that, they used two different electrodes; a conductive hydrogel electrode and a widely-used carbon conductive grease electrode. Moreover, to predict the electric-field induced actuation strains, they used an electro-viscoelastically coupled constitutive model available in the literature [170]. Furthermore, in contrast to the actuator mode of operation, Huang et al. [171] performed experiments on a DE energy generator under an equi-biaxial setting aiming to calculate how much energy was generated in each loading-unloading cycle. Interesting to note here that, similar to the experimental works for the uniaxial and pure shear modes of deformations, all the above-mentioned equi-biaxial studies were conducted only on VHB polymers (3 M).

Despite significant progress in the experimental characterizations of ERPs under pure mechanical and electro-mechanical loads, very few studies are available in which temperature, in addition to the mechanical and electric fields, is considered. For instance, Guo et al. [172] performed thermo-electro-mechanical experiments on a classical acrylic polymer (VHB, 3 M) in which they used uniaxial-type of tests ranging from −20 °C to 80 °C. Mehnert et al. [157,173] also conducted an extensively thermo-electro-viscoelastic study on a VHB polymer. They subsequently developed finite element models accounting for the temperature effects on ERPs. ERP structures experience multiple loading-unloading cycles during their service life, hence fatigue study is crucial for their practical applications. For instance, Fan et al. [174] performed a fatigue study of VHB4910 polymer typically used as ERPs under mechanical loads, while Chen et al. [175] performed a similar experiment under electro-mechanical loading conditions in which high electric voltages were used (5–10 kV).

4. Applications

4.1. Tissue engineering (TE)

TE aims to regenerate tissues or organs more efficiently by adopting approaches that improve the repairment or replacement processes in the damaged tissues. Conventionally, biological grafts have been used for tissue regeneration and healing processes [176]. However, conventional grafts have many drawbacks, such as donor morbidity, potential rejection, inflammation, and prolonged healing time [177]. Recent advances in TE have made it possible to boost the regeneration process by using porous scaffold biomaterials, perfused with nutrients and growth factors to promote cell attachment and migration. Also, the use of electro/ magneto-responsive (polymeric) materials can provide new opportunities to develop smart biomaterials showing certain mechanical or biological cues for tuning the cell mechanobiology.

Natural or synthetic polymeric biomaterials need to posse particular chemical-physical characteristics suitable for TE applications. First and the foremost, they have to be biocompatible that can be integrated into the biological environment without revoking any deleterious immune responses such as inflammation or rejection. Moreover, scaffolds or injected biomaterials may need to gradually be biodegraded at a biodegradation rate comparable to the regeneration growth rate [178]. Also, the by-products of such degradation process should be safe and nontoxic [179]. Finally, those biomaterials have to provide appropriate mechanical properties (*e.g.,* high ductility, tensile and compressive strength, and flexural rigidity).

Among different natural polymers, hydrogel has found its way into the fabrication of 4D-printed biomaterials. This is because hydrogels are biocompatible and can be used for 3D bioprinting of cells making them a great candidate for a broad biomedical applications such as DDSs [180,181] and TE [182]. Hydrogels can also be used as a based material for embedding magneto/electro particles enabling them to exhibit reversible shape-morphing characteristics when triggered by external electric or magnetic stimuli.

The physical stimuli such as electric or magnetic actuation, trigger the mechano-transduction signaling pathways in cells, promoting cell differentiation, proliferation, and immunomodulation [183]. In the engineering of electro-responsive tissues such as cardiac and neural tissues, electro-conductivity is also instrumental. Therefore, most of the endeavors aimed at tuning the electrical properties of the biomaterials (*e.g.,* Polypyrrole (PPy) and PANi as two common ERPs used in TE [184] or embedding various nanoparticles such as CNFs, CNTs, and graphene-based nanomaterials into a polymer as ERPs to make multi-functional biomaterials [184,185]).

Magnetic actuation strategies have been mainly applied in the forms of scaffold-free TE assisted by magnetic particles [186,187] and magneto-responsive biomaterial scaffolds [188–190]. Using magnetic forces as stimuli have several advantages such as improved cell survival and reduced apoptosis by increasing anti-apoptotic agents [191]. Besides, the employment of magnetic particles in conjunction with magnetic actuation offers unique possibilities to remotely control cellular activity. In this section, we summarize the potential applications of MERPs in the engineering of bone, cartilage, cardiac, neural tissues and other organs (see Fig. 10).

4.1.1. Bone tissue engineering

A significant part of research in the applications of magneto-/ electro-responsive biomaterials in TE focuses on bone tissue engineering (BTE). The proper biomaterial scaffolds for BTE need to be biocompatible, bioresorbable (in most cases) and show osteoconductive, or osteoinductive properties to facilitate bone growth [192]. Mineralization and sufficient vascularization are other crucial elements in BTE, particularly for the reconstructions of larger implanted tissues as the core of such scaffolds need to receive enough nutrients and oxygen [193].

Using magnetic-responsive biomaterials can promote osteogenesis gene expression and improve mineralization processes. As an example, Filippi et al. [194] proposed a novel magnetized nanocomposite hydrogel by embedding magnetic particles into PEG-based hydrogel. The scaffold was seeded with stromal vascular fraction cells and was exposed to a static magnetic field, which

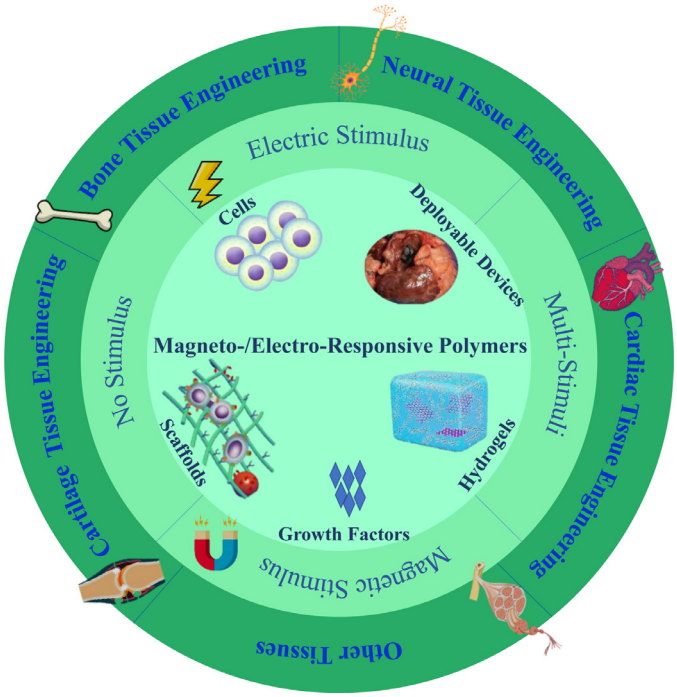

Fig. 10. Schematic illustration of MERPs in TE: process, stimulation methods, and applications.

resulted in a dramatical increase in the expression of osteogenesis-related genes and, consequently, improved mineralization and osteoblastic/ vasculogenic properties.

Furthermore, introducing ECM into the preparation process of magneto-responsive hydrogels may help better mimicking the native microenvironment surrounding the cells, as being demonstrated in past by determining various characteristics of hydrogels such as stiffness, gelatin kinetics, and ultrastructure [195]. As an example, Silva et al. [190] developed a magneto-responsive hydrogel composed of methacrylate chondroitin sulfate (MA-CS) in which MA-CS coated magnetic nanoparticles were covalently linked to the MA-CS matrix. The hydrogel, containing osteogenically differentiated adipose-derived (or tendon-derived) stem cells, resembled the ECM interactions in tendon-to-bone when triggered in the magnetic field. In magnetic scaffolds, given the distribution of magnetic particles, different cell behaviors and regenerations can be achieved. That means, homogenous distribution of magnetic particles accelerates the regeneration process but the new cells may not sufficiently mature; while, inhomogeneous distribution results in less bone formulation but they are relatively mature [196].

Composites of nanohydroxyapatite-coated γ-Fe_2O_3 NPs and Poly(vinyl alcohol) (PVA) results in magneto-responsive hydrogels, which demonstrate outstanding potentials in BTE through promoting the adhesion and proliferation of human osteoblast cells [197]. Implantation of electro-responsive nanofibers and scaffolds can also promote osteogenic differentiation [198] and boost the formation of a mineralized matrix [199]. For example, to improve the inherent osteoinductive, antibacterial and osteoimmunomodulatory properties of collagen scaffolds, bioactive elements possessing the above-mentioned properties can be doped [200]. These strontium and silver collagen scaffolds provided satisfactory osteoimmunomodulatory and antibacterial properties. Bone regeneration is interconnected to other soft tissues (*e.g.,* cartilage, muscles, nerves, and vessels). It is, therefore, crucial to comprehensively consider the key regeneration factors necessary for all of these tissues.

4.1.2. Cartilage

While cartilage damages are common among connective tissue diseases, their avascular nature, and complex ECM prevent their regeneration. One type of hydrogels that has shown positive results in the engineering of cartilage is fibrin-agarose hydrogel with the possibility of encapsulating elastic cartilage-derived chondrocytes [201]. Magnetic particles incorporated in the fibrin-agarose hydrogel showed improved biomechanical properties and expressed native cartilage ECM [202] although it did not fully mimic the native soft tissue. This was because the human hyaline chondrocytes did not fulfill the maturation criteria in the biomaterial during the culture time. The gelatin-based magneto-responsive hydrogels actuated non-invasively by magnetic field have also exhibited great potentials as scaffolds for cartilage tissue repair engineering [203].

The pulsed electro-magnetic field's effects on the bone marrow mesenchymal stem cells (BMSCs) demonstrated drastic improvement in the chondrogenic differentiation and proliferation [204]. Another application of magnetic-responsive hydrogels includes stem-cell therapy for cartilage repair. In a recent study, Yang et al. [205] developed a hydrogel with kartogenin-grafted ultrasmall superparamagnetic iron oxide (SPIO) NPs that improved BMSCs differentiation and demonstrated chondroprotective effects.

4.1.3. Cardiac tissue engineering

Cardiac tissue engineering (CTE) aims to design and fabricate structures to replace the injured or missing cardiac tissue, to improve the cell-based therapies for cardiac regeneration, or to regulate cardiovascular homeostasis by mimicking the heart tissue (with its all physiological and mechanical properties). Considering the inherent conductive nature of cardiac tissue, electroresponsiveness and conductivity of the material can play a key role in obtaining good functionality in electrical signal propagation and synchronous contraction [206]. The PPy-PCL platform shows a resistivity similar to those of the cardiac tissues [207]. The cardiomyocytes cultured on this platform showed a faster calcium transient velocity, and more Cx-34 protein present proximate to the cells. PPy in the form of NPs and PPy coated poly (lactic-co-glycolic acid) (PLGA) scaffolds have been used in CTE to enforce cardiogenic differentiation and synchronous beating [208,209]. The incorporation of CNFs in polymers or hydrogels contributed to the enhanced electro-conductivity, improved synchronous heartbeat, and improved cell survival and intercellular transitions (attributed to an increased expression of connexin-43) in the heart tissue [210,211]. For instance, PVA-chitosan-CNF and multi-walled carbon nanotubes-PVA-chitosan increased the adhesion of MSC to the scaffold and its differentiation to the cardiomyocytes and enhanced its intracellular activities (*i.e.,* calcium handling, phosphatase, transcription factor activation, protein kinase expression and activation [212,213]).

The possibility to increase the flexibility of hydrogels makes them an appropriate candidate for *in-vivo* application, particularly when ventricular remodeling occurs, which may lead to congestive heart failure [214]. As an example, Namdari and Etemadi [215] synthesized a magneto-responsive hydrogel by dissolving N-Isopropylacrylamide-based nanogel in NaOH in the presence of curcumin and magnetic particles. The resulting hydrogel showed cardioprotective effects against the doxorubicin-induced cardiac toxicity. Besides, myocardial infarction occurred when a coronary artery was occluded and, consequently, the heart muscle was irreversibly necrosed. In this case, a mechanically suitable and biocompatible patch could help with conveying oxygen and electroreaction to the damaged tissue. As another example, Kapnisi et al. [216] devised an auxetic cardiopatch based on a network of PANi and phytic acid grown on a chitosan surface. The proposed patch mechanically supported the tissue while being conductive. In a very recent study, cardiac H9C2 and primary cardiomyocyte cells

were magnetically labeled and then relocated using magnetophoresis, resulting in biomimetic multi-layer 3D-aligned cell constructs promising for CTE [217].

4.1.4. Nerve tissue engineering

Central nervous system or peripheral nervous system impairments caused by genetic disorders, injuries, infections, or any other possible reasons, directly affect the quality of life of these patients. Restoring a damaged neural tissue is complicated mainly because of its complex physiology and limited regrowth performance [218]. Natural or synthetic polymers have been used in neural engineered scaffolds. In particular, hydrogels, as an alternative to the conventional grafts have been utilized for the nerve conduit, especially for the peripheral nerves such as sciatic, peroneal, or median [219]. As an example, using polymer fibers with encapsulated SPIO NPs, Omidinia-Anarkoli [220] introduced a magneto-responsive injectable hydrogel with unidirectional signal propagation capability and neurite outgrowth. In this so-called Anisogel, aligned PLGA were electro-spun and micro-cut into short fibers, and then the excess of gel was washed away in the distilled water. These short fibers were later added to a hydrogel precursor and then, under a low magnetic field ($\leq$300 mT), the fibers were oriented (see Fig. 11.a). Another recently investigated biomaterial is electro-responsive collagen/ PPy-b-PCL hydrogel, whose rheological properties and cytotoxicity analysis are auspicious for the 3D-printed neural constructs [221].

4.1.5. Other tissues

As mentioned before, the magnetic and/or electric stimuli can provide dynamic microenvironments (*e.g.,* dynamic cell culture) with better cell responses (cell proliferation and differentiation) rather than static cell culture. For example, in muscle tissue engineering, using the combination of poly(vinylidene fluoride) (PVDF) and magneto-responsive $CoFe_2O_4$ NPs, cell proliferation and differentiation (C2C12 myoblast cells) were enhanced under the mechanical and electrical stimuli [183] (see Fig. 11.b).

Another way to provide a dynamic cell culture is to use a mechanical stimulation of cells, *i.e.,* mechanical bioreactor [222]. This can be done directly using stimuli-responsive materials such as DEs to induce tension/ compression deformations. This deformation can be controlled in such a way to positively affect the gene transfection performance as well [223,224]. From the mechanobiological perspective, it is important to measure the forces applied to cells from the substrates/scaffolds. The stimuli-responsive materials in general and MERPs, in particular, can act as a biosensor to determine the applied cell forces. Another application of MRPs in TE is hyperthermia treatment of the tumor under the application of stents. For this application, iron-based magnetic NPs with different concentrations were added to a polypropylene-based polymer to prepare a tissue-like gel and then the performance of the stent (*e.g.,* heating efficiency upon magnetic field) was investigated under an alternating magnetic field [225].

It is worth mentioning that several numerical and computational studies on the function of electro-responsive hydrogels in the engineering of tissues and organs have recently been conducted to facilitate TE [226,227].

4.1.6. MRSMPs in 4D-printed tissue engineered devices

The applications of SMPs in biomedical engineering and regenerative medicine have become recently more common. This is because SMPs can be combined with 3D/ 4D printing technologies making them morphologically controllable and personalized [228]. SMPs can be used in the design and fabrication of various types of biomedical devices such as bone scaffolds [229], stents [230], or occlusion devices [231]. While various stimuli can trigger SMPs, here we focus only on the MRSMPs and ERSMPs. As an example, 4D-printed PLA/ Fe_3O_4 composites with different mass fractions were investigated in terms of shape fixity and recovery ratio [232]. There are several studies on the biomedical application of MRSMPs based on PLA/MPs such as porous bone tissue scaffolds and bone repair tools [55,115,232]. For example, Zhao et al. [55] proposed a personalized tracheal scaffold that recovered its shape under 30 kHz alternating magnetic field (AMF) in 35 s (see Fig. 11.c). Besides, due to the SME, biodegradability, remote controllability, and fast response of MRSMPs, they are also a prominent candidate against congenital heart diseases as occlusion devices. For such applications, a magneto-responsive 4D-printed occluder made of PLA/Fe_3O_4 was fabricated and implemented into male rats with 16 s deployment time [128] (see Fig. 11.d). Other promising applications of SMPs include injectable ultrathin films in which the polymer can be functionalized by SPIO NPs. As an example of this application, a PLGA-based MRSMP nano-sheet with a height of less than a micrometer was proposed as a possible material for TE and delivery systems (see Fig. 11.e) [233].

4.2. Drug delivery systems (DDSs)

Advance in medicine demonstrates an extensive demand to improve the administration of drug efficacy and safety [235]. Traditional drug managements are not essentially effective and suffered from the rapid clearance from the body leading to the high drug dosage and longtime therapeutic periods. Furthermore, they are not reaching the desired efficacies for the adverse side effects and toxicity as a result of off-target therapy [236,237]. In this regard, DDSs have revealed notable potentials in recent years to address these deficiencies [238]. Up to now, an infinite range of innovative materials and methodologies has been produced and are constantly evolving DDSs to efficiently improve drug therapeutics. The ideal DDS would be applied *in-vivo* providing excellent biocompatibility, controllable drug release, effective cellular uptake and precisely targeting the cells that cause disease. As this is challenging to achieve all the above-mentioned factors at a specific DDS, it has continuously led to expanding research area to design a wide range of materials and methods. Stimuli-responsive materials have shown great potentials promising to impart these desirable properties [235,239].

By rapid advances in the field of nanotechnology, various range of nanostructures has been explored such as drug carriers, which their main role is avoiding both high cytotoxicity (*i.e.,* overdose) and ineffective treatment (*i.e.,* under-dose) [240,241]. However, most drug carriers have been afflicted by a low rate of drug release, deficiency of high drug loading, and poor performance [241]. To overcome these limitations, stimuli-responsive materials are very efficient strategies for specific and effective drug delivery applications [241]. The incorporation of NPs into the functional polymers has become one of the most promising strategies that take the advantage of nanomaterials [242]. Mainly, there are two types of stimuli-responsive materials that respond to: I) intrinsic stimuli, such as acidic pH, high redox potential, up-regulated enzymes, and hypoxia, II) external stimuli, including heat, ultrasound, ionic strength, pressure, electric and magnetic fields [243,244]. By utilizing the external physical stimuli, it is possible to remotely control the drug release and diffusion through the reversible changes in the physical and/or chemical properties of the polymers such as microstructures, surface charge, and phase volume [245–247]. That means, the polymer returns to its original state after the removal of the stimuli. Among these, MERPs attract much attention due to their unique properties, which lead to the capabilities of control over the drug release concerning dosage, location, duration, and even timing [241]. Here, we highlight the recent developments of

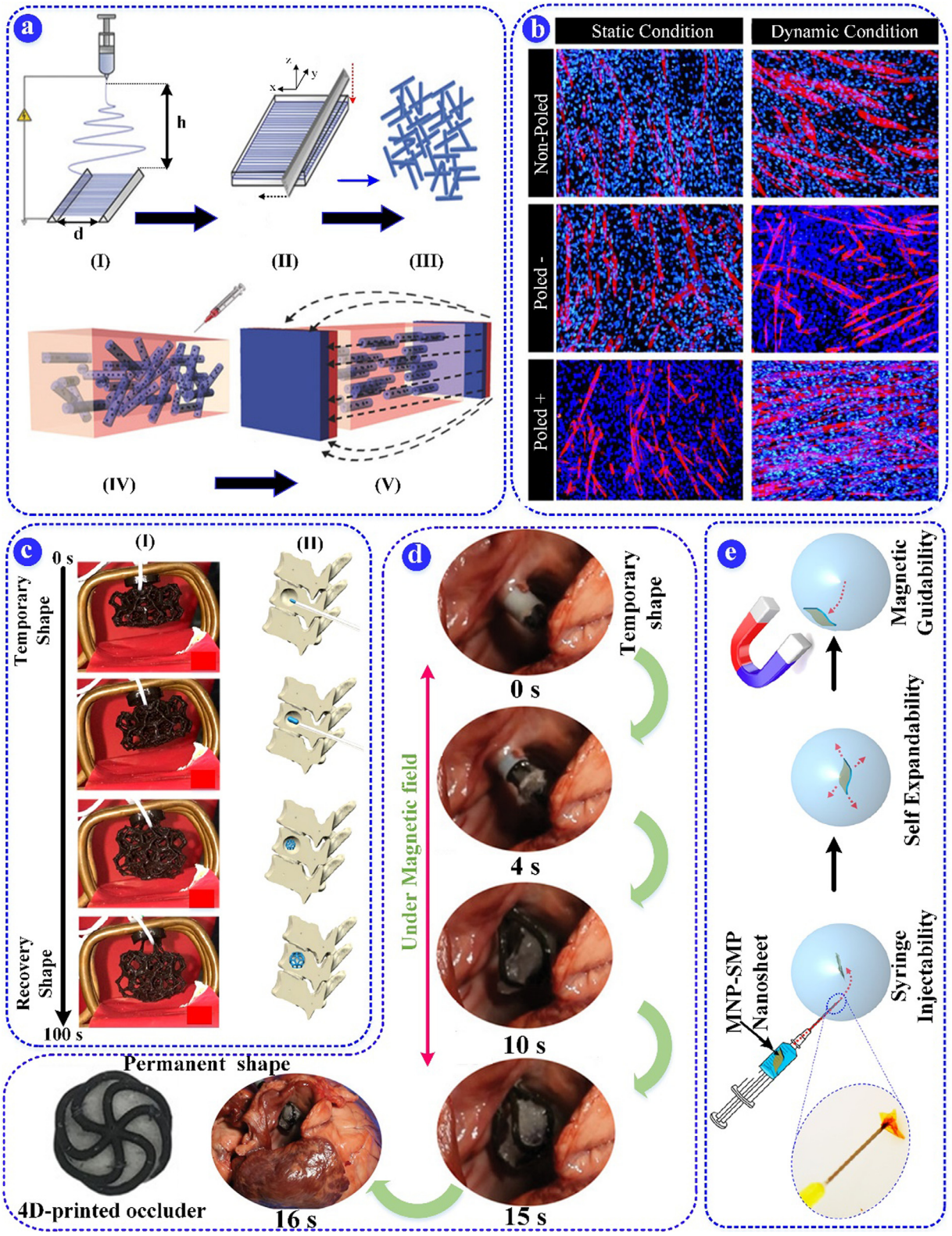

Fig. 11. (a) Schematic illustration of Anisogel Preparation; I) Electro-spinning of aligned fibers II) Rinsing the fibers and micro-cutting III) Adding the short fibers to the hydrogel precursor IV) Exerting magnetic force to obtain Anisogel [220]. (b). Immunofluorescence staining of the C2C12-seeded PVDF/$CoFe_2O_4$ with 10% fetal bovine serum on day 5 under both static and dynamic conditions [183]. Row 1, 2 and 3 show the presence of the C2C12 cells on non-poled, poled – and poled + samples. (c) a 4D-printed magneto-responsive bone scaffold [116]. I) Shape recovery behavior of the 4D-printed composite structure in a magnetic field. (II) a simulation showing the mechanism of the 4D-printed structure as a bone repair tool. (d) The recovery stages of a 4D-printed occluder based on PLA/Fe_3O_4 implemented in a male rat under a magnetic field [234]. (e) Syringe-injectable self-expandable magneto-responsive nanosheet that can be guided by an external magnetic field [233].

various MERPs in DDS with a specific focus on their advances in the control of drug release and targeting of specific locations.

4.2.1. MRPs

There are numerous numbers of magnetic particles among which, IO NPs, including Fe_3O_4 and γ-Fe_2O_3, have been extensively utilized in magneto-responsive DDS due to their easy synthesis, biocompatibility, and low toxicity as they are one of the essential nutrients for mammals and most other life forms [248–250]. In addition, the superparamagnetic properties of iron oxide nanocrystals (*e.g.,* SPIONs), have made them a powerful tool for remotely controlled drug release and rapid response to external magnetic fields [242,251]. Despite all these advantages, IO NPs have a great tendency to self-agglomeration as well as poor loading capacity of drug agents, which limits their efficiency and applications [252]. Therefore, the incorporation of IO NPs into the functional polymeric matrix as smart materials has a significant potential to improve these drawbacks. The surface of functional polymers provides a great opportunity to load or encapsulate the high dosage of drug molecules. One of the key advantages of introducing IO NPs into functional polymers is providing smart polymers, which can recognize and respond to the microenvironment in response to an external magnetic field [253]. This feature is extremely useful in targeting and controlling nanosystems to a specific location.

Targeted and controlled drug release are significantly important features in the field of DDS to regulate drug dosage and location to decrease side effects therapy, and then achieving an efficient treatment [253]. Regarding the magnetic field, there are different mechanisms employed in the MRPs, which lead to the control of drug release. One of the most widely used mechanisms is employing polymers that are sensitive to the variation of temperature. In this mechanism, the AMFs have been used to generate heat [254–256]. AMFs with different frequencies and amplitudes can induce local heats around the magnetic particles due to the quick response of magnetic particles to the variation of magnetic fields [256,257]. The response of thermo-responsive polymers to the generated heat is in the form of the conformational changes (squeezing or expanding) in their matrix, which leads to the drug release [258,259]. This conformational change is due to the displacement of power between hydrophobic and hydrophilic forces in polymers under the influence of temperature changes in aqueous solutions [256]. In general, there are two main mechanisms to tune the rate of drug release in MRPs including changing the direction of magnetic field vector and on-off mechanism of magnetic field (*i.e.,* switching the magnetic field) [253]. As by changing the magnetic direction in MRPs, different properties are achieved, therefore, different drug-release rates are also expected. The second method, seems to be more effective. That is due to that MRPs as stimuli-responsive polymers show quite different behavior under zero magnetic field and a high magnetic field (*i.e.,* on and off). For example, in Fig. 12.d, under zero magnetic field, the drugs have already been encapsulated in the hydrophobic micelles (*i.e.,* magnetic field off) [260]. Once a magnetic field is applied (*i.e.,* magnetic field on), the magnetic particles start moving/aggregating and therefore squeeze the hydrophobic cores, which eventually results in changing the drug-release rate. In this method, relatively low-frequency AMFs is used to stimulate magnetic particles leading to a mechanical change in chitosan hydrogels. Consequently, the retention and release of drug agents can be controlled by tuning external magnetic fields [261].

As mentioned before, an internal heat is generated in MRPs upon a magnetic field due to the rearragment of magnetic particles. Similarly, in MRP-based DDSs, an internal heat is generated by applying an AFM, which results in changing the rate of drug release (see Fig. 12.a, b and c). In such mechanisms, when AMFs are exposed, an internal heat is generated and the polymer becomes hydrophilic, which means losing water and shrinking the structure, as a result, the drug release occurs (see Fig. 12.a) [262]. For example, a PEG-block-PLA (*i.e.,* $PEG_{4.9kD} - PLA_{6.0kD}$) block copolymer incorporating with magnetic particles has exhibited a precisely controlled release of drug cargo under an AMF [263]. In addition, advance in MRPs has provided an attractive opportunity to synchronous and asynchronous multiple deliveries of two or more therapeutic agents with spatially and temporally control. A magneto-responsive hydrogel composed of magnetic IO NPs embedded into the chitosan hydrogel cross-linked with telechelic difunctional poly (ethylene glycol), has been reported that be capable of co-delivery and asynchrony of both doxorubicin and docetaxel for chemotherapy [264].

4.2.2. ERPs

Similar to MRPs, ERPs have attracted much attention are and widely used for spatially and temporally control of drugs in DDSs [265]. Most types of DDSs based on electric sensitivity are implantable and need surgery, which means they are invasive and more harmful than magneto-responsive-based DDSs [265]. There are different types of polymers, which have been employed to respond to an applied electric field. As mentioned previously, some polymers are naturally conductive, such as doped PPy, N-methyl pyrrole, PANi and polytyophene, and other types are neutral polymers that achieve conductivity behaviors by spiking with conductive polymers and nanomaterials such as graphene, CNTs, and metallic nanomaterials [266–269]. The response of electro-responsive polymers to an electric current varies in different mechanisms. One of the popular mechanisms is changing pH due to the electric current, which destroys hydrogen bonding between polymer structures, which leads to the degradation of the polymer matrix and consequently drug release (see Fig. 12.e) [270]. Another mechanism that is broadly used for the control of drug release is the deformation of polymer chains due to stress created by the movement of ionic groups towards cathode or anode under an electric field [267,271]. For example, an implantable electro-responsive hydrogel constructed by PAAm containing nanofibers of PANi loaded with amoxicillin to treat infections so that the antibiotic drug is released under an electric field [272]. Although this device has shown a large potential to control drug release, it should be planted on the target site, that means it needs surgery and is an invasive method. As another example, a transdermal delivery system was developed so that the drug is released from the reservoir under an electric field and increases the rate of permeation through the skin [273].

Conductive transdermal delivery systems are non-invasive and have good control over drug release [274], although they have a lack of on-site delivery benefit so the side effect of off-target delivery is increased and therapy efficiency gets declined [273]. To overcome this issue, an injectable non-invasive electro-/ pH-responsive hydrogel have been developed by mixing chitosan-graft-polyaniline copolymer and oxidized dextran (see Fig. 12) [269]. The release rate of therapeutic agents increases when the smart device is exposed to an applied voltage. This type of mechanism has a great potential for the future of ERPs as DDSs to have effective therapy [269].

4.3. Diagnosis and imaging

Drug delivery imaging is mainly applied to improve drug targeting to pathological sites, which allows easy, non-invasive, and real-time pharmacokinetic and biodistributional analyses [277]. In the last two decades, thanks to the application of stimuli-responsive NPs, diagnosis and real-time imaging have been made possible in conjunction with drug delivery/ release capabilities in the area of drug encapsulation technology. Using these new multi-functional

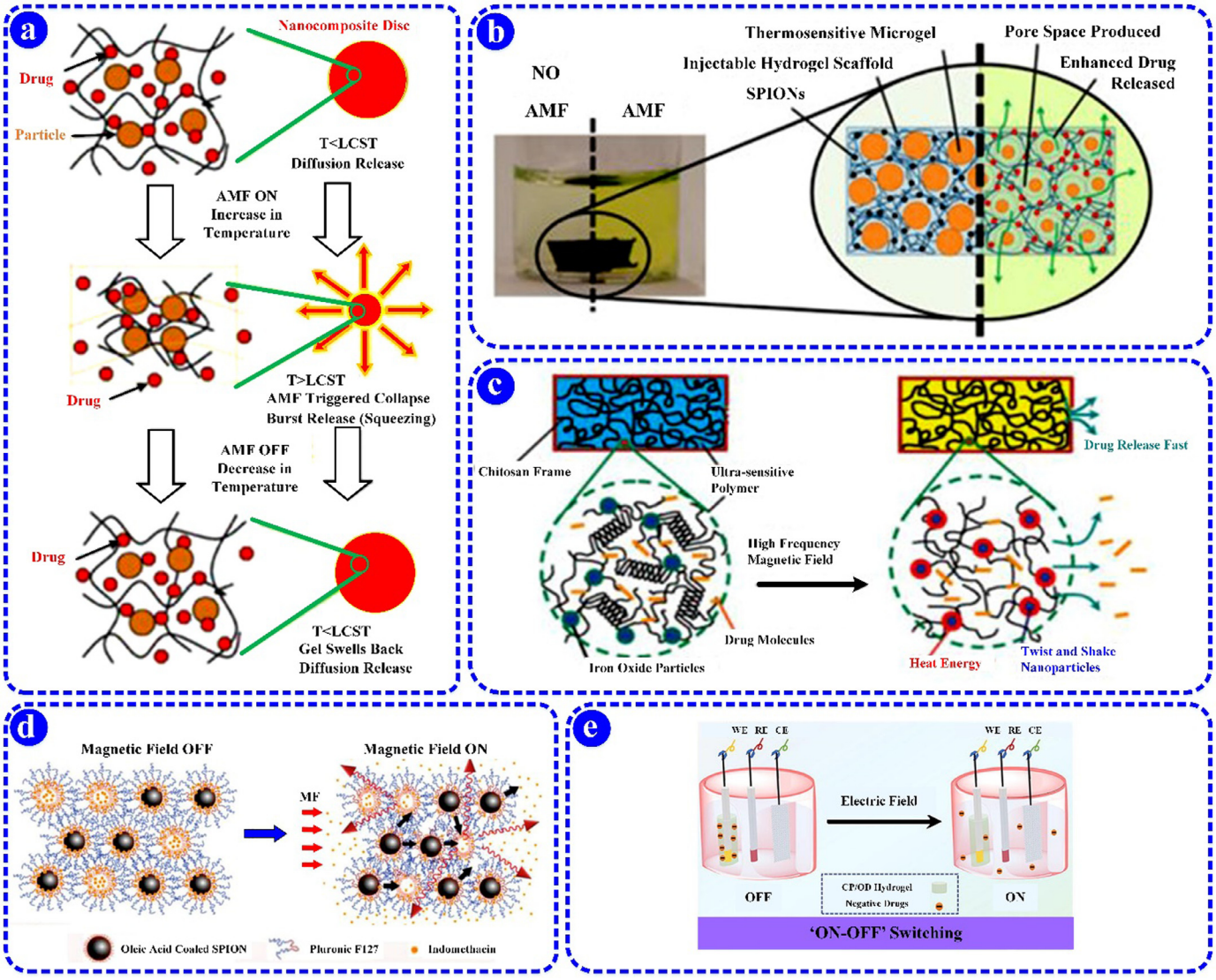

Fig. 12. (a) The schematic of the drug-release of MRPs under an AMF leading to generating an internal heat so that shrinks and squeezes the polymers in such a way that the drug is released [262], (b) Expanding the pore size of a hydrogel scaffold, leading to the increase of drug release [275], (c) Tuning the drug-release based on the heat generated under high-frequency magnetic field [276]. (d) The mechanicsm of drug-release based on the on-off magnetic field, reasulting in the movement of magnetic particles and therefore squeezes the polymer structure [260]. (e) The mechanisms of drug release in ERPs; the electric field changes pH, resulting in the destruction of hydrogen binding of polymers and eventually the drug release is enhanced [269].

medicines, not only the accumulation of therapy at the delivery site is monitored, but also the efficiency of drug release is controlled. In these multi-functional medicines, the core structure has an imaging duty to make sure that the drug has properly targeted, delivered, released, and performed the reaction to the therapy. In this regard, numerous studies on various types of NPs, such as metal oxides, including Fe_3O_4, Fe_2O_3, γ-Fe_2O_3, $CoFe_2O_4$, $NiFe_2O_4$, $MnFe_2O_4$ and CNTs and gold particles, as the core structure of NPs have so far been carried out [278–280]. For example, in liver pathology with magnetic resonance imaging (MRI), tumor sites are characterized by lower absorption of SPIOs in comparison with healthy liver sites due to their low number of macrophages (see Fig. 13.a) [281–283]. In the field of vascular imaging, employing particle sizes of less than 7 nm in diameter brings the ability for the drug to circulate in the vascular compartment for several hours after drug injection. Such NPs can then be used as blood pool agents for endoleaks diagnosis as well as for the evaluation of the relative blood volume in various parts of the body [284,285].

As far as CNT applications in diagnosis are considered, their high surface-area network and their exclusive property of high near-infrared absorbance make them suitable for ultrasensitive photoacoustic imaging [286,287]. In comparison with other reference electrodes, CNT electrodes have resulted in high contrast MRI-tests with almost no distorted images, offering an opportunity to diagnose tumor cells (see Fig. 13.b) [288,289]. It should be mentioned that the imaging quality can be further developed by the utilization of various additives, such as gold and silver NPs [290]. Since these NPs generate thermal energy under various external stimuli, their encapsulation in the stimuli-responsive polymers brings potential application in targeted imaging (MRI contrast and computed tomography contrast), tumor suppression enhancement, controlled release of drugs and time extension of blood circulation, simultaneously [291]. For example, Liu et al. [292] employed magnetic particles in a thermo-responsive polymer, poly(N-isopropylacrylamide), with a glass transition temperature of 32 °C, to develop a multi-functional medicine. As explained in the DDs

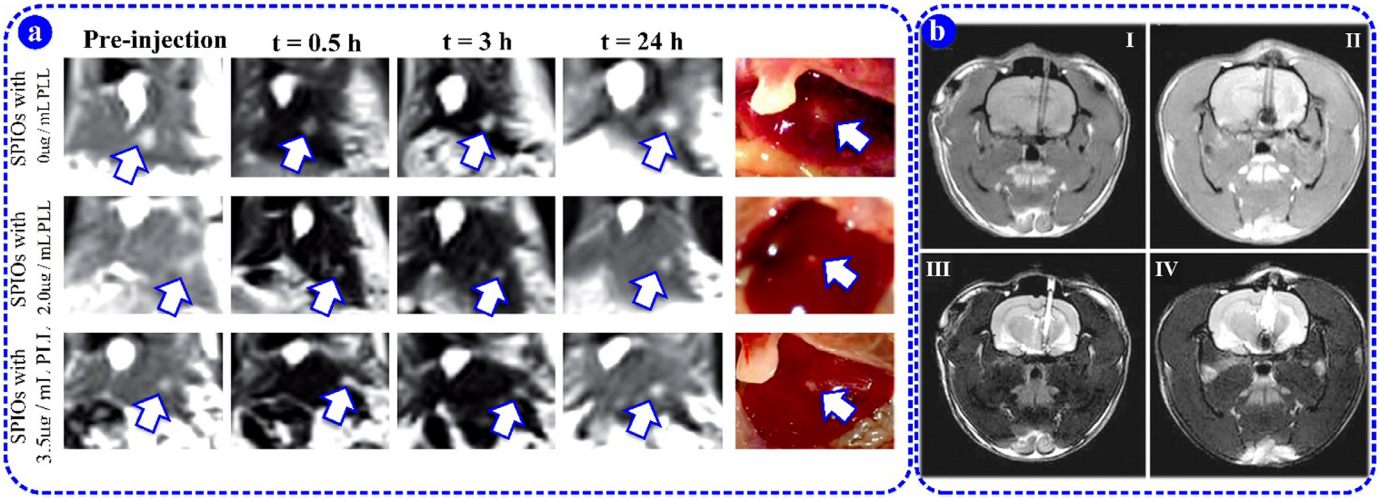

Fig. 13. (a) T2-weighted liver imaging using SPIO nanoclusters as MRI contrast agents, with various particle sizes, 35 nm (0 gml^{-1} of PLL), 80 nm (2.0 gml^{-1} of PLL) and 120 nm (3.5 gml^{-1} of PLL). After 24 h of SPIO injection, the healthy liver sites uptake higher SPIO in comparison with tumour sites (white arrows) [283]. (b) Comparison of T1(I), (II)- and T2 (III), (IV)-weighted MRI results for (I), (III) CNT yarns and (II), (IV) Pt-Ir electrodes implanted into the subthalamic nucleus after 12 weeks [289].

section, when a magnetic field is applied to the polymer, the temperature of the polymer increases, and due to the internally generated heat, the polymeric layer is melted, and therefore, doxorubicin is released. Moreover, as another advantage for magnetic particles, the local heat generated by the core structure has the potential to kill cancer cells. For instance, Jing et al. created a multi-functional medicine using magnetic NPs with a doxorubicin payload for imaging agents as well as therapeutic applications for prostate tumor cells [293]. In the activation of multi-functional drugs with external stimuli, magnetic fields and light emission are the most commonly used stimulation methods for stimuli-responsive polymers. This is while, other methods still face challenges pertaining to thermal control under a narrow range of body functioning temperature [294]. However, economic design, ease of product, biocompatible fabrication of polymeric ligands, and proper core structure employment corresponding to the polymer type are the key factors, which should be considered in drug production. The long-term effects of these smart medicines on organs should also be evaluated to avoid harmful toxic side effects.

4.4. Shape morphing (SM) structures

Shape morphing (SM), shape shifting, reconfigurable, shape changing, and deployable structures refer to transformable structures whose shapes can be transformed between at least two states namely an initial or permanent state and other distinct configurations (*i.e.,* temporary state(s)) when being triggered by external stimuli. SM structures can also be categorized based on their cyclic shape changing behavior or the number of achievable temporary shapes. That means, their shapes may only change in one cycle, *i.e.,* irreversible, so-called as one-way SM structures. They may also save more than one temporary shape, which are referred to as multiple SM structures.

Transferring between multiple shapes means that the Gaussian curvature (defined as the product of the principal curvature at a point of a surface) of SM structures can change. Based on Gauss's theorems Egregium, such morphing is only possible when the deformations are spatially inhomogeneous or non-affine [295,296]. Such spatially inhomogeneous deformation can be generated by magnetic anisotropy (*i.e.,* non-uniform magnetization profile) or electric anisotropy. In deformations such as pure bending, homogenous expansion and contraction so that the Gaussian curvature is not changed, the structures cannot transform between a permanent and temporary shape(s) [296]. Therefore, to create SM structures, non-affine or gradient deformations are required. Residual stress, differential swelling, inhomogeneous stiffness and domain wall motion in MRPs/ERPs are the four main mechanisms to create shape morphing behavior [296]. Among different polymers, hydrogels and SMPs are the two most common polymers showing SM behavior owing to their memory effect, enduring large deformations, and large volume change (in hydrogels) [297,298]. Herein, we specifically focus on magneto-responsive shape morphing (MRSM) and electro-responsive shape morphing (ERSM) structures. In MRSM and ERSM structures there are several important motifs: I) re-programmability (*i.e.,* magnetic or electric memory of the structures can be repeatedly reprogrammed) to achieve numerous SM modes in the structure (without re-producing the structure), II) rationally encoding magnetic (or electric) anisotropy in the structures to achieve complex SM with high spatial resolution, III) energy efficiency (*i.e.,* locking behavior in the absence of external field), IV) fast switching between permanent and temporary shapes (*i.e.,* short response time), V) ease of fabrication and encoding (*e.g.,* single-step process).

4.4.1. MRSM structures

MRSM structures are particularly swift, reversible, safe and can benefit from effective manipulation methods for their SM behaviors (*e.g.,* remote actuation in the enclosed and confined places for biomedical applications) enabling them to undergo complex time-varying morphing shapes at even smaller scales [16,299–301].

One strategy to achieve SM in magneto-responsive materials is to use multi-material (or multi-layer) structures. For example, in multi-layer magneto-responsive hydrogels and elastomers, SM behaviors can induce due to the swelling differences between different layers [302]. The second strategy is to create a local magnetization profile in the MRSM structures. In this technique, time-varying shapes can be achieved by tuning the characteristics of the external magnetic field (*e.g.,* magnitude, direction and spatiotemporal properties of the magnetic field), which make them a promising candidate for creating active materials [301,303].

As mentioned before, the magneto-responsive properties of MRSM structures originate from the magnetic properties of the MPs/NPs distributed within their polymeric matrix. When a magnetic field is applied to such materials, a magnetic-dependent torque will generate up until the magnetization direction of all domains will be along the direction of the applied magnetic field

[304]. The spatial distribution of the magnetization directions, and their magnitude, can thus change the Gaussian curvature of the MRSM structures, which in turn, enables pattern transformation upon external magnetic fields [4].

In general, there exist three strategies to fabricate MRSM structures and to create a corresponding magnetization profile. The first method is template-assisted magnetization. In this method, multi-material (*i.e.,* passive and active components) structures can be fabricated using molding techniques. Examples of passive components are silicone rubbers while the active part can be made from magnetic particles embedded in the silicone. Then, the structures can be sandwiched and deformed between jigs (to fold, bend, or wrap) and by applying a strong magnetic field, magnetization profile can produce [3,305–309]. Using different phases of materials (*i.e.,* active and passive materials) with different geometrical profiles, the magnitude of the magnetization profile can non-uniformly be tuned [301,309]. An example of geometrical changes was the incorporation of auxetic metamaterials in the design of MRSM that could alter the distribution of magnetization profile in individual ligaments, and consequently changed the configuration and mechanical properties of those structures (see Fig. 14.a) [310]. One of the main advantages of this method is the facile encoding of SM [4]. The downside of this method is that only simple SM modes (*i.e.,* bending and folding) can be created [4,311].

The second approach is to use lithographic or 3D printing techniques to enable the physical alignment and fixation of the magnetic particles as well as the adjustment of the local magnetization profiles during the curing processes [1,4,16,312–314]. In this method, the magnetization profile can be locally oriented along the applied magnetic field, during the printing process. This can be done by applying the magnetic field to the dispensing nozzle. In this strategy, unlike the first method, more complex SM structures can be created (*i.e.,* higher programming freedom) [311]. However, a fabrication-dependent permanent magnetization profile will be created that prevents reprogramming after fabricating the structures [4]. Also, the resolution, dispersion of fillers, and the heat during the printing processes are other drawbacks of making these materials particularly in DIW and FDM 3D printing techniques [62]. To settle such issues in 3D printing of MRSM structures, light-assisted AM such as DLP has been utilized as an alternative approach to fabricate isotropic MRPs [62,315]. In this technique, using homogenous dispersion of magnetic particles into the resin and 3D printing them at room temperature, isotropic magnetic structures can be fabricated [62]. More advanced 3D printing techniques, such as voxel-encoding DIW 3D printing have recently been introduced that can program variable magnetic density and direction in such structures [316]. The integration of this method with an evolutionary algorithm, has enabled researchers to create complex SM structures with biomimetic dynamic motions (*e.g.,* crawling motion) of an inchworm [316].

The third method deals with heat-assisted magnetic programming (HAMP) [4,311,317]. In this method, the structures are heated up above the Curie temperature of the MPs. At the temperatures above the Curie temperature, the magnetic particles lose their permanent magnetization [4]. This allows reorienting the magnetization profile when the structure is placed in the magnetic field during the cooling process. It should be noted that in this method, demagnetization can also obtain by heating the samples above the Curie temperature in the absence of a magnetic field. For example, different SM structures including four-segment ring, hemisphere, cubic, and auxetic metamaterial structures with complex pattern transformation have been 3D magnetized and are shown in Fig. 14.b [4]. The heating process in HAMP may change the magnetic properties of embedded magnetic particles or the molecular properties of the base polymers. Therefore, to overcome this issue, other methods have been proposed in which magnetic MPs were encapsulated with oligomeric-PEG with an elastomeric matrix to achieve heat-assisted reprogramming [317].

SM structures can be used in the design of smart materials for biomedical and soft matter engineering applications. As an example, magneto-responsive reconfigurable micro-pillar arrays can add additional (bio-)functionalities (*e.g.,* inducing complex deformations with the coupling of twisting and bending) to the design and fabrication of next-generation biomedical implants [318,319]. In addition, SM structures have been used for the design of smart structures with self-healing properties, which has numerous applications in DDSs and TE scaffolds [320]. For instance, a hydrogel-based construct composed of glycol chitosan and oxidized hyaluronate plus SPIO NPs was recently 3D printed to enable self-healing behavior in magneto-responsive gels in response to magnetic fields [320]. Multi-stimuli ciliary systems is another interesting application of SM structures, which has led to tuning the configuration of cilia using light and magnetic fields in a remotely-controlled multi-stimuli fashion (see Fig. 14.c) [321]. To fabricate a micro-machine that can work in many reversible cycles, specific sequences of magnetic fields with tailored switching fields can be applied to the machine. Toward this aim, by encoding the nano-magnets at small scale, the configurations of arrays of single domain nano-magnets on the machine could be programmed [322].

One of the issues in the design of MRSM structures is incorporating (un-)locking mechanisms in their designs. In most MRSM structures reported in the literature, the temporary shapes cannot be locked and are retrieved quickly once the magnetic field is removed [4,114]. Therefore, a constant magnetic field needs to be present around the structure making it from an energy consumption viewpoint inefficient. In addition, MRSM structures are relatively soft and cannot be applicable to hard materials. Furthermore, one of the weaknesses of the conventional SMPs is their one-way actuation. To address those aforementioned drawbacks, new approaches have been suggested that integrated multi-functional shape manipulations using sequential actuation of such structures in digital logic circuits [3,69]. In this regard, combined soft and hard magnetic particles, including Fe_3O_4 and NdFeB, respectively, were added into an amorphous SMP-based matrix (acrylate-based). The employment of Fe_3O_4 particles induces an internal heat under a high-frequency alternating current applied by a solenoid in a way that can provide (un-)locking mechanisms. NdFeB in contrast provided a magnetization profile for programmable deformation under an actuation under a direct magnetic field by a pair of electro-magnetic coils (see Fig. 15.a) [3]. Such a concept also can be applied using multiple materials (with the same MPs but different base matrices) composed of a magnetic soft material such as an elastomer/NdFeB and a MRSMP including NdFeB particles. Using this approach and employment of magnetic multi-material DIW technique, a multi-modal pop-up structure with sequential deformations has been recently developed (see Fig. 15.b) [69].

4.4.2. ERSM structures

Compared to MRSM structures, there are only a few studies on ERSM ones. As mentioned before, to make reconfigurable SM with different values of negative and positive Gaussian curvatures, spatially electric fields are needed. Such implementation can lead to spatially non-homogeneous deformations. Using this approach, multi-layer electrodes have been proposed to construct ERSM structures [296]. Those multi-layer electrodes contained a set of internal electrode layers with different geometries (or changing the electrode arrangement to achieve spatially-varying electrodes [323]) (see Fig. 15.c). As another approach, concentric rings on the surface of ERPs such as DEs [324], or patterning a dielectric liquid crystal elastomer actuators [325], result in more complex SM. Using multi-polar 3D electric field modulation without pre-programming in a single material, the direction and magnitude

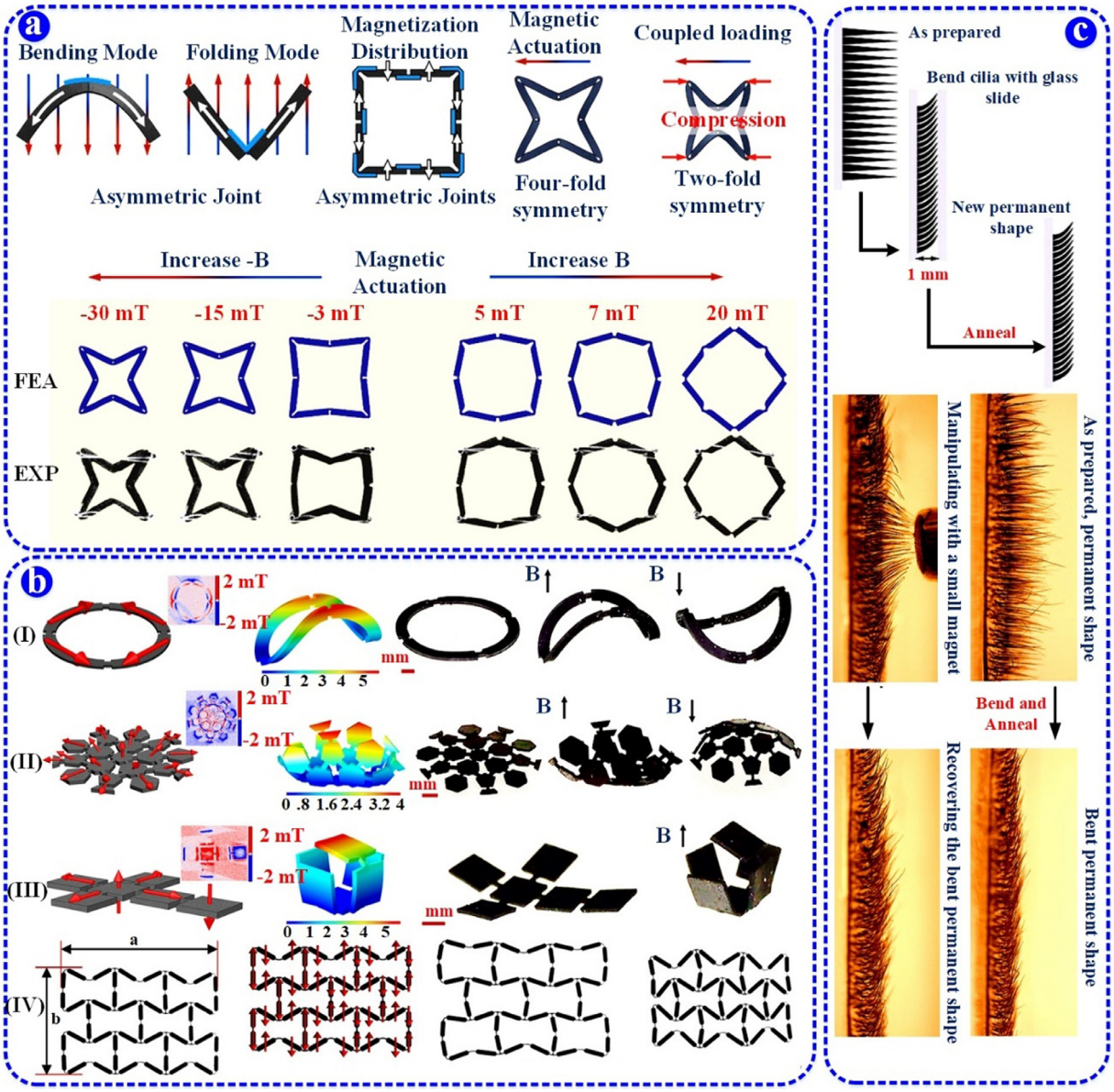

Fig. 14. Applications of MRSM in metamaterials. (a) FE simulation and experiment of the deformation mode of the architected structures under the compression loading at different discrete magnetic field [310]. (b) Reprogrammable 3D reconfigurable structures [4]; I) a four-ligament ring, II) a half-sphere, III) a cubic box and IV) an auxetic metamaterial. (c) a reconfigurable cilia [321] a schematic drawing of the programming of the Irogran magnetic cilia.

of the electric field applied to samples can change. Using such an approach in a single electro-responsive hydrogel, positive and negative bending curvatures have been programmed (see Fig. 15.d). Also, inspired by thermo-responsive SMPs and DEs, multiple distinct configurations have been created. The examples are multilayer of SMP fibers and DEs [92] or solvent casting method [326] or FDM 3D printing of PLA/ CNT filaments [78] in the response of heat and electric fields [326,327].

4.5. Soft robotics

Soft robotics is a growingly emerging paradigm in which soft and flexible materials form the structure of the robots replacing the rigid actuators, sensors, and even central controller units in the conventional robots to deal with delicate objects and media, such as manipulating human and animal organs and tissues [270,320,328,329]. After introducing the McKibben pneumatic artificial muscle in the earlier decades [330], soft robots have drawn the attentions of the researchers recently mainly due to the development of soft polymer materials, such as PDMS, also commercially known as silicone [331], as well as AM [332–334], which make their processing easy. In this section, various state-of-the-art soft robotics mechanisms developed with employing MERPs are presented and categorized by materials and stimuli. The operation principles, manufacturing approaches, and their advantages and drawbacks in terms of resulting deformation and force are discussed, and finally, their future potentials and challenges are foreseen in this section.

4.5.1. MRE soft robots

MREs soft robots are commonly made from dispersing the magnetic particles, such as iron, cobalt, or NdFeB into silicone or rubber-based polymer materials, such as PDMS, which are good electrical insulators [335,336]. The external magnetic field temporarily aligns the randomly oriented particles leading to the stiffness and damping changes [18] and consequently actuations har-

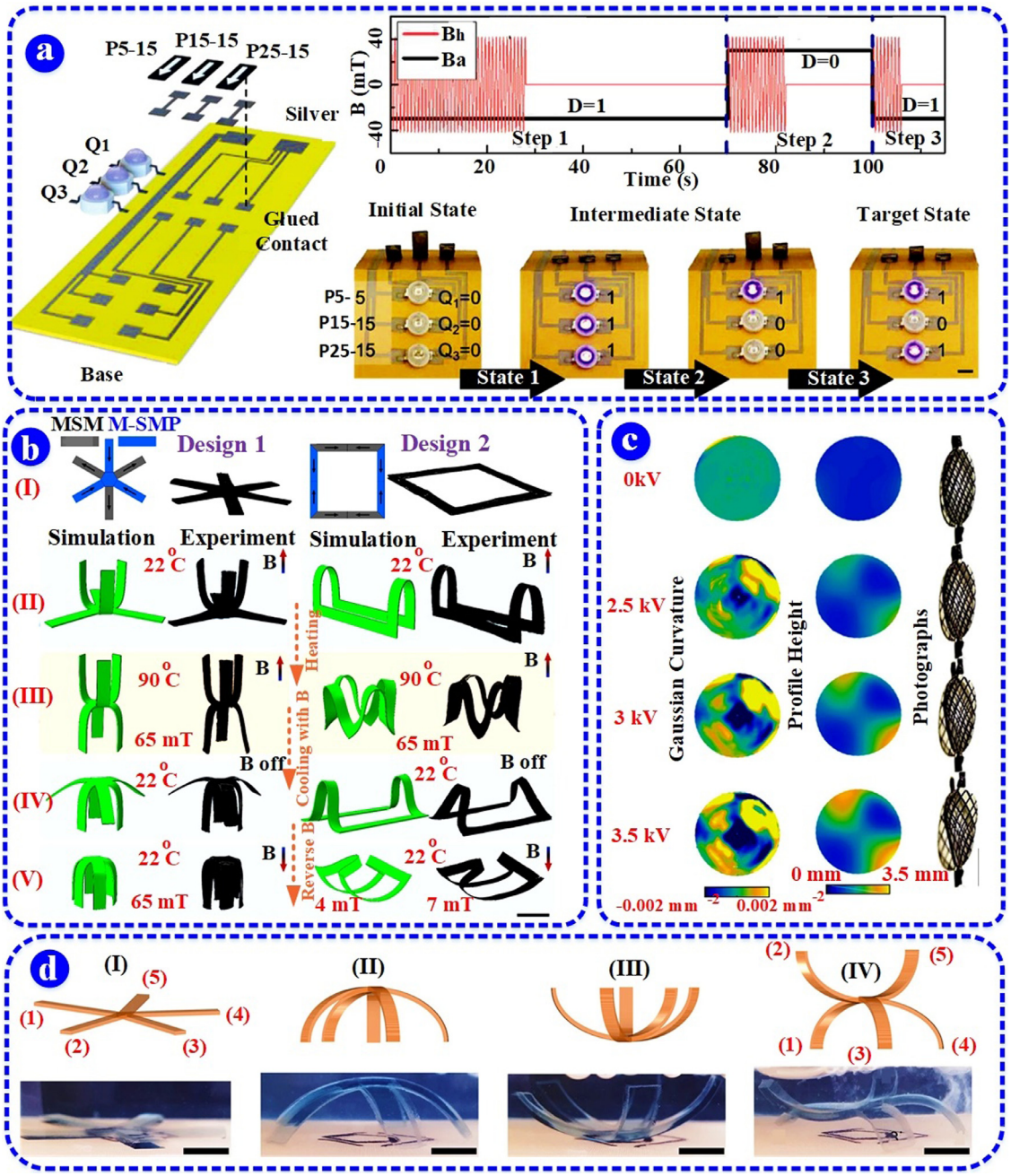

Fig. 15. (a) Application of sequential MRSM with shape locking abilities in digital logic circuits [3]. (b) Computational modelling and experimental results of multi-modal MRSM in a pop-up (design 1) and Asterisk design (design 2) 3D printed by multi-material DIW [69]. (c) ERSM in a DE-based circular sheet; the increasing of negative Gaussian curvature upon increasing applied voltage in a DE [296]. (d) ERSM in electro-responsive hydrogel based on the multipolar spatial electric field to mimic the movement of swollen starfish [140].

nessed (see Fig. 16.a). In other words, the application of the magnetic field increases the stiffness and shear modulus of MREs depending on the size, concentration and magnetic properties of the particles as well as material properties of the elastomer matrix [314]. The studies have revealed that the randomly dispersed magnetic particles experience lower stiffness variation and dielectric response than anisotropic MREs in the presence of a magnetic field [337,338]. Also, further studies have revealed the linear inverse correlation of the particle's concentration with the conformity of MREs soft robot actuators [339]. Therefore, a trade-off between stiffness enhancement and desirable conformity should be achieved in the design of MREs soft robots. The effects of cross-linking degree [340] and the alignment of magnetic particles [341] on the deflection and mechanical properties of MREs actuators are also considerable. A magnetic soft gripper was tested with different magnetic fields as well as magnetic fillers content [340].

Untethered soft robotics have benefited greatly from the advantages of MREs where small-scale soft robots composed of hard magnetic particles embedded in silicone were developed operating under relatively low Reynolds conditions [119,305]. Various fabrications approaches were employed to develop MREs soft robots, including casting [314], spin coating [342], heat- assisted magnetization [4], extrusion [16,343] and voxel-level DOD 3D printing [344]. Soft robotics have benefited from MREs as sensory elements to deal with stress concentration and adhesion issues in deformable bodies too [345].

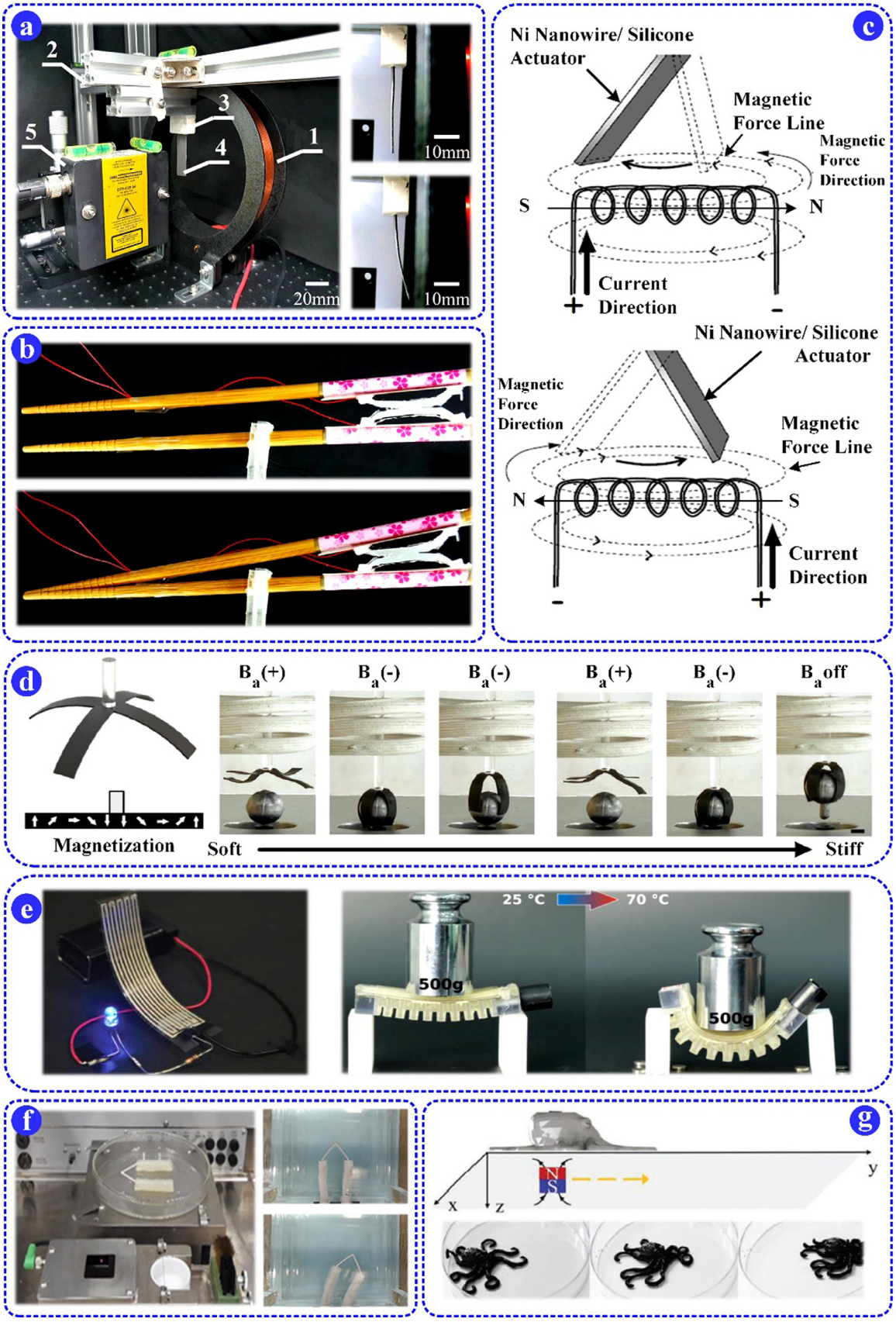

Fig. 16. (a) The MRE soft actuator set up and actuation sequence with application of a magnetic field, 1. Solenoid 2. Structure 3. Sample holder 4. MRE actuator 5. Laser displacement sensor [340]. (b) Chopstick-shape DE soft robot [358]. (c) The EMRE soft actuator under different magnetic fields [376]. (d) a shape locking magnetic SMP with (left) and without (right) locking mechanisms [3]. (e) The printed joule heating circuit of the electric SMP soft gripper (left) and its application in temperature-dependent stiffness variable [389]. (f) 4D-printed electro-responsive hydrogel soft parallel robot and its actuation states [381]. (g) 4D-printed magneto-responsive octopus hydrogel soft robot [36].

4.5.2. DEs soft robots

As mentioned previously, DEs as a subset of ERPs have found significant applications in soft robotics owing to their tremendous configurability, large strains up to 200% [346], and high energy density as against thermo-responsive SMPs [347–350]. The DEs mechanism of operation is following the capacitive principle, based on which the DE material is sandwiched between two flexible electrodes and generates Maxwell electro-static pressure and subsequently motion in response to an electric field [166]. Other featured characteristics of DEs are their agility and light-weight compared to thermo-responsive soft robots, which make them a suitable candidate to mimic artificial muscles [351], crawling [352], walking [353], swimming [349], and flapping [354] soft robots. One drawback of such DEs is their high voltage operation, in kV, which has recently been reduced to 300 V by thinning the membrane close to 3 μm [355].

The spin coating, casting, and spray casting have been practiced as conventional fabrication methods of DEs soft robots due to their efficiency in the production of thin layer, less than 10 μm thickness, silicone membrane [356–358] (see Fig. 16.b). The roll-to-roll processing, including multi-layering and rolling processes, was introduced to develop efficient tubular DEs soft robots with higher compactness and shape deformation [359]. However, those approaches suffered from the production of spatial intricate 3D geometries [360]. The 3D printing technology was introduced to deal with this challenge by developing more customized spatial DEs [41,42,65,361]. It was found that 3D printing has the capability of increasing the actuation force via stacking the DE layers as well as geometric optimizations [362,363].

To improve the performance of DEs in soft robotics, one conventional method is to increase the dielectric constant by including ferro/ piezoelectric ceramics [364] or conductive NPs [365]. Yet, this led to increasing the rigidity of the DEs that consequently resulting in lower longevity and strength. A multi-layer fabrication method was employed to eliminate the rigidity of the crawling DE soft robot [366] while stacking the DEs proved to shorten the response time and lower actuation voltage [360]. A range of folded [296], conned [367], twisted [368], and helical [369] DEs soft robots were developed reporting the increased force and performance compared to plain DEs design. Yet, the main concerns of using DEs in soft robotics are the payload capacity stem from the low mechanical modulus of DEs. Therefore, enhancing approaches such as embedding fibers [370,371] and incorporation of SMPs [372] to adjust the stiffness of the robots at diverse conditions are introduced. Another shortcoming of the DEs soft robots is their short longevity under applied high electric fields. This was recently dealt with the introduction of liquid dielectric embedded in soft membranes known as hydraulically amplified self-healing electro-static soft actuators [373,374]. The principle of hydraulically amplified self-healing electro-static soft actuators is based on the electro-static Maxwell stress, which results in the displacement in response to the applied voltage between the electrodes [375]. Such actuators work up to 1 million cycles with a 15% strain; however, they still require high voltage to operate even with the recent improvements.

4.5.3. Electro-magnetorheological elastomers soft robots

Electro-magnetorheological elastomers (EMREs) have been studied much less than other groups in soft robotics. The soft robot actuators developed based on EMREs principles are generally composites of metal and/or magnetic particles and elastomers with electro-magnetic properties that show actuation in response to electrical stimulus in the presence of the magnetic field. In a pioneering study of such soft robots, a Ni nanowire/ silicone nanocomposite actuator having electro-magnetic properties was tested in response to the magnetic force direction (see Fig. 16.c). The study reported that with increasing the frequency of input voltage for EMREs soft actuators, the strain response decreases with reasonable phase lag [376]. The EMREs soft actuators have shown less hysteresis compared to the ERP soft actuators, however, they were not responding well to the low voltage in high frequencies [376]. The EMREs soft actuators could also be applied in active vibration control of soft robots [377]. However, the inherent time delay in such mechanisms is the main drawback, which should be dealt with. Other groups of EMRE soft robots have been developed based on the electro-rheological fluids in which the magnetic particles are dispersed, and the actuation modulation is controlled through the electric and magnetic fields [378,379]. However, there remain some challenges to use low viscosity electro-rheological fluids to maintain the acceptable speed of soft robots and overall efficiency. Besides, sedimentation and uniform re-dispersion of magnetic particles are other considerable practical issues with EMREs in soft robotic applications.

4.5.4. Magneto-/ electro-responsive shape memory polymers soft robots

The SMPs have been broadly utilized for the fabrication of soft robots. However, the majority of works have been focused on thermo-responsive SMPs [380,381], which are sometimes undesirable due to the difficulty in inducing local controlled deformation in the thermal environment. Therefore, the necessity of SMPs that are responsive to the stimuli with quick and more local controllability is significant. This has led to more recent studies on the development of MRSMPs and ERSMPs in soft robotics and 3D/ 4D printings [16,54] and their constitutive modelling, as well [8].

4.5.4.4. MRSMPs soft robots. Controllability of the both direction and magnitude of a signal as well as its easy penetration in polymers have made magnetic stimulation a favorable choice for polymer and hydrogel-based soft robots [301]. Such soft robots have been benefiting from remote and high bandwidth control abilities as crawling and swimming robots in drug delivery applications [382]. Simultaneous magnetic actuation and photothermal heating have been utilized in a SMP-based magnetically actuated stiffness variable soft robot [382] and a diverse biomedical applications, including catheters [383].

The common mechanism of generating motion using a magnetic field in polymer-based soft robots relies on patterning magnetic fillers on elastomeric substrates. The fillers then align with applying the magnetic field resulting in the generation of different actuation modes such as bending, contraction, elongation, and twist. However, there are some difficulties in the application of magnetic soft robots in terms of the generation of magnetic fields via coils that are mainly bulky and require high power, making them cumbersome in restricted space. The use of micro/ nano-sized magnetic particles in SMPs enabled a new class of reconfigurable soft robots fabricated via different manufacturing methods, including casting, electro-spinning, laser cutting, and 3D printing [34,382,384,385]. The locking mechanism was also introduced in MRSMP soft robots to provide a fast-reversible transformation into the system (Fig. 16.d).

4.5.4.5. ERSMPs soft robots. A common method of developing electro-responsive soft robots made of SMPs is through the electro-thermal or joule heating mechanism. In this approach, the conductive fillers, such as carbon black [386], carbon fiber [387], CNT [68], and antimony-doped tin oxide/TiO_2 (ATO/ TiO_2) [388] are incorporated into SMPs for generating and conducting the required heat for the local deformation control stimulated by an electric current. In other applications of ERSMPs in soft robotics, a stiffness tuneable soft gripper was developed with 3D printing of an electric circuit on a soft actuator made of SMP material [389]. Therefore,

the soft robotic gripper has demonstrated tuneable stiffness at different environmental temperatures enhancing its performance and functionality (see Fig. 16.e).

4.5.5. Magneto-/ electro-responsive hydrogels

As mentioned previously about hydrogels, their vast water content compared to SMPs and reversible shape shifting have received increasing attention in biomedical and soft robotic applications. The main mechanism of harnessing actuation in hydrogel-based soft robots is based on volumetric changes of hydrogels in swelling and un-swelling. There are several approaches of patterning [390], functionally graded cross-linking [232], bi-material [391] and multi-material [392] composites to induce desirable motions, such as bending, morphing, and twisting.

4.5.5.1. Magneto-responsive hydrogels soft robots. Magneto-responsive hydrogels could be controlled remotely in presence of the external magnetic field where the polarity and the magnitude of field determine the actuation direction and bending deflection of the hydrogel in which magnetic particles, such as Fe_2O_3, Fe_3O_4 and $CoFe_2O_4$ are dispersed into the precursor hydrogel [393]. However, the media in which the NPs are dispersed must be viscous enough to prevent particle agglomeration [394]. These types of soft robots have found their applications in pharmaceutical and drug delivery where doses of drugs could be controllably and non-invasively released remotely. The magneto-responsive hydrogel soft robots are recently developed using direct 3D printing methods to fabricate complex shape robots with unique features of functionally graded and variable stiffness, which could be controlled remotely [16,394–396] (see Fig. 16.g). Hydrogel soft actuators were also 3D printed via encapsulating magnetic Fe_3O_4 NPs within an algae-derived alginate ionic hydrogel [397]. However, the mechanical strength of the hydrogels are the main concern in practical soft robotics applications. Therefore, nanocomposites addition has been introduced to increase the mechanical strength of the pure composite in presence of electrical and magnetic fields [395,398].

4.5.5.2. Electro-responsive hydrogels soft robots. Electro-responsive hydrogels could be easily controlled by the application of the external field while the polarity of the electrodes and the magnitude of pulse determine the actuation direction caused by the swelling mismatch of the soft actuator body [40,381]. Generally, there have been two approaches in developing electro-responsive hydrogels soft robots. The first group is ionic hydrogels with a conductivity of around 10 Sm^{-1} in which the hydrogel is sandwiched by composite layers of conductive material similar to the ionic polymer-metal composite (IPMC) actuators [399]. The working mechanism of these electro-responsive hydrogel soft robots is based on the Maxwell stress and DE actuators [400]. The second group comprises ionic conductive polyelectrolytes, which contain ionic groups along the hydrogel chains leading to the motion of the hydrogels in response to electrical triggers [401–403]. This type of electric-based hydrogel soft robots, working based on osmotic pressure and Donnan effects [402,403], was successfully tested for the 3D/4D printing of the soft robot entirely [391,402,404,405].

4.5.6. Discussions on MERP soft robots

The bulky magnetic field generator and high energy demand are the challenges of magnetic soft robots. Therefore, miniature magnetic soft robots are favorable to reduce the required field amplitude for their actuations [1]. Besides, more attention is needed for fabricating highly magnetized thin membranes with low mass density to achieve a high-speed large deformation in such robots [70]. Recent soft robots have been developed benefiting from a combination of dielectric and magnetic responsive principles [406]. A recent example is a double-cone shape soft actuator that was fabricated by a magnetically coupled DE actuator pump driving based on the Maxwell stress in response to an input voltage [407]. The soft robots have shown a significantly amplified output stroke when excited at the resonant frequency of the DE actuators as a result of the repulsive magnetic field. DE soft robots commonly require high operating voltage, kV range, while electro-responsive hydrogel soft robots are not capable of generating sufficient force.

Among all the MERP soft robots investigated in this study, EMREs have found to be the least explored. Therefore, there is a tremendous potential for future research on their applications in soft robotics considering the size, dispersion and type of magnetic/electric particles as well as the optimum viscosity of the electro-rheological fluid to overcome their current challenges. MRSMP soft robots provide more design flexibility via tuning both glass transition temperature and conductive particle concentrations compared to MREs. However, the locking mechanism in MRSMP soft robots are still slow compared to the EMREs and DE soft actuators. Wireless soft robots made from MRSMPs/ERSMPs with capabilities of autonomously navigation as well as hybrid magnetic and electro-responsive hydrogel soft actuators could be a future direction for further exploration [68,360]. There have been tremendous research and achievement in the field of electric and magnetic-response hydrogel soft robots, particularly in medical applications due to biocompatibility, biodegradability, transparency, and compliance of these materials. However, hydrogels have shown not matured yet for the soft robotics application requiring rapid and high force throughput. The current research directions are expected to improve their functionality through the synthesis of hydrogels that could be processed via 3D/ 4D printing and generating higher force. A summary of the advances and challenges of MERP soft robotics is presented in Table 4.

4.6. Dynamic systems

MREs [412], EMREs [413], and ERPs [414] are the most commonly used MERPs in the design of dynamic systems. Moreover, unlike shape morphing applications, in MRP-based dynamic systems, soft magnetic particles such as IOs are mostly used due to their ability in enduring large deformation and stiffening effect upon magnetic fields. Such materials possess incredible importance in vibration control [415], energy harvesting [314], and isolation [416] procedures. It should be noted that there are many studies in the literature on the use of piezoelectrics for vibration energy harvesting and vibration control [417]. However, piezoelectrics are not included in this study and we only focus on MREs, EMREs and ERPs. Given experimental studies, it was observed that vibro-acoustic behaviors of membranes can be controlled by ERPs [418]. Moreover, a novel design of ERP-based damper was accomplished in order to introduce a stiffness variable control, which was never observed before [419]. In addition to the control of the systems' vibrations, ERPs are excellent candidates for the purpose of lowering the dispersion velocity of the waves traveling in continua [420].

EMREs also possess an easy-to-manipulate dynamic behavior due to tunable dependency between electrical, mechanical and magnetic features and were studied well [421–423]. In addition to EMREs, MREs are also of high magnificence in structural dynamic applications. It was shown that the non-linear free and forced oscillation behaviors of shell-type structures were tailored by changing either the thickness of the MR layer or the intensity of the magnetic field [424]. In the framework of an analytical investigation, it was proven that it is possible to attenuate the amplitude of the panels' vibration by aggrandizing the intensity of the magnetic field if an MRE is utilized as the core layer [425]. MREs are also able to tailor the dispersion characteristics of waves scattered in continuous systems [426]. The aforementioned feature can be well utilized for the sake of defect detection via non-destructive

Table 4
Advantages and challenges of MERP soft robots.

	MREs	DEs	EMREs	MRSMPs	ERSMPs	Magneto-Responsive hydrogels	Electro-Responsive hydrogels
Response time (s)	Low (0.02–0.1)	Low (0.1–0.5)	Medium-High (0.1–1)	Medium-High (1–5)	Medium-High (1–5)	High (0.7–10)	High (0.1–5)
Efficiency	Medium-High	High	Medium	Medium	Medium	Low-Medium	Low-Medium
Strain	Low (0.08–0.2)	Low (0.03–0.4)	Medium (0.02–0.8)	Medium (0.1–1)	Medium (0.1–1)	High (1–2)	High (0.8–2)
Stress (MPa)	Low-Medium (0.01–0.1)	High (0.1–10)	Medium (0.1–7)	High (0.1–10)	Medium (0.02–1)	Low (0.01–0.05)	Low (0.01–0.05)
3D/ 4D printing	[4,70,314,343,344]	[41,42,65,362,363]	NA	[34]	[54,68,389]	[16,36,54,231,395,396]	[397,398,402,404,405]
Conventional	[16,335,340]	[296,358,367-369]	[376,378,379]	[3,382]	[408,409]	[1,410]	[411]
Advantages	Remotely controlled	Simple control High bandwidth	Little hysteresis	Easy process Locking	Low cost	Low temperature Low operating voltage	Degradable Environment friendly Low operating voltage
Challenges	Low force External field interference	High voltage (kV-MV/m^{-1}) Pre-strain	Sedimentation Redispersion	High voltage	Medium strength	Low strength	Low strength

testing by checking wave propagation curves of desired continua [427]. The dependency of the linear natural frequency of the laminated composite structures containing an MRE core on the magnetic flux intensity was shown in recent studies [412,428]. Furthermore, an experiment has been carried out to highlight the incredible impact of the magnetic field on the manipulation of the natural frequency responses of a three-layered composite with an MRE core [429]. Moreover, MREs can be implemented as vibration isolators [430,431]. Tunable properties of the MREs were gathered to protect mechanical instruments against fluctuations caused by seismic excitations. In such applications, the variable stiffness (*i.e.,* magnetic-dependent) of MREs plays a key role in the isolation procedure (*e.g.,* magnetic-dependent natural frequencies and loss factors in free vibration analysis of MRE composites) [412].

5. Discussion and outlook

In this extensive review article, we have focused on the state-of-the-art MERPs and their multifunctional and dynamic capabilities in creating smart and active (bio-)materials. We have highlighted various manufacturing techniques and characterization methods employed for the development of MERPs. The recent progress and applications of MERPs in biomedical engineering (*e.g.,* DDSs, diagnosis/imaging and TE), soft matter engineering, SM structures and dynamic systems were discussed. Although MERPs benefit from several unique characteristics such as swiftness in response, safety in operation, flexibility in programmability, and capability for remote control, there are still multiple limitations in developing or utilizing them.

5.1. Comparison between ERPs and MRPs

The 3D/4D printing of MRPs, in general, is comparatively more straightforward than that of ERPs. Therefore, more complex structures or functionalities (*e.g.,* adaptable actuation rates in soft robotics applications [232]) can be incorporated into the design of MRPs. Although it is possible to obtain highly delicate structures and prompt shape morphing using MRPs, ERPs can achieve larger deformations. On the other hand, some of ERPs such as DEs need a high electric source (or actuation voltage), which are not suitable for biomedical applications and may result in cytotoxicity and irreversible dielectric breakdown as compared to MRPs [432,433]. It should, however, be noted that there have already been alternative approaches suggested to overcome these drawbacks, for example, to use IPMCs, which need low actuation voltage for their actuations [432,434]. From the mechanical point of view, DEs ad IPMCs are not mechanically strong enough. To enhance their elastic stiffness it is required to embed fibres or to use SMPs in their designs. This is another reason that the MRPs are relatively more favourable in biomedical applications, particularly, *in-vitro* TE. Furthermore, it is also possible to lock the temporary shape(s) of MRPs in the absence of an external magnetic field when SMP is used as a matrix in the MRPs [3]. Although it is still a challenge to actuate a single system using both electric and magnetic fields as the external stimuli, recently, methods have been offered to synergistically couple multiple stimuli (*e.g.,* magnetic, ultrasonic, humidity and UV lights) leading to structures with multiple-functionalities (*e.g.,* multi-form deformations desirable in soft robotics [435]). Therefore, it can be anticipated that the electric and magnetic energies will be coupled to take the individual advantages offered by the MRPs and ERPs in a single system.

5.2. Challenges and future directions of MERPs

From a development point of view, we have discussed 3D/4D printing techniques and their great capabilities/flexibilities for developing MERPs. One of the main challenges in 3D/4D printing of MERPs is that the well-established or commercially available materials cannot directly be used and need to be modified by adding magneto-/electro-responsive fillers. The modification of printing materials requires an optimization/customization of the printing processes, which is a time-consuming procedure and is different for individual 3D printing process. Therefore, more studies should be performed to extend the knowledge of materials science, polymer chemistry, and 3D/4D printing techniques in order to facilitate the procedure of 4D-printed MERP-based objects. Moreover, for the characterization of MERPs, there is a lack of standard procedure or protocol for the characterizations, testing, and performance measurements of MERPs. Therefore, there is a need for developing standardized methods or protocols for MERPs characterization [73].

From an application viewpoint, there are still many aspects of MERPs, which require further investigation. For instance, some of the available studies on MERPs applications in TE, DDSs, and diagnosis systems are considered to be conceptual designs and the current knowledge concerned with the biocompatibility of various MERPs is still very limited [241]. Therefore, it is necessary to investigate the biological performance of MERPs and their interactions with different types of living cells. MERPs have great potentials to be utilized in smart multi-functional materials such as self-healing and self-reparability systems, which will have vast applications in biomedical engineering including engineering of artificial organs, muscles, and self-healing bone [436]. Also, new functionalities such as re-programmability, rationally encoding magnetic (or electric) anisotropy, energy efficiency, fast switching between permanent and temporary shapes (*i.e.,* fast response time) and

easiness of the fabrication and encoding (*e.g.*, single-step process) are the areas that need to take into account for the designing and fabrication of MRSM/ ERSM structures in the future.

With the world moving toward making everything smart, there is a great desire to assist the MERPs-related systems with artificial intelligence, including machine learning or deep learning approaches. First, there are limited studies regarding integrated 4D-printed sensors and actuators made by MERPs, and thus should be investigated strongly. Second, there is an extended need for self-programming or intelligent MERPs robots particularly for the systems that might be used in the human body. Another point is to find ways to mediate the unpleasant effects of external stimuli (*i.e.*, high voltage or magnetic field).

In summary, the trend of future research is to develop new knowledge for boosting the application of MERPs by developing advanced computational models for predicting their behavior, proposing new fabrication tools for creating multi-functional structures and studying their performance and their interaction with different biological materials.

Declaration of Competing Interest

The authors declare that they have no known competing financial interests or personal relationships that could have appeared to influence the work reported in this paper.

References

[1] S.R. Goudu, I.C. Yasa, X. Hu, H. Ceylan, W. Hu, M. Sitti, Biodegradable untethered magnetic hydrogel Milli-Grippers, Adv. Funct. Mater. 30 (50) (2020) 2004975.

[2] S. Wu, W. Hu, Q. Ze, M. Sitti, R. Zhao, Multifunctional magnetic soft composites: a review, Multifunct. Mater. 3 (2020) 042003.

[3] Q. Ze, X. Kuang, S. Wu, J. Wong, S.M. Montgomery, R. Zhang, J.M. Kovitz, F. Yang, H.J. Qi, R. Zhao, Magnetic shape memory polymers with integrated multifunctional shape manipulation, Adv. Mater. 32 (4) (2020) 1906657.

[4] Y. Alapan, A.C. Karacakol, S.N. Guzelhan, I. Isik, M. Sitti, Reprogrammable shape morphing of magnetic soft machines, Sci. Adv. 6 (38) (2020) eabc6414.

[5] P. Testa, R.W. Style, J.Z. Cui, C. Donnelly, E. Borisova, P.M. Derlet, E.R. Dufresne, L.J. Heyderman, Magnetically addressable shape-memory and stiffening in a composite elastomer, Adv. Mater. 31 (29) (2019) 1900561.

[6] Y.W. Lee, H. Ceylan, I.C. Yasa, U. Kilic, M. Sitti, Interfaces, 3D-Printed Multi-Stimuli-Responsive Mobile Micromachines, ACS Appl. Mater. Interfaces. 13 (11) (2020) 12759–12766.

[7] E. Yarali, M. Baniasadi, M. Bodaghi, M. Baghani, Structures, 3D constitutive modeling of electro-magneto-visco-hyperelastic elastomers: a semi-analytical solution for cylinders under large torsion–extension deformation, Smart Mater. Struct. 29 (8) (2020) 085031.

[8] M. Baniasadi, E. Yarali, M. Bodaghi, A. Zolfagharian, M. Baghani, Constitutive Modeling of multi-stimuli-responsive shape memory polymers with multi–functional capabilities, Int. J. Mech. Sci. 192 (2021) 106082.

[9] A.K. Bastola, M. Hossain, The shape–morphing performance of magnetoactive soft materials, Mater. Des. 211 (2021) 110172.

[10] T. Liu, T. Zhou, Y. Yao, F. Zhang, L. Liu, Y. Liu, J. Leng, Stimulus methods of multi-functional shape memory polymer nanocomposites: a review, Compos. Part A 100 (2017) 20–30.

[11] E. Yarali, A. Mohammadi, S. Mafakheri, M. Baghani, H. Adibi, Mathematical modeling and experimental evaluation of a prototype double-tube Magnetorheological damper, SN Appl. Sci. 1 (11) (2019) 1–10.

[12] R.G. Nikov, N. Nedyalkov, D. Karashanova, Laser ablation of Ni in the presence of external magnetic field: selection of microsized particles, Appl. Surf. Sci. 518 (2020) 146211.

[13] J. S. Leng, W. M. Huang, X. Lan, Y. J. Liu, S. Y. Du, Significantly reducing electrical resistivity by forming conductive Ni chains in a polyurethane shape-memory polymer/carbon-black composite, Appl. Phys. Lett. 92 (20) (2008) 204101.

[14] M. Hossain, P. Saxena, P. Steinmann, Modelling the curing process in magneto-sensitive polymers: rate-dependence and shrinkage, Int. J. Non. Linear Mech. 74 (2015) 108–121.

[15] S. Lucarini, M. Hossain, D. Garcia-Gonzalez, Recent advances in hard-magnetic soft composites: synthesis, characterisation, computational modelling, and applications, Compos. Struct. (2021) 114800.

[16] Y. Kim, H. Yuk, R. Zhao, S.A. Chester, X. Zhao, Printing ferromagnetic domains for untethered fast-transforming soft materials, Nature 558 (7709) (2018) 274–279.

[17] R. Zhao, Y. Kim, S.A. Chester, P. Sharma, X. Zhao, Mechanics of hard-magnetic soft materials, J. Mech. Phys. Solids 124 (2019) 244–263.

[18] A.K. Bastola, M. Paudel, L. Li, W. Li, Recent progress of magnetorheological elastomers: a review, Smart Mater. Struct. 29 (2020) 123002.

[19] P. Brochu, Q. Pei, Dielectric elastomers for actuators and artificial muscles, in: Electroactivity in Polymeric Materials, Springer, 2012, pp. 1–56.

[20] L. J. Romasanta, M. A. López-Manchado, R. Verdejo, Increasing the performance of dielectric elastomer actuators: A review from the materials perspective, Prog. Polym. Sci. 51 (2015) 188–211.

[21] M.J. Mirzaali, H. Pahlavani, E. Yarali, A.A. Zadpoor, Non-affinity in multi-material mechanical metamaterials, Sci. Rep. 10 (1) (2020) 11488.

[22] E. Dogan, A. Bhusal, B. Cecen, A.K. Miri, 3D Printing metamaterials towards tissue engineering, Appl. Mater. Today. 20 (2020) 100752.

[23] H. Rahman, E. Yarali, A. Zolfagharian, A. Serjouei, M. Bodaghi, Energy absorption and mechanical performance of functionally graded soft–hard lattice structures, Materials 14 (6) (2021) 1366.

[24] S. Tibbits, The emergence of "4D printing"| TED Talk, 2013.

[25] S. Joshi, K. Rawat, C. Karunakaran, V. Rajamohan, A.T. Mathew, K. Koziol, V.K. Thakur, A.S.S. Balan, 4D printing of materials for the future: opportunities and challenges, Appl. Mater. Today. 18 (2020) 100490.

[26] E. Pei, G.H. Loh, S. Nam, Concepts and Terminologies in 4D Printing, Appl. Sci. 10 (13) (2020) 4443.

[27] X. Xin, L. Liu, Y. Liu, J. Leng, 4D printing auxetic metamaterials with tunable, programmable, and reconfigurable mechanical properties, Adv. Funct. Mater. 30 (43) (2020) 2004226.

[28] T. van Manen, S. Janbaz, K.M. Jansen, A.A. Zadpoor, 4D printing of reconfigurable metamaterials and devices, Commun. Mater. 2 (1) (2021) 1–8.

[29] E. MacDonald, R. Wicker, Multiprocess 3D printing for increasing component functionality, Science 353 (6307) (2016).

[30] M. Falahati, P. Ahmadvand, S. Safaee, Y.-C. Chang, Z. Lyu, R. Chen, L. Li, Y. Lin, Smart polymers and nanocomposites for 3D and 4D printing, Mater. Today 40 (2020) 215–245.

[31] X. Wan, L. Luo, Y. Liu, J. Leng, Direct ink writing based 4D printing of materials and their applications, Adv. Sci. 7 (16) (2020) 2001000.

[32] A.K. Bastola, M. Paudel, L. Li, Development of hybrid magnetorheological elastomers by 3D printing, Polymer (Guildf) 149 (2018) 213–228.

[33] H. Yuk, X. Zhao, A new 3D printing strategy by harnessing deformation, instability, and fracture of viscoelastic inks, Adv. Mater. 30 (6) (2018) 1704028.

[34] H. Wei, Q. Zhang, Y. Yao, L. Liu, Y. Liu, J. Leng, Direct-write fabrication of 4D active shape-changing structures based on a shape memory polymer and its nanocomposite, ACS Appl. Mater. Interfaces 9 (1) (2017) 876–883.

[35] M. Hossain, Z. Liao, An additively manufactured silicone polymer: thermo-viscoelastic experimental study and computational modelling, Addit. Manuf. 35 (2020) 101395.

[36] Z. Chen, D. Zhao, B. Liu, G. Nian, X. Li, J. Yin, S. Qu, W. Yang, 3D printing of multifunctional hydrogels, Adv. Funct. Mater. 29 (20) (2019) 1900971.

[37] B. Derby, Inkjet printing of functional and structural materials: fluid property requirements, feature stability, and resolution, Annu. Rev. Mater. Res. 40 (2010) 395–414.

[38] F. Zhang, C. Tuck, R. Hague, Y. He, E. Saleh, Y. Li, C. Sturgess, R. Wildman, Inkjet printing of polyimide insulators for the 3 D printing of dielectric materials for microelectronic applications, J. Appl. Polym. Sci. 133 (18) (2016).

[39] D. Jang, D. Kim, J. Moon, Influence of fluid physical properties on ink-jet printability, Langmuir 25 (5) (2009) 2629–2635.

[40] S. De Pedro, V. Cadarso, X. Muñoz-Berbel, J. Plaza, J. Sort, J. Brugger, S. Büttgenbach, A. Llobera, PDMS-based, magnetically actuated variable optical attenuators obtained by soft lithography and inkjet printing technologies, Sens. Actuat. A 215 (2014) 30–35.

[41] D. McCoul, S. Rosset, S. Schlatter, H. Shea, Inkjet 3D printing of UV and thermal cure silicone elastomers for dielectric elastomer actuators, Smart Mater. Struct. 26 (12) (2017) 125022.

[42] J. Rossiter, P. Walters, B. Stoimenov, Printing 3D dielectric elastomer actuators for soft robotics, Electroactive Polymer Actuators and Devices (EAPAD) 2009, Int. Soc. Opt. Photon. (2009) 72870H.

[43] S. Schlatter, S. Rosset, H. Shea, Inkjet printing of carbon black electrodes for dielectric elastomer actuators, Electroactive Polymer Actuators and Devices (EAPAD) 2017, Int. Soc. Opt. Photon. (2017) 1016311.

[44] C. Baechler, S. Gardin, H. Abuhimd, G. Kovacs, Inkjet printed multiwall carbon nanotube electrodes for dielectric elastomer actuators, Smart Mater. Struct. 25 (5) (2016) 055009.

[45] C. de Saint-Aubin, S. Rosset, S. Schlatter, H. Shea, High-cycle electromechanical aging of dielectric elastomer actuators with carbon-based electrodes, Smart Mater. Struct. 27 (7) (2018) 074002.

[46] R. Mikkonen, P. Puistola, I. Jönkkäri, M. Mäntysalo, Inkjet printable polydimethylsiloxane for all-inkjet-printed multilayered soft electrical applications, ACS Appl. Mater. Interfaces 12 (10) (2020) 11990–11997.

[47] E. Saleh, 3D and 4D printed polymer composites for electronic applications, in: 3D and 4D Printing of Polymer Nanocomposite Materials, Elsevier, 2020, pp. 505–525.

[48] N. Berdozzi, Y. Chen, L. Luzi, M. Fontana, I. Fassi, L.M. Tosatti, R. Vertechy, Rapid fabrication of electro-adhesive devices with inkjet printed electrodes, IEEE Robot. Automat. Lett. 5 (2) (2020) 2770–2776.

[49] A. Chortos, E. Hajiesmaili, J. Morales, D.R. Clarke, J.A. Lewis, 3D Printing of interdigitated dielectric elastomer actuators, Adv. Funct. Mater. 30 (1) (2020) 1907375.

[50] G.-.K. Lau, M. Shrestha, Ink-jet printing of micro-electro-mechanical systems (MEMS), Micromachines (Basel) 8 (6) (2017) 194.

[51] J.Y. Lee, J. An, C.K. Chua, Fundamentals and applications of 3D printing for novel materials, Appl. Mater. Today. 7 (2017) 120–133.

[52] C. Yang, X. Tian, T. Liu, Y. Cao, D. Li, 3D printing for continuous fiber reinforced thermoplastic composites: mechanism and performance, Rapid Prototyping J (2017).
[53] G.D. Goh, V. Dikshit, J. An, W.Y. Yeong, Structures, Process-structure-property of additively manufactured continuous carbon fiber reinforced thermoplastic: an investigation of mode I interlaminar fracture toughness, Mech. Adv. Mater. Struct. (2020) 1–13.
[54] L.-H. Shao, B. Zhao, Q. Zhang, Y. Xing, K. Zhang, 4D printing composite with electrically controlled local deformation, Extreme Mech. Lett. (2020) 100793.
[55] W. Zhao, F. Zhang, J. Leng, Y. Liu, Personalized 4D printing of bioinspired tracheal scaffold concept based on magnetic stimulated shape memory composites, Compos. Sci. Technol. 184 (2019) 107866.
[56] E. Dohmen, A. Saloum, J. Abel, Field-structured magnetic elastomers based on thermoplastic polyurethane for fused filament fabrication, Philosoph. Trans. R. Soc. A 378 (2171) (2020) 20190257.
[57] N. Prem, D. Sindersberger, G.J. Monkman, Mini-extruder for 3D magnetoactive polymer printing, Adv. Mater. Sci. Eng. 2019 (2019) 8715718.
[58] S. Kumar, R. Singh, T. Singh, A. Batish, On mechanical characterization of 3-D printed PLA-PVC-wood dust-Fe3O4 composite, J. Thermoplast. Compos. Mater. 0 (0) (2019) 1–18 0892705719879195, doi:10.1177/0892705719879195.
[59] D. Fan, U. Staufer, A. Accardo, Engineered 3D polymer and hydrogel microenvironments for cell culture applications, Bioengineering (Basel) 6 (4) (2019) 113.
[60] K.-S. Lee, R.H. Kim, D.-Y. Yang, S.H. Park, Advances in 3D nano/microfabrication using two-photon initiated polymerization, Prog. Polym. Sci. 33 (6) (2008) 631–681.
[61] B. Nagarajan, P. Mertiny, A.J. Qureshi, Magnetically loaded polymer composites using stereolithography—Material processing and characterization, Mater. Today Commun. 25 (2020) 101520.
[62] S. Lantean, G. Barrera, C.F. Pirri, P. Tiberto, M. Sangermano, I. Roppolo, G. Rizza, 3D printing of magnetoresponsive polymeric materials with tunable mechanical and magnetic properties by digital light processing, Adv. Mater. Technol. 4 (11) (2019) 1900505.
[63] T. Hupfeld, S. Salamon, J. Landers, A. Sommereyns, C. Doñate-Buendía, J. Schmidt, H. Wende, M. Schmidt, S. Barcikowski, B. Gökce, 3D printing of magnetic parts by laser powder bed fusion of iron oxide nanoparticle functionalized polyamide powders, J. Mater. Chem. C (2020) 12204–12217.
[64] S. Yuan, C.K. Chua, K. Zhou, 3D-printed mechanical metamaterials with high energy absorption, Adv. Mater. Technol. 4 (3) (2019) 1800419.
[65] G. Haghiashtiani, E. Habtour, S.-H. Park, F. Gardea, M.C. McAlpine, 3D printed electrically-driven soft actuators, Extreme Mech. Lett. 21 (2018) 1–8.
[66] K. Tian, J. Bae, S.E. Bakarich, C. Yang, R.D. Gately, G.M. Spinks, M. In Het Panhuis, Z. Suo, J.J. Vlassak, 3D printing of transparent and conductive heterogeneous hydrogel–elastomer systems, Adv. Mater. 29 (10) (2017) 1604827.
[67] H. Wei, X. Cauchy, I.O. Navas, Y. Abderrafai, K. Chizari, U. Sundararaj, Y. Liu, J. Leng, D. Therriault, Direct 3D printing of hybrid nanofiber-based nanocomposites for highly conductive and shape memory applications, ACS Appl. Mater. Interfaces 11 (27) (2019) 24523–24532.
[68] X. Kuang, D.J. Roach, J. Wu, C.M. Hamel, Z. Ding, T. Wang, M.L. Dunn, H.J. Qi, Advances in 4D printing: materials and applications, Adv. Funct. Mater. 29 (2) (2019) 1805290.
[69] C. Ma, S. Wu, Q. Ze, X. Kuang, R. Zhang, H.J. Qi, R. Zhao, Magnetic multimaterial printing for multimodal shape transformation with tunable properties and shiftable mechanical behaviors, ACS Appl. Mater. Interfaces 13 (11) (2021) 12639–12648.
[70] P. Zhu, W. Yang, R. Wang, S. Gao, B. Li, Q. Li, 4D printing of complex structures with a fast response time to magnetic stimulus, ACS Appl. Mater. Interfaces 10 (42) (2018) 36435–36442.
[71] D. Kokkinis, M. Schaffner, A.R. Studart, Multimaterial magnetically assisted 3D printing of composite materials, Nat. Commun. 6 (1) (2015) 1–10.
[72] A. Bastola, V. Hoang, L. Li, A novel hybrid magnetorheological elastomer developed by 3D printing, Mater. Des. 114 (2017) 391–397.
[73] A.K. Bastola, M. Hossain, A review on magneto-mechanical characterizations of magnetorheological elastomers, Compos. Part B 200 (2020) 108348.
[74] A. Bastola, M. Paudel, L. Li, Line-patterned hybrid magnetorheological elastomer developed by 3D printing, J. Intell. Mater. Syst. Struct. 31 (3) (2020) 377–388.
[75] D. Sindersberger, A. Diermeier, N. Prem, G.J. Monkman, Printing of hybrid magneto active polymers with 6 degrees of freedom, Mater. Today Commun. 15 (2018) 269–274.
[76] J.D. Carrico, N.W. Traeden, M. Aureli, K.K. Leang, Fused filament 3D printing of ionic polymer-metal composites (IPMCs), Smart Mater. Struct. 24 (12) (2015) 125021.
[77] S. Trabia, Z. Olsen, K.J. Kim, Searching for a new ionomer for 3D printable ionic polymer–metal composites: aquivion as a candidate, Smart Mater. Struct. 26 (11) (2017) 115029.
[78] C. Zeng, L. Liu, W. Bian, Y. Liu, J. Leng, 4D printed electro-induced continuous carbon fiber reinforced shape memory polymer composites with excellent bending resistance, Compos. Part B (2020) 108034.
[79] H. Shinoda, S. Azukizawa, K. Maeda, F. Tsumori, Bio-mimic motion of 3D-printed gel structures dispersed with magnetic particles, J. Electrochem. Soc. 166 (9) (2019) B3235.
[80] J.J. Martin, B.E. Fiore, R.M. Erb, Designing bioinspired composite reinforcement architectures via 3D magnetic printing, Nat. Commun. 6 (1) (2015) 8641.
[81] W. Zhu, J. Li, Y.J. Leong, I. Rozen, X. Qu, R. Dong, Z. Wu, W. Gao, P.H. Chung, J. Wang, 3D-printed artificial microfish, Adv. Mater. 27 (30) (2015) 4411–4417.
[82] R. Domingo-Roca, J. Jackson, J. Windmill, 3D-printing polymer-based permanent magnets, Mater. Des. 153 (2018) 120–128.
[83] J.A. Jackson, M.C. Messner, N.A. Dudukovic, W.L. Smith, L. Bekker, B. Moran, A.M. Golobic, A.J. Pascall, E.B. Duoss, K.J. Loh, Field responsive mechanical metamaterials, Sci. Adv. 4 (12) (2018) eaau6419.
[84] Z. Al-Dulimi, M. Wallis, D.K. Tan, M. Maniruzzaman, A. Nokhodchi, 3D printing technology as innovative solutions for biomedical applications, Drug Discovery Today 26 (2) (2021) 360–383.
[85] T.D. Ngo, A. Kashani, G. Imbalzano, K.T. Nguyen, D. Hui, Additive manufacturing (3D printing): a review of materials, methods, applications and challenges, Compos. Part B 143 (2018) 172–196.
[86] V.D. Phadtare, V.G. Parale, K.Y. Lee, T. Kim, V.R. Puri, H.H. Park, Flexible and lightweight Fe3O4/polymer foam composites for microwave-absorption applications, J. Alloys Compd. 805 (2019) 120–129.
[87] Z. Xu, C. Ding, D.-w. Wei, R.-y. Bao, K. Ke, Z. Liu, M.-b. Yang, W. Yang, Electro and Light-Active Actuators Based on Reversible Shape- Memory Polymer Composites with Segregated Conductive Networks, ACS Appl. Mater. Interfaces 11 (2019) 30332–30340.
[88] S.-t. Xing, P.-p. Wang, S.-q. Liu, Y.-h. Xu, R.-m. Zheng, Z.-f. Deng, Z.-f. Peng, J.-y. Li, Y.-y. Wu, L. Liu, A shape-memory soft actuator integrated with reversible electric/moisture actuating and strain sensing, Compos. Sci. Technol. 193 (2020) 108133.
[89] T.G. Polat, K. Ateş, S. Bilgin, O. Duman, Ş. Özen, S. Tunç, Carbon nanotube, poly(3,4-ethylenedioxythiophene): poly(styrenesulfonate) and Ag nanoparticle doped gelatin based electro-active hydrogel systems, Colloids Surf. A 580 (2019) 123751.
[90] L. Peng, Y. Liu, J. Huang, J. Li, J. Gong, J. Ma, Microfluidic fabrication of highly stretchable and fast electro-responsive graphene oxide/polyacrylamide/alginate hydrogel fibers, Eur. Polym. J. 103 (2018) 335–341.
[91] F. Zhao, C. Zhang, J. Liu, L. Liu, X. Cao, X. Chen, B. Lei, L. Shao, Periosteum structure/function-mimicking bioactive scaffolds with piezoelectric/chem/nano signals for critical-sized bone regeneration, Chem. Eng. J. 402 (2020) 126203.
[92] B. Aksoy, H. Shea, Reconfigurable and latchable shape-morphing dielectric elastomers based on local stiffness modulation, Adv. Funct. Mater. 30 (27) (2020) 2001597.
[93] L. Vannozzi, P. Gouveia, P. Pingue, C. Canale, L. Ricotti, Novel ultrathin films based on a blend of PEG- b-PCL and PLLA and doped with ZnO nanoparticles, ACS Appl. Mater. Interfaces 12 (2020) 21398–21410.
[94] R.V. Chernozem, M.A. Surmeneva, S.N. Shkarina, K. Loza, M. Epple, M. Ulbricht, A. Cecilia, B. Krause, T. Baumbach, A.A. Abalymov, B.V. Parakhonskiy, A.G. Skirtach, R.A. Surmenev, Piezoelectric 3-D Fibrous Poly(3-hydroxybutyrate)-based scaffolds ultrasound-mineralized with calcium carbonate for bone tissue engineering: inorganic phase formation, osteoblast cell adhesion, and proliferation, ACS Appl. Mater. Interfaces 11 (2019) 19522–19533.
[95] A. Dargahi, R. Sedaghati, S. Rakheja, On the properties of magnetorheological elastomers in shear mode: design, fabrication and characterization, Compos. Part B 159 (2019) 269–283.
[96] A. Cafarelli, P. Losi, A.R. Salgarella, M.C. Barsotti, I.B. Di Cioccio, I. Foffa, L. Vannozzi, P. Pingue, G. Soldani, L. Ricotti, Small-caliber vascular grafts based on a piezoelectric nanocomposite elastomer: mechanical properties and biocompatibility, J. Mech. Behav. Biomed. Mater. 97 (2019) 138–148.
[97] T. Kubo, K. Tachibana, T. Naito, S. Mukai, K. Akiyoshi, J. Balachandran, K. Otsuka, Magnetic field stimuli-sensitive drug release using a magnetic thermal seed coated with thermal-responsive molecularly imprinted polymer, ACS Biomater. Sci. Eng. 5 (2019) 759–767.
[98] G.Z. Lum, Z. Ye, X. Dong, H. Marvi, O. Erin, W. Hu, M. Sitti, Shape-programmable magnetic soft matter, Proc. Natl. Acad. Sci. U.S.A. 113 (2016) E6007–E6015.
[99] M.Y. Razzaq, M. Behl, A. Lendlein, Memory-effects of magnetic nanocomposites, Nanoscale 4 (2012) 6181–6195.
[100] K.K. Patel, R. Purohit, Improved shape memory and mechanical properties of microwave-induced shape memory polymer/MWCNTs composites, Mater. Today Commun. 20 (2019) 100579.
[101] M. Ansari, M. Golzar, M. Baghani, M. Soleimani, Shape memory characterization of poly(ε-caprolactone) (PCL)/polyurethane (PU) in combined torsion-tension loading with potential applications in cardiovascular stent, Polym. Test 68 (2018) 424–432.
[102] E. Tekay, Preparation and characterization of electro-active shape memory PCL/SEBS-g-MA/MWCNT nanocomposites, Polymer (Guildf) 209 (2020) 122989.
[103] G.D. Soto, C. Meiorin, D.G. Actis, P. Mendoza Zélis, O. Moscoso Londoño, D. Muraca, M.A. Mosiewicki, N.E. Marcovich, Magnetic nanocomposites based on shape memory polyurethanes, Eur. Polym. J. 109 (2018) 8–15.
[104] R.V. Chernozem, M.A. Surmeneva, S.N. Shkarina, K. Loza, M. Epple, M. Ulbricht, A. Cecilia, B. Krause, T. Baumbach, A.A. Abalymov, B.V. Parakhonskiy, A.G. Skirtach, R.A. Surmenev, Piezoelectric 3-D Fibrous Poly(3-hydroxybutyrate)-based scaffolds ultrasound-mineralized with calcium carbonate for bone tissue engineering: inorganic phase formation, osteoblast cell adhesion, and proliferation, ACS Appl. Mater. Interfaces 11 (21) (2019) 19522–19533.

[105] M. Ansari, M. Golzar, M. Baghani, M.J.P.T. Soleimani, Shape memory characterization of poly (ε-caprolactone)(PCL)/polyurethane (PU) in combined torsion-tension loading with potential applications in cardiovascular stent, Polym. Test 68 (2018) 424–432.
[106] M. Ansari, M. Golzar, M. Baghani, M. Abbasishirsavar, M.J.S.M. Taghavimehr, structures, Force recovery evaluation of thermo-induced shape-memory polymer stent: material, process and thermo-viscoelastic characterization, Smart Mater. Struct. 28 (9) (2019) 095022.
[107] X.X. Wang, G.F. Yu, J. Zhang, M. Yu, S. Ramakrishna, Y.Z. Long, Conductive polymer ultrafine fibers via electrospinning: preparation, physical properties and applications, Prog. Mater. Sci. 115 (2020) 100704.
[108] M. Udayakumar, M. Kollar, F. Kristaly, M. Lesko, T. Szabo, K. Marossy, I. Tasnadi, Z. Nemeth, Temperature and Time Dependence of the Solvent-Induced Crystallization of Poly(l-lactide), Polymers (Basel) 12 (5) (2020) 1065.
[109] M. Sabzi, M. Babaahmadi, M. Rahnama, Thermally and Electrically Triggered Triple-Shape Memory Behavior of Poly(vinyl acetate)/Poly(lactic acid) Due to Graphene-Induced Phase Separation, ACS Applied Materials and Interfaces 9 (2017) 24061–24070.
[110] A.N. Boyandin, A.A. Sukhanova, V.V. Orlova, A.I.J.M.L. Volchek, A novel method of fabricating polymer tubes using the casting solution technique, Mater Lett 282 (2021) 128833.
[111] T. Calvo-correas, A. Shirole, A. Alonso-varona, C. Weder, M.A. Corcuera, A. Eceiza, Impact of the Combined Use of Magnetite Nanoparticles and Cellulose Nanocrystals on the Shape-Memory Behavior of Hybrid Polyurethane Bionanocomposites, Biomacromolecules 21 (2020) 6.
[112] M.-q. Li, J.-m. Wu, F. Song, D.-d. Li, X.-l. Wang, L. Chen, Y.-z. Wang, Flexible and electro-induced shape memory Poly (Lactic Acid) -based material constructed by inserting a main-chain liquid crystalline and selective localization of carbon nanotubes, Compos. Sci. Technol. 173 (2019) 1–6.
[113] A. Bratek-Skicki, Towards a new class of stimuli-responsive polymer-based materials–Recent advances and challenges, Appl. Surf. Sci. Adv. 4 (2021) 100068.
[114] P. Testa, R.W. Style, J. Cui, C. Donnelly, E. Borisova, P.M. Derlet, E.R. Dufresne, L.J. Heyderman, Magnetically addressable shape-memory and stiffening in a composite elastomer, Adv. Mater. 31 (29) (2019) 1900561.
[115] W. Zhao, Z. Huang, L. Liu, W. Wang, J. Leng, Y. Liu, Porous bone tissue scaffold concept based on shape memory PLA/Fe3O4, Compos. Sci. Technol. 203 (2020) 108563.
[116] F. Zhang, L. Wang, Z. Zheng, Y. Liu, J. Leng, Magnetic Programming of 4D Printed Shape Memory Composite Structures, Elsevier, 2019.
[117] K. Dong, M. Panahi-Sarmad, Z. Cui, X. Huang, X. Xiao, Electro-induced shape memory effect of 4D printed auxetic composite using PLA/TPU/CNT filament embedded synergistically with continuous carbon fiber: a theoretical & experimental analysis, Composites, Part B 220 (2021) 108994.
[118] L.Z. Guan, L. Zhao, Y.J. Wan, L.C. Tang, Three-dimensional graphene-based polymer nanocomposites: preparation, properties and applications, Nanoscale 10 (2018) 14788–14811.
[119] J. Chai, D. Zhang, J. Cheng, Y. Jia, X. Ba, Y. Gao, L. Zhu, H. Wang, M. Cao, Facile synthesis of highly conductive MoS2/graphene nanohybrids with hetero-structures as excellent microwave absorbers, RSC Adv. 8 (2018) 36616–36624.
[120] B.S. Dakshayini, K.R. Reddy, A. Mishra, N.P. Shetti, S.J. Malode, S. Basu, S. Naveen, A.V. Raghu, Role of conducting polymer and metal oxide-based hybrids for applications in ampereometric sensors and biosensors, Microchem. J. 147 (2019) 7–24.
[121] M.R.U.D. Biswas, K.Y. Cho, J.D. Na, W.C. Oh, Highly electro-conductive graphene-decorated PANI-BiVO4 polymer-semiconductor nanocomposite with outstanding photocatalytic performance, Mater. Sci. Eng. B 251 (2019).
[122] A. Kumar, K. Patra, M.J.P.C. Hossain, Silicone composites cured under a high electric field: an electromechanical experimental study, Polym. Compos. 42 (2) (2021) 914–930.
[123] M. Dai, Y. Tao, L. Fang, C. Wang, J. Sun, Q. Fang, Low Dielectric polymers with high thermostability derived from biobased vanillin, ACS Sustain. Chem. Eng. 8 (39) (2020) 15013–15019.
[124] Y. Alapan, A.C. Karacakol, S.N. Guzelhan, I. Isik, M. Sitti, Reprogrammable shape morphing of magnetic soft machines, Sci. Adv. 6 (38) (2020) eabc6414.
[125] X. Gong, F. Xie, L. Liu, Y. Liu, J. Leng, Electro-active variable-stiffness corrugated structure based on shape-memory polymer composite, Polymers (Basel) 12 (2020).
[126] M.J. Lee, M.J. Kim, J.S. Kwon, S.B. Lee, K.M. Kim, Cytotoxicity of light-cured dental materials according to different sample preparation methods, Materials (Basel) 10 (3) (2017) 288.
[127] N. Zobeiry, R. Vaziri, A. Poursartip, Manufacturing, Computationally efficient pseudo-viscoelastic models for evaluation of residual stresses in thermoset polymer composites during cure, Compos. Part A 41 (2) (2010) 247–256.
[128] S. Araujo-Custodio, M. Gomez-Florit, A.R. Tomas, B.B. Mendes, P.S. Babo, S.M. Mithieux, A. Weiss, R.M.A. Domingues, R.L. Reis, M.E. Gomes, Injectable and magnetic responsive hydrogels with bioinspired ordered structures, ACS Biomater. Sci. Eng. 5 (3) (2019) 1392–1404.
[129] L.F. Fan, H.I. Hsiang, J.J. Hung, Silane surface modification effects on the electromagnetic properties of phosphatized iron-based SMCs, Appl. Surf. Sci. 433 (2018) 133–138.
[130] M. Bansal, A. Dravid, Z. Aqrawe, J. Montgomery, Z. Wu, D. Svirskis, Conducting polymer hydrogels for electrically responsive drug delivery, J. Control. Release 328 (2020) 192–209.
[131] A.S. Timin, A.R. Muslimov, M.V. Zyuzin, O.O. Peltek, T.E. Karpov, I.S. Sergeev, A.I. Dotsenko, A.A. Goncharenko, N.D. Yolshin, A. Sinelnik, B. Krause, T. Baumbach, M.A. Surmeneva, R.V. Chernozem, G.B. Sukhorukov, R.A. Surmenev, Multifunctional scaffolds with improved antimicrobial properties and osteogenicity based on piezoelectric electrospun fibers decorated with bioactive composite microcapsules, ACS Appl. Mater. Interfaces 10 (2018) 34849–34868.
[132] V. Beachley, X. Wen, Effect of electrospinning parameters on the nanofiber diameter and length, Mater. Sci. Eng. C Mater. Biol. Appl. 29 (3) (2009) 663–668.
[133] A. Reizabal, R. Brito-Pereira, M.M. Fernandes, N. Castro, V. Correia, C. Ribeiro, C.M. Costa, L. Perez, J.L. Vilas, S. Lanceros-Méndez, Silk fibroin magnetoactive nanocomposite films and membranes for dynamic bone tissue engineering strategies, Materialia 12 (2020).
[134] D. Barati, O. Karaman, S. Moeinzadeh, S. Kader, E. Jabbari, Material and regenerative properties of an osteon-mimetic cortical bone-like scaffold, Regener. Biomater. 6 (2) (2019) 89–98.
[135] X. Wan, F. Zhang, Y. Liu, J. Leng, CNT-based electro-responsive shape memory functionalized 3D printed nanocomposites for liquid sensors, Carbon.155 (2019) 77–87.
[136] P. Testa, R.W. Style, J. Cui, C. Donnelly, E. Borisova, P.M. Derlet, E.R. Dufresne, L.J. Heyderman, Magnetically addressable shape-memory and stiffening in a composite elastomer, Adv. Mater. 31 (29) (2019) 1900561.
[137] T. Calvo-Correas, A. Shirole, F. Crippa, A. Fink, C. Weder, M.A. Corcuera, A. Eceiza, Biocompatible thermo-and magneto-responsive shape-memory polyurethane bionanocomposites, Mater. Sci. Eng., C. 97 (2019) 658–668.
[138] M. Helminger, B. Wu, T. Kollmann, D. Benke, D. Schwahn, V. Pipich, D. Faivre, D. Zahn, H. Cölfen, Synthesis and characterization of gelatin-based magnetic hydrogels, Adv. Funct. Mater. 24 (21) (2014) 3187–3196.
[139] J. Liao, H. Huang, Green magnetic hydrogels synthesis, characterization and flavourzyme immobilization based on chitin from Hericium erinaceus residue and polyvinyl alcohol, Int. J. Biol. Macromol. 138 (2019) 462–472.
[140] M.-Y. Choi, Y. Shin, H.S. Lee, S.Y. Kim, J.-H. Na, Multipolar spatial electric field modulation for freeform electroactive hydrogel actuation, Sci. Rep. 10 (1) (2020) 1–8.
[141] S.R. Goudu, I.C. Yasa, X. Hu, H. Ceylan, W. Hu, M. Sitti, Biodegradable untethered magnetic hydrogel milli-grippers, Adv. Funct. Mater. 30 (2020) 2004975 50 n/a(n/a) 2004975.
[142] M. Kallio, The Elastic and Damping Properties of Magnetorheological Elastomers, VTT Espoo, Finland, 2005.
[143] F. Gordaninejad, X. Wang, P. Mysore, Behavior of thick magnetorheological elastomers, J. Intell. Mater. Syst. Struct. 23 (9) (2012) 1033–1039.
[144] G. Stepanov, S. Abramchuk, D. Grishin, L. Nikitin, E.Y. Kramarenko, A. Khokhlov, Effect of a homogeneous magnetic field on the viscoelastic behavior of magnetic elastomers, Polymer (Guildf) 48 (2) (2007) 488–495.
[145] G. Schubert, P. Harrison, Large-strain behaviour of magneto-rheological elastomers tested under uniaxial compression and tension, and pure shear deformations, Polym. Test 42 (2015) 122–134.
[146] C.G. Soria-Hernández, L.M. Palacios-Pineda, A. Elías-Zúñiga, I.A. Perales-Martínez, O. Martínez-Romero, Investigation of the effect of carbonyl iron micro-particles on the mechanical and rheological properties of isotropic and anisotropic MREs: constitutive magneto-mechanical material model, Polymers (Basel) 11 (10) (2019) 1705.
[147] G. Schubert, P. Harrison, Equi-biaxial tension tests on magneto-rheological elastomers, Smart Mater. Struct. 25 (1) (2015) 015015.
[148] Y. Zhou, S. Jerrams, L. Chen, Multi-axial fatigue in magnetorheological elastomers using bubble inflation, Mater. Des. 50 (2013) 68–71.
[149] D. Gorman, N. Murphy, R. Ekins, S. Jerrams, The evaluation of the effect of strain limits on the physical properties of Magnetorheological Elastomers subjected to uniaxial and biaxial cyclic testing, Int. J. Fatigue 103 (2017) 1–4.
[150] M. Hossain, D.K. Vu, P. Steinmann, Experimental study and numerical modelling of VHB 4910 polymer, Comput. Mater. Sci. 59 (2012) 65–74.
[151] M. Hossain, R. Navaratne, D. Perić, 3D printed elastomeric polyurethane: viscoelastic experimental characterizations and constitutive modelling with nonlinear viscosity functions, Int. J. Non Linear Mech. 126 (2020) 103546.
[152] M. Wissler, E. Mazza, Physical, Electromechanical coupling in dielectric elastomer actuators, Sens. Actuators, A. 138 (2) (2007) 384–393.
[153] R.K. Sahu, K. Patra, Structures, Rate-dependent mechanical behavior of VHB 4910 elastomer, Adv. Mater. Struct. 23 (2) (2016) 170–179.
[154] F. Carpi, D. De Rossi, Electroactive polymer-based devices for e-textiles in biomedicine, IEEE Trans. Inf. Technol. Biomed. 9 (3) (2005) 295–318.
[155] R. Pelrine, P. Sommer-Larsen, R.D. Kornbluh, R. Heydt, G. Kofod, Q. Pei, P. Gravesen, Applications of dielectric elastomer actuators, Smart Structures and Materials 2001: electroactive Polymer Actuators and Devices, Int. Soc. Opt. Photon. (2001) 335–349.
[156] Y. Zhao, J.-.W. Zha, L.-.J. Yin, Z.-.S. Gao, Y.-.Q. Wen, Z.-.M. Dang, Remarkable electrically actuation performance in advanced acrylic-based dielectric elastomers without pre-strain at very low driving electric field, Polymer (Guildf) 137 (2018) 269–275.
[157] M. Mehnert, M. Hossain, P. Steinmann, Experimental and numerical investigations of the electro-viscoelastic behavior of VHB 4905TM, Eur. J. Mech.-A/Solids 77 (2019) 103797.
[158] M. Shariff, R. Bustamante, J. Merodio, A nonlinear spectral rate-dependent constitutive equation for electro-viscoelastic solids, Z. Angewand. Math. Phys. 71 (4) (2020) 1–22.

[159] Y. Chen, G. Kang, J. Yuan, Y. Hu, T. Li, S. Qu, An electro-mechanically coupled visco-hyperelastic-plastic constitutive model for cyclic deformation of dielectric elastomers, Mech. Mater. 150 (2020) 103575.
[160] M. Hossain, D.K. Vu, P. Steinmann, A comprehensive characterization of the electro-mechanically coupled properties of VHB 4910 polymer, Arch. Appl. Mech. 85 (4) (2015) 523–537.
[161] X. Zhao, Q.J.A.P.R. Wang, Harnessing large deformation and instabilities of soft dielectrics:, Theory Exp. Appl. 1 (2) (2014) 021304.
[162] H. Godaba, C.C. Foo, Z.Q. Zhang, B.C. Khoo, J. Zhu, Giant voltage-induced deformation of a dielectric elastomer under a constant pressure, Appl. Phys. Lett. 105 (11) (2014) 112901.
[163] H.P. James, R. John, A. Alex, K. Anoop, Smart polymers for the controlled delivery of drugs–a concise overview, Acta Pharmaceutica Sinica B 4 (2) (2014) 120–127.
[164] J.S. Plante, S. Dubowsky, structures, Large-scale failure modes of dielectric elastomer actuators, Int. J. Solids Struct. 43 (25–26) (2006) 7727–7751.
[165] Y. Chen, G. Kang, J. Yuan, T. Li, S. Qu, Experimental investigation on electro-mechanically coupled cyclic deformation of laterally constrained dielectric elastomer, Polym. Test. 81 (2020) 106220.
[166] M. Wissler, E. Mazza, Electromechanical coupling in dielectric elastomer actuators, Sens. Actuat. A 138 (2) (2007) 384–393.
[167] X. Zhao, Q. Wang, Harnessing large deformation and instabilities of soft dielectrics: theory, experiment, and application, Appl. Phys. Rev. 1 (2) (2014) 021304.
[168] J.-.S. Plante, S. Dubowsky, Large-scale failure modes of dielectric elastomer actuators, Int. J. Solids Struct. 43 (25–26) (2006) 7727–7751.
[169] Y. Bai, Y. Jiang, B. Chen, C. Chiang Foo, Y. Zhou, F. Xiang, J. Zhou, H. Wang, Z. Suo, Cyclic performance of viscoelastic dielectric elastomers with solid hydrogel electrodes, Appl. Phys. Lett. 104 (6) (2014) 062902.
[170] W. Hong, Modeling viscoelastic dielectrics, J. Mech. Phys. Solids 59 (3) (2011) 637–650.
[171] J. Huang, S. Shian, Z. Suo, D.R. Clarke, Maximizing the energy density of dielectric elastomer generators using equi-biaxial loading, Adv. Funct. Mater. 23 (40) (2013) 5056–5061.
[172] J. Guo, R. Xiao, H.S. Park, T.D. Nguyen, The temperature-dependent viscoelastic behavior of dielectric elastomers, J. Appl. Mech. 82 (9) (2015).
[173] M. Mehnert, M. Hossain, P. Steinmann, P.o. Solids, A complete thermo-electro-viscoelastic characterization of dielectric elastomers, Part I: Exp. Investigat. 157 (2021) 104603.
[174] W. Fan, Y. Wang, S. Cai, Fatigue fracture of a highly stretchable acrylic elastomer, Polym. Test. 61 (2017) 373–377.
[175] Y. Chen, L. Agostini, G. Moretti, G. Berselli, M. Fontana, R. Vertechy, Fatigue life performances of silicone elastomer membranes for dielectric elastomer transducers: preliminary results, Electroactive Polymer Actuators and Devices (EAPAD) XXI, International Society for Optics and Photonics, 2019.
[176] N. Sultana, Biodegradable polymer-based scaffolds for bone tissue engineering, Biodegradable Polymer-Based Scaffolds For Bone Tissue Engineering, Springer, Berlin, Germany, 2013.
[177] T.T. Roberts, A.J. Rosenbaum, Bone grafts, bone substitutes and orthobiologics: the bridge between basic science and clinical advancements in fracture healing, Organogenesis 8 (4) (2012) 114–124.
[178] J.A. Hubbell, Biomaterials in tissue engineering, Bio/Technology 13 (6) (1995) 565–576.
[179] A. Dolcimascolo, G. Calabrese, S. Conoci, R. Parenti, Innovative Biomaterials for Tissue Engineering, Biomaterial-Supported Tissue Reconstruction or Regeneration, IntechOpen (2019), doi:10.5772/intechopen.83839.
[180] Y. Dong, S. Wang, Y. Ke, L. Ding, X. Zeng, S. Magdassi, Y. Long, 4D Printed hydrogels: fabrication, materials, and applications, Adv. Mater. Technol. (2020) 2000034.
[181] Q. Shi, H. Liu, D. Tang, Y. Li, X. Li, F. Xu, Bioactuators based on stimulus-responsive hydrogels and their emerging biomedical applications, NPG Asia Mater. 11 (1) (2019) 1–21.
[182] M. Champeau, D.A. Heinze, T.N. Viana, E.R. de Souza, A.C. Chinellato, S. Titotto, 4D printing of hydrogels: a review, Adv. Funct. Mater. 30 (2020) 1910606.
[183] S. Ribeiro, C. Ribeiro, E.O. Carvalho, C.R. Tubio, N. Castro, N. Pereira, V. Correia, A.C. Gomes, S. Lanceros-Méndez, Magnetically activated electroactive microenvironments for skeletal muscle tissue, regeneration 3 (7) (2020) 4239–4252.
[184] K. Ashtari, H. Nazari, H. Ko, P. Tebon, M. Akhshik, M. Akbari, S.N. Alhosseini, M. Mozafari, B. Mehravi, M. Soleimani, Electrically conductive nanomaterials for cardiac tissue engineering, Adv. Drug Deliv. Rev. 144 (2019) 162–179.
[185] S. Ahadian, R. Obregón, J. Ramón-Azcón, G. Salazar, H. Shiku, M. Ramalingam, T. Matsue, Carbon nanotubes and graphene-based nanomaterials for stem cell differentiation and tissue regeneration, J. Nanosci. Nanotechnol. 16 (9) (2016) 8862–8880.
[186] T. Gupta, S. Aithal, S. Mishriki, R.P. Sahu, F. Geng, I.K. Puri, Label-free magnetic field-assisted assembly of layer-on-layer cellular structures, ACS Biomater. Sci. Eng. 6 (2020) 4294–4303 8.
[187] F. Mushtaq, H. Torlakcik, Q. Vallmajo-Martin, E.C. Siringil, J. Zhang, C. Röhrig, Y. Shen, Y. Yu, X.Z. Chen, R. Müller, B. J. Nelson, S. Pané, Magnetoelectric 3D scaffolds for enhanced bone cell proliferation, Appl. Mater. Today. 16 (2019) 290–300.
[188] Y. Du, J.L. Guo, J. Wang, A.G. Mikos, S. Zhang, Hierarchically designed bone scaffolds: from internal cues to external stimuli, Biomaterials 218 (2019) 119334.
[189] S. Panseri, A. Russo, G. Giavaresi, M. Sartori, F. Veronesi, M. Fini, D. Salter, A. Ortolani, A. Strazzari, A. Visani, Innovative magnetic scaffolds for orthopedic tissue engineering, J. Biomed. Mater. Res. Part A 100 (9) (2012) 2278–2286.
[190] E.D. Silva, P.S. Babo, R. Costa-Almeida, R.M. Domingues, B.B. Mendes, E. Paz, P. Freitas, M.T. Rodrigues, P.L. Granja, M.E. Gomes, Multifunctional magnetic-responsive hydrogels to engineer tendon-to-bone interface, Nanomedicine 14 (7) (2018) 2375–2385.
[191] C. Fanelli, S. Coppola, R. Barone, C. Colussi, G. Gualandi, P. Volpe, L. Ghibelli, Magnetic fields increase cell survival by inhibiting apoptosis via modulation of Ca2+ influx, The FASEB journal 13 (1) (1999) 95–102.
[192] C.J. Kowalczewski, J.M. Saul, Biomaterials for the delivery of growth factors and other therapeutic agents in tissue engineering approaches to bone regeneration, Front. Pharmacol. 9 (2018) 513.
[193] J. Rouwkema, N.C. Rivron, C.A. van Blitterswijk, Vascularization in tissue engineering, Trends Biotechnol. 26 (8) (2008) 434–441.
[194] M. Filippi, B. Dasen, J. Guerrero, F. Garello, G. Isu, G. Born, M. Ehrbar, I. Martin, A. Scherberich, Magnetic nanocomposite hydrogels and static magnetic field stimulate the osteoblastic and vasculogenic profile of adipose-derived cells, Biomaterials 223 (2019) 119468.
[195] Z. Liu, J. Liu, X. Cui, X. Wang, L. Zhang, P. Tang, Recent advances on magnetic sensitive hydrogels in tissue engineering, Front. Chem. 8 (2020).
[196] Y. Xia, J. Sun, L. Zhao, F. Zhang, X.-J. Liang, Y. Guo, M.D. Weir, M.A. Reynolds, N. Gu, H.H. Xu, Magnetic field and nano-scaffolds with stem cells to enhance bone regeneration, Biomaterials 183 (2018) 151–170.
[197] R. Hou, G. Zhang, G. Du, D. Zhan, Y. Cong, Y. Cheng, J. Fu, Magnetic nanohydroxyapatite/PVA composite hydrogels for promoted osteoblast adhesion and proliferation, Colloids Surf. B 103 (2013) 318–325.
[198] C. Ribeiro, J. Pärssinen, V. Sencadas, V. Correia, S. Miettinen, V.P. Hytönen, S. Lanceros-Méndez, Dynamic piezoelectric stimulation enhances osteogenic differentiation of human adipose stem cells, J. Biomed. Mater. Res. Part A 103 (6) (2015) 2172–2175.
[199] T. Zheng, Y. Huang, X. Zhang, Q. Cai, X. Deng, X. Yang, Mimicking the electrophysiologic microenvironment of bone tissue using electroactive materials to promote its regeneration, J. Mater. Chem. B 8 (2020) 45.
[200] H. Liu, M. Lin, X. Liu, Y. Zhang, Y. Luo, Y. Pang, H. Chen, D. Zhu, X. Zhong, S. Ma, Doping bioactive elements into a collagen scaffold based on synchronous self-assembly/mineralization for bone tissue engineering, Bioactive Mater. 5 (4) (2020) 844–858.
[201] L. García-Martínez, F. Campos, C. Godoy-Guzmán, M. del Carmen Sánchez-Quevedo, I. Garzón, M. Alaminos, A. Campos, V. Carriel, Encapsulation of human elastic cartilage-derived chondrocytes in nanostructured fibrin-agarose hydrogels, Histochem. Cell Biol. 147 (1) (2017) 83–95.
[202] A.B. Bonhome-Espinosa, F. Campos, D. Durand-Herrera, J.D. Sánchez-López, S. Schaub, J.D. Durán, M.T. Lopez-Lopez, V. Carriel, *In vitro* characterization of a novel magnetic fibrin-agarose hydrogel for cartilage tissue engineering, J. Mech. Behav. Biomed. Mater. 104 (2020) 103619.
[203] J. Huang, Y. Liang, Z. Jia, J. Chen, L. Duan, W. Liu, F. Zhu, Q. Liang, W. Zhu, W. You, Development of magnetic nanocomposite hydrogel with potential cartilage tissue engineering, ACS Omega 3 (6) (2018) 6182–6189.
[204] J. Huang, Y. Liang, Z. Huang, P. Zhao, Q. Liang, Y. Liu, L. Duan, W. Liu, F. Zhu, L. Bian, Magnetic enhancement of chondrogenic differentiation of mesenchymal stem cells, ACS Biomater. Sci. Eng. 5 (5) (2019) 2200–2207.
[205] W. Yang, P. Zhu, H. Huang, Y. Zheng, J. Liu, L. Feng, H. Guo, S. Tang, R. Guo, Functionalization of novel theranostic hydrogels with kartogenin-grafted USPIO nanoparticles to enhance cartilage regeneration, ACS Appl. Mater. Interfaces 11 (38) (2019) 34744–34754.
[206] H. Esmaeili, A. Patino-Guerrero, M. Hasany, M.O. Aansari, A. Memic, A. Dolatshahi-Pirouz, M. Nikkhah, Electroconductive biomaterials for cardiac tissue engineering, Acta Biomater (2021) In press, doi:10.1016/j.actbio.2021.08.031.
[207] B.S. Spearman, A.J. Hodge, J.L. Porter, J.G. Hardy, Z.D. Davis, T. Xu, X. Zhang, C.E. Schmidt, M.C. Hamilton, E.A. Lipke, Conductive interpenetrating networks of polypyrrole and polycaprolactone encourage electrophysiological development of cardiac cells, Acta Biomater. 28 (2015) 109–120.
[208] A. Gelmi, A. Cieslar-Pobuda, E. de Muinck, M. Los, M. Rafat, E.W. Jager, Direct mechanical stimulation of stem cells: a beating electromechanically active scaffold for cardiac tissue engineering, Adv. Healthc. Mater. 5 (12) (2016) 1471–1480.
[209] L. Wang, J. Jiang, W. Hua, A. Darabi, X. Song, C. Song, W. Zhong, M.M. Xing, X. Qiu, Mussel-inspired conductive cryogel as cardiac tissue patch to repair myocardial infarction by migration of conductive nanoparticles, Adv. Funct. Mater. 26 (24) (2016) 4293–4305.
[210] M. Sabzi, M. Babaahmadi, M. Rahnama, Thermally and electrically triggered triple-shape memory behavior of poly (vinyl acetate)/poly (lactic acid) due to graphene-induced phase separation, ACS Appl. Mater. Interfaces 9 (28) (2017) 24061–24070.
[211] M. Cabiati, F. Vozzi, F. Gemma, F. Montemurro, C. De Maria, G. Vozzi, C. Domenici, S. Del Ry, Cardiac tissue regeneration: a preliminary study on carbon-based nanotubes gelatin scaffold, J. Biomed. Mater. Res. Part B 106 (8) (2018) 2750–2762.
[212] S. Mombini, J. Mohammadnejad, B. Bakhshandeh, A. Narmani, J. Nourmohammadi, S. Vahdat, S. Zirak, Chitosan-PVA-CNT nanofibers as electrically conductive scaffolds for cardiovascular tissue engineering, Int. J. Biol. Macromol. 140 (2019) 278–287.

[213] A. Abedi, B. Bakhshandeh, A. Babaie, J. Mohammadnejad, S. Vahdat, R. Mombeiny, S.R. Moosavi, J. Amini, L. Tayebi, Concurrent application of conductive biopolymeric chitosan/polyvinyl alcohol/MWCNTs nanofibers, intracellular signaling manipulating molecules and electrical stimulation for more effective cardiac tissue engineering, Mater. Chem. Phys. (2020) 123842.
[214] A.Le Huu, A. Paul, L. Xu, S. Prakash, D. Shum-Tim, Recent advancements in tissue engineering for stem cell-based cardiac therapies, Ther. Deliv. 4 (4) (2013) 503–516.
[215] M. Namdari, A. Eatemadi, Cardioprotective effects of curcumin-loaded magnetic hydrogel nanocomposite (nanocurcumin) against doxorubicin-induced cardiac toxicity in rat cardiomyocyte cell lines, Artificial cells, Nanomed. Biotechnol. 45 (4) (2017) 731–739.
[216] M. Kapnisi, C. Mansfield, C. Marijon, A.G. Guex, F. Perbellini, I. Bardi, E.J. Humphrey, J.L. Puetzer, D. Mawad, D.C. Koutsogeorgis, Auxetic cardiac patches with tunable mechanical and conductive properties toward treating myocardial infarction, Adv. Funct. Mater. 28 (21) (2018) 1800618.
[217] S. Richard, A.K. Silva, G.t. Mary, H. Ragot, J.E. Perez, C. Ménager, F. Gazeau, I. Boucenna, O. Agbulut, C. Wilhelm, 3D magnetic alignment of cardiac cells in, hydrogels 3 (10) (2020) 6802–6810.
[218] R. Boni, A. Ali, A. Shavandi, A.N. Clarkson, Current and novel polymeric biomaterials for neural tissue engineering, J. Biomed. Sci. 25 (1) (2018) 90.
[219] G.C. De Ruiter, M.J. Malessy, M.J. Yaszemski, A.J. Windebank, R.J. Spinner, Designing ideal conduits for peripheral nerve repair, Neurosurg. Focus 26 (2) (2009) E5.
[220] A. Omidinia-Anarkoli, S. Boesveld, U. Tuvshindorj, J.C. Rose, T. Haraszti, L. De Laporte, An injectable hybrid hydrogel with oriented short fibers induces unidirectional growth of functional nerve cells, Small 13 (36) (2017) 1702207.
[221] S. Vijayavenkataraman, N. Vialli, J.Y. Fuh, W.F. Lu, Conductive collagen/polypyrrole-b-polycaprolactone hydrogel for bioprinting of neural tissue constructs, Int. J. Bioprint. 5 (2.1) (2019).
[222] J. Costa, M. Ghilardi, V. Mamone, V. Ferrari, J.J. Busfield, A. Ahluwalia, F. Carpi, Bioreactor with electrically deformable curved membranes for mechanical stimulation of cell cultures, Frong Bioeng. Biotechnol. 8 (2020) 22.
[223] C. Gao, Z. Li, J. Zou, J. Cheng, K. Jiang, C. Liu, G. Gu, W. Tao, J. Song, Mechanical effect on gene transfection based on dielectric elastomer, ACS Appl. Bio Mater. 3 (5) (2020) 2617–2625.
[224] A. Poulin, M. Imboden, F. Sorba, S. Grazioli, C. Martin-Olmos, S. Rosset, H.J. Shea, An ultra-fast mechanically active cell culture substrate, Sci. Rep. 8 (1) (2018) 1–10.
[225] B. Mues, B. Bauer, A.A. Roeth, J. Ortega, E.M. Buhl, P. Radon, F. Wiekhorst, T. Gries, T. Schmitz-Rode, I. Slabu, Nanomagnetic actuation of hybrid stents for hyperthermia treatment of hollow organ tumors, Nanomaterials (Basal) 11 (3) (2021) 618.
[226] A.R. Farooqi, J. Zimmermann, R. Bader, U. van Rienen, Computational study on electromechanics of electroactive hydrogels for cartilage-tissue repair, Comput. Methods Programs Biomed. (2020) 105739.
[227] A.R. Farooqi, J. Zimmermann, R. Bader, U. van Rienen, Numerical simulation of electroactive hydrogels for cartilage–tissue engineering, Materials (Basel) 12 (18) (2019) 2913.
[228] Y. Xia, Y. He, F. Zhang, Y. Liu, J. Leng, A review of shape memory polymers and composites: mechanisms, materials, and applications, J. Adv. Mater. 33 (6) (2021) 2000713.
[229] C. Zhang, D. Cai, P. Liao, J.-.W. Su, H. Deng, B. Vardhanabhuti, B.D. Ulery, S.-Y. Chen, J. Lin, 4D Printing of shape-memory polymeric scaffolds for adaptive biomedical implantation, J. Acta Biomater. 122 (2021) 101–110.
[230] J.Y. Park, J.B. Lee, W.B. Shin, M.L. Kang, Y.C. Shin, D.H. Son, S.W. Yi, J.K. Yoon, J.Y. Kim, J. Ko, et al., Nasolacrimal stent with shape memory as an advanced alternative to silicone products, Acta Biomater 101 (2020) 273–284.
[231] C. Lin, J. Lv, Y. Li, F. Zhang, J. Li, Y. Liu, L. Liu, J. Leng, 4D-printed biodegradable and remotely controllable shape memory occlusion devices, Adv. Funct. Mater. 29 (51) (2019) 1906569.
[232] Y. Wu, J.K. Yim, J. Liang, Z. Shao, M. Qi, J. Zhong, Z. Luo, X. Yan, M. Zhang, X. Wang, et al., Insect-scale fast moving and ultrarobust soft robot, Sci. Rob. 4 (32) (2019).
[233] K. Yamagishi, A. Nojiri, E. Iwase, M. Hashimoto, Syringe-injectable, self-expandable, and ultraconformable magnetic ultrathin films, ACS Appl. Mater. Interfaces 11 (44) (2019) 41770–41779.
[234] C. Lin, J. Lv, Y. Li, F. Zhang, J. Li, Y. Liu, L. Liu, J. Leng, 4D-printed biodegradable and remotely controllable shape memory occlusion devices, Adv. Funct. Mater. 29 (51) (2019) 1906569.
[235] M.W. Tibbitt, J.E. Dahlman, R. Langer, Emerging frontiers in drug delivery, J. Am. Chem. Soc. 138 (3) (2016) 704–717.
[236] T.R. Hoare, D.S. Kohane, Hydrogels in drug delivery: progress and challenges, Polymer (Guildf) 49 (8) (2008) 1993–2007.
[237] J. Li, D.J. Mooney, Designing hydrogels for controlled drug delivery, Nat. Rev. Mater. 1 (12) (2016) 1–17.
[238] G. Tiwari, R. Tiwari, B. Sriwastawa, L. Bhati, S. Pandey, P. Pandey, S.K. Bannerjee, Drug delivery systems: an updated review, Int. J. Pharm. Investig. 2 (1) (2012) 2.
[239] S. Bhatia, Nanoparticles types, classification, characterization, fabrication methods and drug delivery applications, in: Natural Polymer Drug Delivery Systems, Springer, 2016, pp. 33–93.
[240] R.B. KC, B. Thapa, P. Xu, pH and redox dual responsive nanoparticle for nuclear targeted drug delivery, Mol. Pharm. 9 (9) (2012) 2719–2729.
[241] A. Zhang, K. Jung, A. Li, J. Liu, C. Boyer, Recent advances in stimuli-responsive polymer systems for remotely controlled drug release, Prog. Polym. Sci. 99 (2019) 101164.
[242] M. Shahrousvand, M.S. Hoseinian, M. Ghollasi, A. Karbalaeimahdi, A. Salimi, F.A. Tabar, Flexible magnetic polyurethane/Fe2O3 nanoparticles as organic-inorganic nanocomposites for biomedical applications: properties and cell behavior, Mater. Sci. Eng. 74 (2017) 556–567.
[243] C. Alvarez-Lorenzo, A. Concheiro, Smart drug delivery systems: from fundamentals to the clinic, Chem. Commun. 50 (58) (2014) 7743–7765.
[244] M. Pereira-Silva, I. Jarak, A.C. Santos, F. Veiga, A. Figueiras, Micelleplex-based nucleic acid therapeutics: from targeted stimuli-responsiveness to nanotoxicity and regulation, Eur. J. Pharm. Sci. 153 (2020) 105461.
[245] S. Chaterji, I.K. Kwon, K. Park, Smart polymeric gels: redefining the limits of biomedical devices, Prog. Polym. Sci. 32 (8–9) (2007) 1083–1122.
[246] M. Ebara, Y. Kotsuchibashi, K. Uto, T. Aoyagi, Y.-J. Kim, R. Narain, N. Idota, J.M. Hoffman, in: Smart Hydrogels, Smart Biomaterials, Springer, 2014, pp. 9–65.
[247] D. Qureshi, S.K. Nayak, S. Maji, A. Anis, D. Kim, K. Pal, Environment sensitive hydrogels for drug delivery applications, Eur. Polym. J. 120 (2019) 109220.
[248] T. Vangijzegem, D. Stanicki, S. Laurent, Magnetic iron oxide nanoparticles for drug delivery: applications and characteristics, Expert Opin. Drug Deliv. 16 (1) (2019) 69–78.
[249] E. Ying, H.-.M. Hwang, *In vitro* evaluation of the cytotoxicity of iron oxide nanoparticles with different coatings and different sizes in A3 human T lymphocytes, Sci. Tot. Environ. 408 (20) (2010) 4475–4481.
[250] W. Chen, M. Sun, X. Fan, H. Xie, Magnetic/pH-sensitive double-layer microrobots for drug delivery and sustained release, Appl. Mater. Today. 19 (2020) 100583.
[251] S. Kralj, T. Potrc, P. Kocbek, S. Marchesan, D. Makovec, Design and fabrication of magnetically responsive nanocarriers for drug delivery, Curr. Med. Chem. 24 (5) (2017) 454–469.
[252] R. Münter, K. Kristensen, D. Pedersbæk, T.L. Andresen, J.B. Simonsen, J.B. Larsen, Quantitative methods for investigating dissociation of fluorescently labeled lipids from drug delivery liposomes, in: Nanotechnology Characterization Tools For Tissue Engineering and Medical Therapy, Springer, 2019, pp. 333–359.
[253] J. Liao, H. Huang, Review on magnetic natural polymer constructed hydrogels as vehicles for drug delivery, Biomacromolecules 21 (7) (2020) 2574–2594.
[254] M. Häring, J. Schiller, J. Mayr, S. Grijalvo, R. Eritja, D.D. Díaz, Magnetic gel composites for hyperthermia cancer therapy, Gels 1 (2) (2015) 135–161.
[255] K. Hu, J. Sun, Z. Guo, P. Wang, Q. Chen, M. Ma, N. Gu, A novel magnetic hydrogel with aligned magnetic colloidal assemblies showing controllable enhancement of magnetothermal effect in the presence of alternating magnetic field, Adv. Mater. 27 (15) (2015) 2507–2514.
[256] E. Guisasola, M. Vallet-Regí, A. Baeza, Magnetically responsive polymers for drug delivery applications, in: Stimuli Responsive Polymeric Nanocarriers for Drug Delivery Applications, Volume 1, Elsevier, 2018, pp. 143–168.
[257] R.V. Stigliano, F. Shubitidze, J.D. Petryk, L. Shoshiashvili, A.A. Petryk, P.J. Hoopes, Mitigation of eddy current heating during magnetic nanoparticle hyperthermia therapy, Int. J. Hyperther. 32 (7) (2016) 735–748.
[258] C.A. Cezar, S.M. Kennedy, M. Mehta, J.C. Weaver, L. Gu, H. Vandenburgh, D.J. Mooney, Biphasic ferrogels for triggered drug and cell delivery, Adv. Healthc. Mater. 3 (11) (2014) 1869–1876.
[259] A.M. Hawkins, N.S. Satarkar, J.Z. Hilt, Nanocomposite degradable hydrogels: demonstration of remote controlled degradation and drug release, Pharm. Res. 26 (3) (2009) 667–673.
[260] J. Qin, I. Asempah, S. Laurent, A. Fornara, R.N. Muller, M. Muhammed, Injectable superparamagnetic ferrogels for controlled release of hydrophobic drugs, Adv. Mater. 21 (13) (2009) 1354–1357.
[261] Y. Wang, B. Li, F. Xu, Z. Han, D. Wei, D. Jia, Y. Zhou, Tough magnetic chitosan hydrogel nanocomposites for remotely stimulated drug release, Biomacromolecules 19 (8) (2018) 3351–3360.
[262] N.S. Satarkar, J.Z. Hilt, Magnetic hydrogel nanocomposites for remote controlled pulsatile drug, release 130 (3) (2008) 246–251.
[263] E.G. Fuller, H. Sun, R.D. Dhavalikar, M. Unni, G.M. Scheutz, B.S. Sumerlin, C. Rinaldi, Externally triggered heat and drug release from magnetically controlled nanocarriers, ACS Appl. Polym. Mater. 1 (2) (2019) 211–220.
[264] W. Xie, Q. Gao, Z. Guo, D. Wang, F. Gao, X. Wang, Y. Wei, L. Zhao, Injectable and self-healing thermosensitive magnetic hydrogel for asynchronous control release of doxorubicin and docetaxel to treat triple-negative breast cancer, ACS Appl. Mater. Interfaces 9 (39) (2017) 33660–33673.
[265] Q. Yan, J. Yuan, Z. Cai, Y. Xin, Y. Kang, Y. Yin, Voltage-responsive vesicles based on orthogonal assembly of two homopolymers, J. Am. Chem. Soc. 132 (27) (2010) 9268–9270.
[266] G. Kaur, R. Adhikari, P. Cass, M. Bown, P. Gunatillake, Electrically conductive polymers and composites for biomedical applications, RSC Adv. 5 (47) (2015) 37553–37567.
[267] J. Kolosnjaj-Tabi, L. Gibot, I. Fourquaux, M. Golzio, M.-.P. Rols, Electric field-responsive nanoparticles and electric fields: physical, chemical, biological mechanisms and therapeutic prospects, Adv. Drug Deliv. Rev. 138 (2019) 56–67.
[268] D. Uppalapati, B.J. Boyd, S. Garg, J. Travas-Sejdic, D. Svirskis, Conducting polymers with defined micro-or nanostructures for drug delivery, Biomaterials 111 (2016) 149–162.

[269] J. Qu, et al., Injectable antibacterial conductive hydrogels with dual response to an electric field and pH for localized “smart” drug release, Acta Biomater. 72 (2018) 55–69.
[270] J.Z. GulZeb, M. Sajid, M.M. Rehman, G.U. Siddiqui, I. Shah, K.H. Kim, K.H. Choi, 3D printing for soft robotics–a review, Sci. Technol. Adv. Mater. 19 (1) (2018) 243–262.
[271] T. Manouras, M. Vamvakaki, Field responsive materials: photo-, electro-, magnetic-and ultrasound-sensitive polymers, Polym. Chem. 8 (1) (2017) 74–96.
[272] C. Pérez-Martínez, S.D.M. Chávez, T. del Castillo-Castro, T.E.L. Ceniceros, M. Castillo-Ortega, D. Rodríguez-Félix, J.C.G. Ruiz, Electroconductive nanocomposite hydrogel for pulsatile drug release, React. Funct. Polym. 100 (2016) 12–17.
[273] S.B. Patil, S.Z. Inamdar, K.K. Das, K.G. Akamanchi, A.V. Patil, A.C. Inamadar, K.R. Reddy, A.V. Raghu, R.V. Kulkarni, Tailor-made electrically-responsive poly (acrylamide)-graft-pullulan copolymer based transdermal drug delivery systems: synthesis, characterization, in-vitro and ex-vivo evaluation, J. Drug Deliv. Sci. Technol. 56 (2020) 101525.
[274] M.R. Prausnitz, R. Langer, Transdermal drug delivery, Nat. Biotechnol. 26 (11) (2008) 1261–1268.
[275] S. Campbell, D. Maitland, T. Hoare, Enhanced pulsatile drug release from injectable magnetic hydrogels with embedded thermosensitive microgels, ACS Macro Lett. 4 (3) (2015) 312–316.
[276] S.H. Hu, T.Y. Liu, D.M. Liu, S. Y. Chen, Controlled pulsatile drug release from a ferrogel by a high-frequency magnetic field, Macromolecules 40 (19) (2007) 6786–6788.
[277] T. Lammers, S. Aime, W.E. Hennink, G. Storm, F. Kiessling, Theranostic nanomedicine, Acc. Chem. Res. 44 (10) (2011) 1029–1038.
[278] J. Salamon, J. Dieckhoff, M. Kaul, C. Jung, G. Adam, M. Möddel, T. Knopp, S. Draack, F. Ludwig, H. Ittrich, Visualization of spatial and temporal temperature distributions with magnetic particle imaging for liver tumor ablation therapy, Sci. Rep. 10 (1) (2020) 1–11.
[279] C. Rümenapp, B. Gleich, H. Axel, Magnetic nanoparticles in magnetic resonance imaging and diagnostics, Pharm. Res. 29 (5) (2012) 1165–1179.
[280] K.T. Arul, E. Manikandan, P. Murmu, J. Kennedy, M. Henini, Enhanced magnetic properties of polymer-magnetic nanostructures synthesized by ultrasonication, J. Alloys Comp. 720 (2017) 395–400.
[281] L.M. Ali, P. Marzola, E. Nicolato, S. Fiorini, S. Heras Guillamón, R. Piñol, L. Gabilondo, A. Millán, F. Palacio, Polymer-coated superparamagnetic iron oxide nanoparticles as T2 contrast agent for MRI and their uptake in liver, Fut. Sci. OA (2019) FSO235 (0).
[282] S. Miao, M. Nowicki, H. Cui, S.-J. Lee, X. Zhou, D.K. Mills, L.G. Zhang, 4D anisotropic skeletal muscle tissue constructs fabricated by staircase effect strategy, Biofabrication 11 (3) (2019) 035030.
[283] Y. Wei, R. Liao, H. Liu, H. Li, H. Xu, Q. Zhou, Biocompatible low-retention superparamagnetic iron oxide nanoclusters as contrast agents for magnetic resonance imaging of liver tumor, J. Biomed. Nanotechnol. 11 (5) (2015) 854–864.
[284] S.M. Dadfar, K. Roemhild, N.I. Drude, S. von Stillfried, R. Knüchel, F. Kiessling, T. Lammers, Iron oxide nanoparticles: diagnostic, therapeutic and theranostic applications, Adv. Drug Deliv. Rev. 138 (2019) 302–325.
[285] H. Sakuma, Coronary CT *versus* MR angiography: the role of MR angiography, Radiology 258 (2) (2011) 340–349.
[286] H. Gong, R. Peng, Z. Liu, Carbon nanotubes for biomedical imaging: the recent advances, Adv. Drug Deliv. Rev. 65 (15) (2013) 1951–1963.
[287] M.-A. Shahbazi, L. Faghfouri, M.P. Ferreira, P. Figueiredo, H. Maleki, F. Sefat, J. Hirvonen, H.A. Santos, The versatile biomedical applications of bismuth-based nanoparticles and composites: therapeutic, diagnostic, biosensing, and regenerative properties, Chem. Soc. Rev. 49 (4) (2020) 1253–1321.
[288] G. Chen, B. Dodson, F. Johnson, I. Hancu, E. Fiveland, W. Zhang, C. Galligan, C. Puleo, R.C. Davis, J. Ashe, Tissue-susceptibility matched carbon nanotube electrodes for magnetic resonance imaging, J. Magn. Reson. 295 (2018) 72–79.
[289] Y. Guo, W. Duan, C. Ma, C. Jiang, Y. Xie, H. Hao, R. Wang, L. Li, Biocompatibility and magnetic resonance imaging characteristics of carbon nanotube yarn neural electrodes in a rat model, Biomed. Eng. Online 14 (1) (2015) 1–13.
[290] L. Minati, V. Antonini, M. Dalla Serra, G. Speranza, Multifunctional branched gold–carbon nanotube hybrid for cell imaging and drug delivery, Langmuir 28 (45) (2012) 15900–15906.
[291] K. Hola, Z. Markova, G. Zoppellaro, J. Tucek, R. Zboril, Tailored functionalization of iron oxide nanoparticles for MRI, drug delivery, magnetic separation and immobilization of biosubstances, Biotechnol. Adv. 33 (6) (2015) 1162–1176.
[292] F. Momeni, X. Liu, J. Ni, A review of 4D printing, Mater. Des. 122 (2017) 42–79.
[293] L. Jing, X. Liang, X. Li, Y. Yang, Z. Dai, Covalent attachment of Mn-porphyrin onto doxorubicin-loaded poly (lactic acid) nanoparticles for potential magnetic resonance imaging and pH-sensitive drug delivery, Acta Biomater. 9 (12) (2013) 9434–9441.
[294] L. Sun, X. Gao, D. Wu, Q. Guo, Advances in physiologically relevant actuation of shape memory polymers for biomedical applications, Polym. Rev. (2020) 1–39.
[295] U. Nath, B.C. Crawford, R. Carpenter, E. Coen, Genetic control of surface curvature, Science 299 (5611) (2003) 1404–1407.
[296] E. Hajiesmaili, D.R. Clarke, Reconfigurable shape-morphing dielectric elastomers using spatially varying electric fields, Nat. Commun. 10 (1) (2019) 1–7.
[297] Y.S. Zhang, A. Khademhosseini, Advances in engineering hydrogels, Science 356 (6337) (2017).
[298] H. Guo, J. Cheng, K. Yang, K. Demella, T. Li, S.R. Raghavan, Z. Nie, Programming the shape transformation of a composite hydrogel sheet via erasable and rewritable nanoparticle patterns, ACS Appl. Mater. Interfaces 11 (45) (2019) 42654–42660.
[299] Z. Ren, W. Hu, X. Dong, M. Sitti, Multi-functional soft-bodied jellyfish-like swimming, Nat. Commun. 10 (1) (2019) 1–12.
[300] X. Yu, Z. Xie, Y. Yu, J. Lee, A. Vazquez-Guardado, H. Luan, J. Ruban, X. Ning, A. Akhtar, D. Li, Skin-integrated wireless haptic interfaces for virtual and augmented reality, Nature 575 (7783) (2019) 473–479.
[301] G.Z. Lum, Z. Ye, X. Dong, H. Marvi, O. Erin, W. Hu, M. Sitti, Shape-programmable magnetic soft matter, Proc. Nat. Acad. Sci. 113 (41) (2016) E6007–E6015.
[302] J. Tang, Q. Yin, Y. Qiao, T. Wang, Shape morphing of hydrogels in alternating magnetic field, ACS Appl. Mater. Interfaces 11 (23) (2019) 21194–21200.
[303] Y. Zhang, Q. Wang, S. Yi, Z. Lin, C. Wang, Z. Chen, L. Jiang, Interfaces, 4D printing of magnetoactive soft materials for on-demand magnetic actuation transformation, ACS Appl. Mater. Interfaces. 13 (3) (2021) 4174–4184.
[304] J.J. Abbott, E. Diller, A.J. Petruska, Magnetic methods in robotics, annual review of control, Robot. Auton. Syst. 3 (1) (2020) 57–90.
[305] S.M. Montgomery, S. Wu, X. Kuang, C.D. Armstrong, C. Zemelka, Q. Ze, R. Zhang, R. Zhao, H.J. Qi, Magneto-mechanical metamaterials with widely tunable mechanical properties and acoustic bandgaps, Adv. Funct. Mater.31(3) (2020).
[306] G.Z. Lum, Z. Ye, X. Dong, H. Marvi, O. Erin, W. Hu, M. Sitti, Shape-programmable magnetic soft matter, Proc. Natl. Acad. Sci. U. S. A. 113 (41) (2016) E6007–E6015.
[307] Y. Li, Z. Qi, J. Yang, M. Zhou, X. Zhang, W. Ling, Y. Zhang, Z. Wu, H. Wang, B.J.A.F.M. Ning, Origami NdFeB flexible magnetic membranes with enhanced magnetism and programmable sequences of polarities, Adv. Funct. Mater. 29 (44) (2019) 1904977.
[308] W. Hu, G.Z. Lum, M. Mastrangeli, M. Sitti, Small-scale soft-bodied robot with multimodal locomotion, Nature 554 (7690) (2018) 81–85.
[309] X. Gong, K. Tan, Q. Deng, S. Shen, Athermal shape memory effect in magnetoactive elastomers, ACS Appl. Mater. Interfaces 12 (14) (2020) 16930–16936.
[310] S.M. Montgomery, S. Wu, X. Kuang, C.D. Armstrong, C. Zemelka, Q. Ze, R. Zhang, R. Zhao, H.J. Qi, Magneto-mechanical metamaterials with widely tunable mechanical properties and acoustic bandgaps, Adv. Funct. Mater. (2020) 2005319 n/a(n/a).
[311] H. Deng, K. Sattari, Y. Xie, P. Liao, Z. Yan, J. Lin, Laser reprogramming magnetic anisotropy in soft composites for reconfigurable 3D shaping, Nat. Commun. 11 (1) (2020) 6325.
[312] J. Kim, S.E. Chung, S.E. Choi, H. Lee, J. Kim, S. Kwon, Programming magnetic anisotropy in polymeric microactuators, Nat. Mater. 10 (10) (2011) 747–752.
[313] T. Xu, J. Zhang, M. Salehizadeh, O. Onaizah, E. Diller, Millimeter-scale flexible robots with programmable three-dimensional magnetization and motions, Sci. Robot. 4 (29) (2019).
[314] T. Xu, J. Zhang, M. Salehizadeh, O. Onaizah, E. Diller, Millimeter-scale flexible robots with programmable three-dimensional magnetization and motions, Sci. Robot. 4 (29) (2019).
[315] Y. Lei, Z. Sheng, J. Zhang, J. Liu, W. Lv, X. Hou, Building magnetoresponsive composite elastomers for bionic locomotion applications, J. Bionic. Eng. 17 (2020) 405–420.
[316] S. Wu, C.M. Hamel, Q. Ze, F. Yang, H.J. Qi, R. Zhao, Evolutionary algorithm-guided voxel-encoding printing of functional hard-magnetic soft active materials, Adv. Intell. Syst. (2020) 2000060.
[317] H. Song, H. Lee, J. Lee, J.K. Choe, S. Lee, J.Y. Yi, S. Park, J.-.W. Yoo, M.S. Kwon, J. Kim, Reprogrammable ferromagnetic domains for reconfigurable soft magnetic actuators, Nano Lett. 20 (7) (2020) 5185–5192.
[318] J. Jeon, J.E. Park, S.J. Park, S. Won, H. Zhao, S. Kim, B.S. Shim, A. Urbas, A.J. Hart, Z. Ku, Shape-Programmed Fabrication and Actuation of Magnetically Active Micropost Arrays, ACS Appl. Mater. Interfaces 12 (14) (2020) 17113–17120.
[319] J.E. Park, J. Jeon, S.J. Park, S. Won, Z. Ku, J.J. Wie, Enhancement of magneto-mechanical actuation of micropillar arrays by anisotropic stress distribution, Small 16 (38) (2020) 2003179.
[320] A. Zolfagharian, A. Kaynak, M. Bodaghi, A.Z. Kouzani, S. Gharaie, S. Nahavandi, Control-based 4D printing: adaptive 4D-printed systems, Appl. Sci. 10 (9) (2020) 3020.
[321] J.A.C. Liu, B.A. Evans, J.B. Tracy, Photothermally reconfigurable shape memory magnetic cilia, Adv. Mater. Technol. 5 (7) (2020) 2000147.
[322] J. Cui, T.-Y. Huang, Z. Luo, P. Testa, H. Gu, X.-Z. Chen, B.J. Nelson, L.J. Heyderman, Nanomagnetic encoding of shape-morphing micromachines, Nature 575 (7781) (2019) 164–168.
[323] F. Chen, K. Liu, X. Zhu, Buckling-induced Shape Morphing using Dielectric Elastomer Actuators Patterned with Spatially-varying Electrodes, in: 2019 IEEE/RSJ International Conference on Intelligent Robots and Systems (IROS), IEEE, 2019, pp. 8306–8311.
[324] E. Hajiesmaili, E. Khare, A. Chortos, J. Lewis, D.R. Clarke, Voltage-controlled morphing of dielectric elastomer circular sheets into conical surfaces, Extreme Mech. Lett. 30 (2019) 100504.
[325] Z.S. Davidson, H. Shahsavan, A. Aghakhani, Y. Guo, L. Hines, Y. Xia, S. Yang, M. Sitti, Monolithic shape-programmable dielectric liquid crystal elastomer actuators, Sci. Adv. 5 (11) (2019) eaay0855.
[326] S. Pringpromsuk, H. Xia, Q.-.Q. Ni, Multifunctional stimuli-responsive shape memory polyurethane gels for soft actuators, Sens. Actuat. A 313 (2020) 112207.

[327] B. Aksoy, H. Shea, Reconfigurable and latchable shape-morphing dielectric elastomers based on local stiffness modulation, Adv. Funct. Mater. 30 (27) (2020) 2001597.
[328] A. Zolfagharian, A.Z. Kouzani, S.Y. Khoo, A.A.A. Moghadam, I. Gibson, A. Kaynak, Evolution of 3D printed soft actuators, Sens. Actuat. A 250 (2016) 258–272.
[329] Y.L. Yap, S.L. Sing, W.Y. Yeong, A review of 3D printing processes and materials for soft robotics, Rapid Prototyping Journal 26 (8) (2020) 1345–1361.
[330] C.-P. Chou, B. Hannaford, Measurement and modeling of McKibben pneumatic artificial muscles, IEEE Trans. Robot. Automat. 12 (1) (1996) 90–102.
[331] G.M. Whitesides, Soft robotics, Angew. Chem. Int. Ed. 57 (16) (2018) 4258–4273.
[332] A. Zolfagharian, A. Kaynak, A. Kouzani, Closed-loop 4D-printed soft robots, Mater. Des. 188 (2020) 108411.
[333] G.L. Goh, S. Agarwala, W.Y. Yong, 3D printing of microfludic sensor for soft robots: a preliminary study in design and fabrication, in: Conference on Progress in Additive Manufacturing (Pro–AM 2016), 2016, p. 181.
[334] B. Shih, C. Christianson, K. Gillespie, S. Lee, J. Mayeda, Z. Huo, M.T. Tolley, Design considerations for 3D printed, soft, multimaterial resistive sensors for soft, Frontiers in Robotics and AI 6 (2019) 30.
[335] X. Li, Z. Zhang, M. Sun, H. Wu, Y. Zhou, H. Wu, S. Jiang, A magneto-active soft gripper with adaptive and controllable motion, Smart Mater. Struct. 30 (2021) 015024.
[336] X. Cao, S. Xuan, S. Sun, Z. Xu, J. Li, X. Gong, Interfaces, 3D printing magnetic actuators for biomimetic applications, ACS Appl. Mater. Interfaces. (2021).
[337] R. Moucka, M. Sedlacik, M. Cvek, Dielectric properties of magnetorheological elastomers with different microstructure, Appl. Phys. Lett. 112 (12) (2018) 122901.
[338] H. Vatandoost, M. Hemmatian, R. Sedaghati, S. Rakheja, Dynamic characterization of isotropic and anisotropic magnetorheological elastomers in the oscillatory squeeze mode superimposed on large static pre-strain, Compos. Part B 182 (2020) 107648.
[339] R. Fuhrer, C.M. Schumacher, M. Zeltner, W.J. Stark, Soft Iron/Silicon composite tubes for magnetic peristaltic pumping: frequency-dependent pressure and volume flow, Adv. Funct. Mater. 23 (31) (2013) 3845–3849.
[340] M. Lee, T. Park, C. Kim, S.-M. Park, Characterization of a magneto-active membrane actuator comprising hard magnetic particles with varying crosslinking degrees, Mater. Des. 195 (2020) 108921.
[341] T. Tian, M. Nakano, Fabrication and characterisation of anisotropic magnetorheological elastomer with 45 iron particle alignment at various silicone oil concentrations, J. Intell. Mater. Syst. Struct. 29 (2) (2018) 151–159.
[342] X. Wang, G. Mao, J. Ge, M. Drack, G.S.C. Bermúdez, D. Wirthl, R. Illing, T. Kosub, L. Bischoff, C. Wang, Untethered and ultrafast soft-bodied robots, Commun. Mater. 1 (1) (2020) 1–10.
[343] S. Qi, H. Guo, J. Fu, Y. Xie, M. Zhu, M. Yu, 3D printed shape-programmable magneto-active soft matter for biomimetic applications, Compos. Sci. Technol. 188 (2020) 107973.
[344] S. Sundaram, M. Skouras, D.S. Kim, L. van den Heuvel, W. Matusik, Topology optimization and 3D printing of multimaterial magnetic actuators and displays, Sci. Adv. 5 (7) (2019) eaaw1160.
[345] H. Wang, M. Totaro, A.A. Blandin, L. Beccai, A wireless inductive sensing technology for soft pneumatic actuators using magnetorheological elastomers, in: 2019 2nd IEEE International Conference on Soft Robotics (RoboSoft), IEEE, 2019, pp. 242–248.
[346] F. Carpi, D. De Rossi, R. Kornbluh, R.E. Pelrine, P. Sommer-Larsen, Dielectric Elastomers As Electromechanical Transducers: Fundamentals, Materials, Devices, Models and Applications of an Emerging Electroactive Polymer Technology, Elsevier, 2011.
[347] X. Gao, C. Cao, J. Guo, A. Conn, Elastic electroadhesion with rapid release by integrated resonant vibration, Adv. Mater. Technol. 4 (1) (2019) 1800378.
[348] V. Cacucciolo, J. Shintake, Y. Kuwajima, S. Maeda, D. Floreano, H. Shea, Stretchable pumps for soft machines, Nature 572 (7770) (2019) 516–519.
[349] J. Shintake, S. Rosset, B. Schubert, D. Floreano, H. Shea, Versatile soft grippers with intrinsic electroadhesion based on multifunctional polymer actuators, Adv. Mater. 28 (2) (2016) 231–238.
[350] E. Yarali, R. Noroozi, A. Yousefi, M. Bodaghi, M. Baghani, Multi-trigger thermo-electro-mechanical soft actuators under large deformations, Polymers (Basel) 12 (2) (2020) 489.
[351] M.W.M. Tan, G. Thangavel, P.S. Lee, Enhancing dynamic actuation performance of dielectric elastomer actuators by tuning viscoelastic effects with polar crosslinking, NPG Asia Mater. 11 (1) (2019) 1–10.
[352] J. Cao, L. Qin, J. Liu, Q. Ren, C.C. Foo, H. Wang, H.P. Lee, J. Zhu, Untethered soft robot capable of stable locomotion using soft electrostatic actuators, Extreme Mech. Lett. 21 (2018) 9–16.
[353] C.T. Nguyen, H. Phung, P.T. Hoang, T.D. Nguyen, H. Jung, H. Moon, J.C. Koo, H.R. Choi, A novel bioinspired hexapod robot developed by soft dielectric elastomer actuators, in: 2017 IEEE/RSJ International Conference on Intelligent Robots and Systems (IROS), IEEE, 2017, pp. 6233–6238.
[354] Y. Chen, H. Zhao, J. Mao, P. Chirarattananon, E.F. Helbling, N.-s.P. Hyun, D.R. Clarke, R.J. Wood, Controlled flight of a microrobot powered by soft artificial muscles, Nature 575 (7782) (2019) 324–329.
[355] Y. Bar-Cohen, Electroactive Polymer Actuators and Devices (EAPAD) XX, SPIE, 2018.
[356] C. Racles, M. Cazacu, B. Fischer, D.M. Opris, Synthesis and characterization of silicones containing cyanopropyl groups and their use in dielectric elastomer actuators, Smart Mater. Struct. 22 (10) (2013) 104004.
[357] P. Lotz, M. Matysek, H.F. Schlaak, Fabrication and application of miniaturized dielectric elastomer stack actuators, IEEE/ASME Trans. Mechatr. 16 (1) (2010) 58–66.
[358] K. Song, Y. Cha, in: Chopstick Robot Driven By X-shaped Soft Actuator, Actuators, Multidisciplinary Digital Publishing Institute, 2020, p. 32.
[359] H. Zhang, M. Dai, Z. Zhang, Application of viscoelasticity to nonlinear analyses of circular and spherical dielectric elastomers, AIP Adv. 9 (4) (2019) 045010.
[360] N. El-Atab, R.B. Mishra, F. Al-Modaf, L. Joharji, A.A. Alsharif, H. Alamoudi, M. Diaz, N. Qaiser, M.M. Hussain, Soft actuators for soft robotic applications: a review, Adv. Intell. Syst. 2 (10) (2020) 2000128.
[361] A.D. Valentine, T.A. Busbee, J.W. Boley, J.R. Raney, A. Chortos, A. Kotikian, J.D. Berrigan, M.F. Durstock, J.A. Lewis, Hybrid 3D printing of soft electronics, Adv. Mater. 29 (40) (2017) 1703817.
[362] J. Cai, 4D printing dielectric elastomer actuator based soft robots, University of Arkansas, 2016.
[363] F. Zhou, M. Zhang, X. Cao, Z. Zhang, X. Chen, Y. Xiao, Y. Liang, T.-W. Wong, T. Li, Z. Xu, Fabrication and modeling of dielectric elastomer soft actuator with 3D printed thermoplastic frame, Sens. Actuat. A 292 (2019) 112–120.
[364] F. Carpi, D.D. Rossi, Improvement of electromechanical actuating performances of a silicone dielectric elastomer by dispersion of titanium dioxide powder, IEEE Trans. Dielectr. Electr. Insul. 12 (4) (2005) 835–843.
[365] I.S. Park, K.J. Kim, J.D. Nam, J. Lee, W. Yim, Mechanical, dielectric, and magnetic properties of the silicone elastomer with multi-walled carbon nanotubes as a nanofiller, Polym. Eng. Sci. 47 (9) (2007) 1396–1405.
[366] S. Chen, Y. Cao, M. Sarparast, H. Yuan, L. Dong, X. Tan, C. Cao, Soft crawling robots: design, actuation, and locomotion, Adv. Mater. Technol. 5 (2) (2020) 1900837.
[367] S. Hau, G. Rizzello, S. Seelecke, A novel dielectric elastomer membrane actuator concept for high-force applications, Extreme Mech. Lett. 23 (2018) 24–28.
[368] H.S. Jung, S.Y. Yang, K.H. Cho, M.G. Song, C.T. Nguyen, H. Phung, U. Kim, H. Moon, J.C. Koo, J.-.D. Nam, Design and fabrication of twisted monolithic dielectric elastomer actuator, Int. J. Control Autom. Syst. 15 (1) (2017) 25–35.
[369] F. Carpi, A. Migliore, G. Serra, D. De Rossi, Helical dielectric elastomer actuators, Smart Mater. Struct. 14 (6) (2005) 1210.
[370] J.-.T. Miao, M. Ge, S. Peng, J. Zhong, Y. Li, Z. Weng, L. Wu, L. Zheng, Dynamic imine bonds based shape memory polymers with permanent shape reconfigurability for 4D printing, ACS Appl. Mater. Interfaces (2019).
[371] L. Liu, J. Zhang, M. Luo, H. Chen, Z. Yang, D. Li, P. Li, A bio-inspired soft-rigid hybrid actuator made of electroactive dielectric elastomers, Appl. Mater. Today. 21 (2020) 100814.
[372] D. McCoul, S. Rosset, N. Besse, H. Shea, Multifunctional shape memory electrodes for dielectric elastomer actuators enabling high holding force and low–voltage multisegment addressing, Smart Mater. Struct. 26 (2) (2016) 025015.
[373] N. Kellaris, V.G. Venkata, G.M. Smith, S.K. Mitchell, C. Keplinger, Peano-HASEL actuators: muscle-mimetic, electrohydraulic transducers that linearly contract on activation, Sci. Robot. 3 (14) (2018) eaar3276.
[374] P. Rothemund, N. Kellaris, S.K. Mitchell, E. Acome, C. Keplinger, HASEL artificial muscles for a new generation of lifelike robots—recent progress and future opportunities, Adv. Mater. (2020) 2003375.
[375] X. Wang, S.K. Mitchell, E.H. Rumley, P. Rothemund, C. Keplinger, High-strain peano-HASEL actuators, Adv. Funct. Mater. 30 (7) (2020) 1908821.
[376] J.-.M. Park, S.-J. Kim, J.-H. Jang, Z. Wang, P.-G. Kim, D.-J. Yoon, J. Kim, G. Hansen, K.L. DeVries, Actuation of electrochemical, electro-magnetic, and electro-active actuators for carbon nanofiber and Ni nanowire reinforced polymer composites, Compos. Part B 39 (7–8) (2008) 1161–1169.
[377] M. Zhu, S. Qi, Y. Xie, J. Fu, M. Yu, Transient responses of magnetorheological elastomer and isolator under shear mode, Smart Mater. Struct. 28 (4) (2019) 044002.
[378] A.K. Bastola, L. Li, M. Paudel, A hybrid magnetorheological elastomer developed by encapsulation of magnetorheological fluid, J. Mater. Sci. 53 (9) (2018) 7004–7016.
[379] A. Sadeghi, L. Beccai, B. Mazzolai, Innovative soft robots based on electro-rheological fluids, in: 2012 IEEE/RSJ International Conference on Intelligent Robots and Systems, IEEE, 2012, pp. 4237–4242.
[380] M. Bodaghi, A. Damanpack, W. Liao, Self-expanding/shrinking structures by 4D printing, Smart Mater. Struct. 25 (10) (2016) 105034.
[381] A. Zolfagharian, A.Z. Kouzani, S.Y. Khoo, A. Noshadi, A. Kaynak, 3D printed soft parallel actuator, Smart Mater. Struct. 27 (4) (2018) 045019.
[382] J.A.-C. Liu, J.H. Gillen, S.R. Mishra, B.A. Evans, J.B. Tracy, Photothermally and magnetically controlled reconfiguration of polymer composites for soft robotics, Sci. Adv. 5 (8) (2019) eaaw2897.
[383] C. Chautems, A. Tonazzini, D. Floreano, B.J. Nelson, A variable stiffness catheter controlled with an external magnetic field, in: 2017 IEEE/RSJ International Conference on Intelligent Robots and Systems (IROS), IEEE, 2017, pp. 181–186.
[384] F. Zhang, Z. Zhang, C. Luo, I.-T. Lin, Y. Liu, J. Leng, S.K. Smoukov, Remote, fast actuation of programmable multiple shape memory composites by magnetic fields, J. Mater. Chem. C 3 (43) (2015) 11290–11293.
[385] R. Mohr, K. Kratz, T. Weigel, M. Lucka-Gabor, M. Moneke, A. Lendlein, Initiation of shape-memory effect by inductive heating of magnetic nanoparticles in thermoplastic polymers, Proc. Nat. Acad. Sci. 103 (10) (2006) 3540–3545.
[386] L. Ma, J. Zhao, X. Wang, M. Chen, Y. Liang, Z. Wang, Z. Yu, R.C. Hedden, Effects of carbon black nanoparticles on two-way reversible shape memory in crosslinked polyethylene, Polymer (Guildf) 56 (2015) 490–497.

[387] J. Guo, Z. Wang, L. Tong, H. Lv, W. Liang, Shape memory and thermo-mechanical properties of shape memory polymer/carbon fiber composites, Compos. Part A 76 (2015) 162–171.
[388] W. Liu, H. Chen, M. Ge, Q.-.Q. Ni, Q. Gao, Electroactive shape memory composites with TiO2 whiskers for switching an electrical circuit, Mater. Des. 143 (2018) 196–203.
[389] Z. Ji, C. Yan, B. Yu, X. Zhang, M. Cai, X. Jia, X. Wang, F. Zhou, 3D printing of hydrogel architectures with complex and controllable shape deformation, Adv. Mater. Technol. 4 (4) (2019) 1800713.
[390] R.M. Erb, J.S. Sander, R. Grisch, A.R. Studart, Self-shaping composites with programmable bioinspired microstructures, Nat. Commun. 4 (1) (2013) 1–8.
[391] A. Zolfagharian, M. Denk, M. Bodaghi, A.Z. Kouzani, A. Kaynak, Topology-optimized 4D printing of a soft actuator, Acta Mech. Solida Sin. (2019) 1–13.
[392] A. Zolfagharian, M. Denk, A.Z. Kouzani, M. Bodaghi, S. Nahavandi, A. Kaynak, Effects of topology optimization in multimaterial 3D bioprinting of soft actuators, Int. J. Bioprint. 6 (2) (2020) 260.
[393] A. Zolfagharian, A.Z. Kouzani, S.Y. Khoo, I. Gibson, A. Kaynak, in: 3D Printed Hydrogel Soft actuators, 2016 IEEE Region 10 Conference (TENCON), IEEE, 2016, pp. 2272–2277.
[394] Y. Kim, G.A. Parada, S. Liu, X. Zhao, Ferromagnetic soft continuum robots, Sci. Robot. 4 (33) (2019).
[395] D. Podstawczyk, M. Nizioł, P. Szymczyk, P. Wiśniewski, A. Guiseppi-Elie, 3D printed stimuli-responsive magnetic nanoparticle embedded alginate-methylcellulose hydrogel actuators, Addit. Manuf. (2020) 101275.
[396] D. Kim, S. Song, S. Jang, G. Kim, J. Lee, Y. Lee, S. Park, Untethered gripper–type hydrogel microrobot actuated by electric field and magnetic field, Smart Mater. Struct. (2020).
[397] J.M. McCracken, B.M. Rauzan, J.C. Kjellman, H. Su, S.A. Rogers, R.G. Nuzzo, Ionic hydrogels with biomimetic 4D-printed mechanical gradients: models for soft-bodied aquatic organisms, Adv. Funct. Mater. 29 (28) (2019) 1806723.
[398] J.H. Lee, W.J. Han, H.S. Jang, H.J. Choi, Highly tough, biocompatible, and magneto-responsive Fe 3 O 4/Laponite/PDMAAm nanocomposite hydrogels, Sci. Rep. 9 (1) (2019) 1–13.
[399] R. Jain, N. Jadon, A. Pawaiya, Polypyrrole based next generation electrochemical sensors and biosensors: a review, TrAC Trends Anal. Chem. 97 (2017) 363–373.
[400] Y. Lee, W.J. Song, Y. Jung, H. Yoo, M.-.Y. Kim, H.-Y. Kim, J.-Y. Sun, Ionic spiderwebs, Sci. Robot. 5 (44) (2020).
[401] L. Song, M.F. Ahmed, Y. Li, C. Zeng, Y. Li, Vascular differentiation from pluripotent stem cells in 3-D auxetic scaffolds, J. Tissue Eng. Regener. Med. 12 (7) (2018) 1679–1689.
[402] A. Zolfagharian, A. Kaynak, S.Y. Khoo, A.Z. Kouzani, Polyelectrolyte soft actuators: 3D printed chitosan and cast gelatin, 3D Print. Addit. Manufac. 5 (2) (2018) 138–150.
[403] A. Zolfagharian, A.Z. Kouzani, S.Y. Khoo, B. Nasri-Nasrabadi, A. Kaynak, Development and analysis of a 3D printed hydrogel soft actuator, Sens. Actuat. A 265 (2017) 94–101.
[404] Y. Zhai, Z. Wang, K.S. Kwon, S. Cai, D.J. Lipomi, T.N. Ng, Printing multi-material organic haptic actuators, Adv. Mater. (2020) 2002541.
[405] A. Zolfagharian, A. Kouzani, A.A.A. Moghadam, S.Y. Khoo, S. Nahavandi, A. Kaynak, Rigid elements dynamics modeling of a 3D printed soft actuator, J. Smart Mater. Struct. 28 (2) (2018) 025003.
[406] Y. Li, Y. Shen, S. Cao, X. Zhang, Y. Meng, Thermally triggered tunable vibration mitigation in Hoberman spherical lattice metamaterials, Appl. Phys. Lett. 114 (19) (2019) 191904.
[407] C. Cao, X. Gao, A.T. Conn, A magnetically coupled dielectric elastomer pump for soft robotics, Adv. Mater. Technol. 4 (8) (2019) 1900128.
[408] H. Lu, Y. Yao, W.M. Huang, J. Leng, D. Hui, Significantly improving infrared light-induced shape recovery behavior of shape memory polymeric nanocomposite via a synergistic effect of carbon nanotube and boron nitride, Compos. Part B 62 (2014) 256–261.
[409] J. Kim, B. Kim, E. Kim, H. Park, H. Jeong, Synthesis and shape memory performance of polyurethane/graphene nanocomposites, React. Funct. Polym. 74 (2014) 16–21.
[410] Y. Zhou, N. Sharma, P. Deshmukh, R.K. Lakhman, M. Jain, R.M. Kasi, Hierarchically structured free-standing hydrogels with liquid crystalline domains and magnetic nanoparticles as dual physical cross-linkers, J. Am. Chem. Soc. 134 (3) (2012) 1630–1641.
[411] D. Morales, E. Palleau, M.D. Dickey, O.D. Velev, Electro-actuated hydrogel walkers with dual responsive legs, Soft Matter 10 (9) (2014) 1337–1348.
[412] E. Yarali, M.A. Farajzadeh, R. Noroozi, A. Dabbagh, M.J. Khoshgoftar, M.J. Mirzaali, Magnetorheological elastomer composites: Modeling and dynamic finite element analysis, Compos. Struct. (2020) 112881.
[413] F. Ebrahimi, M.R. Barati, V. Mahesh, Dynamic modeling of smart magneto–electro-elastic curved nanobeams, Adv. Nano Res. 7 (3) (2019) 145.
[414] A. Ghorbanpour Arani, S.A. Jamali, The vibration of the cylindrically curved sandwich plate with rheological core and nanocomposite face sheets rested on the Winkler–Pasternak foundation, J. Sandwich Struct. Mater. 0 (0) (2020) 1099636220909818.
[415] T. Soleymani, A. Ghorbanpour Arani, On aeroelastic stability of a piezo-MRE sandwich plate in supersonic airflow, Compos. Struct. 230 (2019) 111532.
[416] A.K. Bastola, L. Li, A new type of vibration isolator based on magnetorheological elastomer, Mater. Des. 157 (2018) 431–436.
[417] A.K. Miri, A. Khalilpour, B. Cecen, S. Maharjan, S.R. Shin, A. Khademhosseini, Multiscale bioprinting of vascularized models, Biomaterials 198 (2019) 204–216.
[418] T. Hiruta, N. Hosoya, S. Maeda, I. Kajiwara, Experimental validation of vibration control in membrane structures using dielectric elastomer actuators in a vacuum environment, Int. J. Mech. Sci. 191 (2020) 106049.
[419] N. Ma, Y. Yao, Q. Wang, C. Niu, X.J.S.M. Dong, Structures, Properties and mechanical model of a stiffness tunable viscoelastic damper based on electrorheological elastomers, Smart Mater. Struct. 29 (4) (2020) 045041.
[420] M. Schwabe, S.A. Khrapak, S.K. Zhdanov, M.Y. Pustylnik, C. Räth, M. Fink, M. Kretschmer, A.M. Lipaev, V.I. Molotkov, A.S. Schmitz, M.H. Thoma, A.D. Usachev, A.V. Zobnin, G.I. Padalka, V.E. Fortov, O.F. Petrov, H.M. Thomas, Slowing of acoustic waves in electrorheological and string-fluid complex plasmas, New J. Phys. 22 (8) (2020) 083079.
[421] M. Vinyas, On frequency response of porous functionally graded magneto–electro-elastic circular and annular plates with different electro-magnetic conditions using HSDT, Compos. Struct. 240 (2020) 112044.
[422] M. Vinyas, Computational analysis of smart magneto-electro-elastic materials and structures: review and classification, Arch. Comput. Methods Eng. (2020).
[423] X.L. Zhang, Q. Xu, X. Zhao, Y.H. Li, J. Yang, Nonlinear analyses of magneto-electro-elastic laminated beams in thermal environments, Compos. Struct. 234 (2020) 111524.
[424] M. Karimiasl, F. Ebrahimi, Large amplitude vibration of viscoelastically damped multiscale composite doubly curved sandwich shell with flexible core and MR layers, Thin-Walled Struct. 144 (2019) 106128.
[425] G.I. Mikhasev, V.A. Eremeyev, K. Wilde, S.S. Maevskaya, Assessment of dynamic characteristics of thin cylindrical sandwich panels with magnetorheological core, J. Intell. Mater. Syst. Struct. 30 (18–19) (2019) 2748–2769.
[426] F. Ebrahimi, S. Bayrami Sedighi, Wave propagation analysis of a rectangular sandwich composite plate with tunable magneto-rheological fluid core, J. Vib. Control 0 (0) (2020) 1077546320938189.
[427] F. Ebrahimi, A. Dabbagh, Wave Propagation Analysis of Smart Nanostructures, 1st ed., CRC Press, Boca Raton, FL, 2019.
[428] A. Omidi Soroor, M. Asgari, H. Haddadpour, Effect of axially graded constraining layer on the free vibration properties of three layered sandwich beams with magnetorheological fluid core, Compos. Struct. (2020) 112899.
[429] R. Selvaraj, M. Ramamoorthy, Dynamic analysis of laminated composite sandwich beam containing carbon nanotubes reinforced magnetorheological elastomer, J. Sandwich Struct. Mater. 0 (0) (2020) 1099636220905253.
[430] S.M.M. Mofidian, H. Bardaweel, A dual-purpose vibration isolator energy harvester: experiment and model, Mech. Syst. Signal Process. 118 (2019) 360–376.
[431] B. Yan, H. Ma, L. Zhang, W. Zheng, K. Wang, C. Wu, A bistable vibration isolator with nonlinear electromagnetic shunt damping, Mech. Syst. Signal Process. 136 (2020) 106504.
[432] P. Motreuil-Ragot, A. Hunt, D. Kasi, B. Brajon, A. van den Maagdenberg, V. Orlova, M. Mastrangeli, P.M. Sarro, Enabling actuation and sensing in organs-on-chip using electroactive polymers, in: 2020 3rd IEEE International Conference on Soft Robotics (RoboSoft), IEEE, 2020, pp. 530–535.
[433] N. Kellaris, V.G. Venkata, G.M. Smith, S.K. Mitchell, C. Keplinger, Peano-HASEL actuators: muscle-mimetic, electrohydraulic transducers that linearly contract on activation, Sci. Rob. 3 (14) (2018).
[434] E.A. Sideris, H.C. de Lange, A. Hunt, An ionic polymer metal composite (ipmc)-driven linear peristaltic microfluidic pump, IEEE Rob. Autom. Lett. 5 (4) (2020) 6788–6795.
[435] B. Han, Y.Y. Gao, Y.L. Zhang, Y.Q. Liu, Z.C. Ma, Q. Guo, L. Zhu, Q.D. Chen, H.B. Sun, Multi-field-coupling energy conversion for flexible manipulation of graphene-based soft robots, Nano Energy 71 (2020) 104578.
[436] S. Miao, N. Castro, M. Nowicki, L. Xia, H. Cui, X. Zhou, W. Zhu, S.J. Lee, K. Sarkar, G. Vozzi, Y. Tabata, J. Fisher, L.G. Zhang, 4D printing of polymeric materials for tissue and organ regeneration, Mater Today (Kidlington) 20 (10) (2017) 577–591.